

THESIS ON NATURAL AND EXACT SCIENCES B204

**A Macromolecular Imprinting Approach to
Design Synthetic Receptors for
Label-Free Biosensing Applications**

ALEKSEI TRETJAKOV

TUT
PRESS

TALLINN UNIVERSITY OF TECHNOLOGY
Faculty of Chemical and Materials Technology
Department of Materials Science
Chair of Physical Chemistry

This dissertation was accepted for the defence of the degree of Doctor of Philosophy in Natural and Exact Sciences on March 17, 2016.

Supervisor: Dr. Vitali Syritski, Department of Materials Science,
Tallinn University of Technology

Co-supervisors: Prof. Andres Õpik, Faculty of Chemical and Materials
Technology, Tallinn University of Technology

Dr. Jekaterina Reut, Department of Materials Science,
Tallinn University of Technology

Opponents: Dr. Michael J Whitcombe, Department of Chemistry,
University of Leicester, UK

Prof. Arunas Ramanavicius, Faculty of Chemistry, Vilnius
University, Lithuania

Defence of the thesis: April 19, 2016 at 12.00
Lecture hall: U06a-201
Tallinn University of Technology, Ehitajate tee 5,
Tallinn

Declaration:

Hereby I declare that this doctoral thesis, my original investigation and achievement, submitted for the doctoral degree at Tallinn University of Technology, has not previously been submitted for any academic degree.

/Aleksi Tretjakov/



Copyright: Aleksi Tretjakov, 2016
ISSN 1406-4723
ISBN 978-9949-23-911-5 (publication)
ISBN 978-9949-23-912-2 (PDF)

LOODUS- JA TÄPPISTEADUSED B204

**Sünteesilised retseptorid molekulaarselt
jäljendatud polümeeridest biomakromolekulide
mürgisevabaks määramiseks**

ALEKSEI TRETJAKOV

TABLE OF CONTENTS

LIST OF PUBLICATIONS	7
THE AUTHOR'S CONTRIBUTION TO PUBLICATIONS.....	7
OTHER PUBLICATIONS	7
LIST OF ABBREVIATIONS.....	8
INTRODUCTION	9
1. THEORY AND LITERATURE REVIEW.....	12
1.1. Introduction to molecular imprinting technology	12
1.1.1. Principle of molecular imprinting	12
1.2. MIP formats	14
1.3. MIPs for biosensing applications.....	16
1.3.1. Protein-MIPs	16
1.3.2. Surface molecular imprinting.....	17
1.3.3. Immobilization of proteins on a surface.....	17
1.3.4. Electrosynthesis approach for protein-MIPs.....	18
1.4. Immunoglobulin G as a template protein.....	20
1.5. Label-free biosensor platforms	21
1.5.1. Quartz Crystal Microbalance sensor	22
1.5.2. Surface Acoustic Wave sensor.....	24
1.6. Characterization of MIP recognition properties.....	25
1.6.1. Binding kinetics	25
1.6.2. Adsorption isotherms	27
1.7. Summary of the literature review and objectives of the study	29
2. EXPERIMENTAL PART.....	30
2.1. A macromolecular imprinting approach for the protein-MIP film fabrication	30
2.2. Protein immobilization on a gold electrode surface.....	30
2.2.1. Surface functionalization via the <i>p</i> -MP/Cys-peptide linker system.....	31
2.2.2. Surface functionalization via 4-aminotiophenol/DTSSP linker system.....	31
2.3. Polymer matrix formation by electropolymerization	31
2.3.1. Electrodeposition of PDA films	32
2.3.2. Electrodeposition of PmPD films.....	32
2.4. IgG removal from polymeric matrix	33
2.5. Characterization of the IgG-MIP film.....	33
2.5.1. Rebinding study by QCM	33
2.5.2. Rebinding study by SAW.....	34
3. RESULTS AND DISCUSSION	36
3.1. Immobilization of IgG on a gold surface	36
3.1.1. Immobilization through the <i>p</i> -MP/Cys-peptide linker system....	36
3.1.2. Immobilization via 4-aminotiophenol/DTSSP.....	36
3.2. Fabrication of the IgG-MIP films	37
3.2.1. Formation of the polymer matrix by electropolymerization	38
3.2.2. Removal of IgG from the polymeric matrix.....	39
3.3. Characterization of the IgG-MIP films	40

3.3.1. Rebinding study by QCM	40
3.3.2. Rebinding study by SAW.....	41
3.3.3. Comparison of QCM and SAW devices	42
3.3.4. Selectivity of the IgG-MIP.....	42
4. CONCLUSIONS.....	43
ABSTRACT.....	45
KOKKUVÕTE.....	47
ACKNOWLEDGMENTS	49
REFERENCES.....	50
APPENDIX A.....	59
APPENDIX B.....	91

LIST OF PUBLICATIONS

The thesis is based on the following publications, which are referred to in the text by the Roman numerals I-III:

I. Xin Zhang, **Aleksei Tretjakov**, Marc Hovestaedt, Guoguang Sun, Vitali Syritski, Jekaterina Reut, Rudolf Volkmer, Karsten Hinrichs, Joerg Rappich, Electrochemical functionalization of gold and silicon surfaces by a maleimide group as a biosensor for immunological application, *Acta Biomaterialia*, 9(3) (2013) 5838–5844.

II. **Aleksei Tretjakov**, Vitali Syritski, Jekaterina Reut, Roman Boroznjak, Olga Volobujeva, and Andres Öpik, Surface molecularly imprinted polydopamine films for recognition of immunoglobulin G, *Microchimica Acta*, 180(15) (2013) 1433-1442.

III. **Aleksei Tretjakov**, Vitali Syritski, Jekaterina Reut, Roman Boroznjak, and Andres Öpik, Molecularly imprinted polymer film interfaced with Surface Acoustic Wave technology as a sensing platform for label-free protein detection, *Analytica Chimica Acta*, 902 (2016) 182-188.

Copies of these articles are included in Appendix A.

THE AUTHOR'S CONTRIBUTION TO PUBLICATIONS

The contribution by the author to the papers included in the thesis is as follows:

I. Carrying out of QCM measurements, participation in data processing, minor role in the manuscript writing.

II. Carrying out a major part of the experimental work, participation in data processing and in the manuscript writing.

III. Carrying out a major part of the experimental work, participation in data processing and in the manuscript writing.

OTHER PUBLICATIONS

Akinrinade George Ayankojo, **Aleksei Tretjakov**, Jekaterina Reut, Roman Boroznjak, Andres Öpik, Jörg Rappich, Andreas Furchner, Karsten Hinrichs, and Vitali Syritski, Molecularly Imprinted Polymer Integrated with a Surface Acoustic Wave Technique for Detection of Sulfamethizole, *Analytical Chemistry*, 88(2) (2016) 1476–1484.

LIST OF ABBREVIATIONS

4-ATP	4-aminothiophenol
Ag/AgCl/KCl _{Sat.}	Silver/Silver Chloride Electrode
CVA	Cyclic Voltammetry
DA	Dopamine
DMSO	Dimethyl Sulfoxide
DTSSP	3, 3'-dithiobis [sulfosuccinimidylpropionate]
EIS	Electrochemical Impedance Spectroscopy
EQCM	Electrochemical Quartz Crystal Microbalance
FIA	Flow Injection Analysis
HSA	Human Serum Albumin
IF	Imprinting factor
IgG	Immunoglobulin G
IgA	Immunoglobulin A
<i>m</i> -PD	<i>m</i> -Phenylenediamine
MIP	Molecularly Imprinted Polymer
NIP	Non-imprinted Polymer
PBS	Phosphate Buffered Saline
PDA	Polydopamine
PmPD	Poly (<i>m</i> -phenylenediamine)
<i>p</i> -mP	Para-maleimidophenyl
QCM	Quartz Crystal Microbalance
SAW	Surface Acoustic Wave
SPR	Surface Plasmon Resonance
SDS	Sodium Dodecyl Sulfate
SEM	Scanning Electron Microscope
SI	Surface Imprinting

INTRODUCTION

Recognition of one molecule by another is a phenomenon that plays a crucial role in many biological processes of living systems. The principles of molecular recognition, as one of the fundamental mechanisms found in nature, inspire modern molecular engineering science to design synthetic receptors capable of binding various analytes with affinity and selectivity comparable to their biological counterparts, at the same time being much more mechanically and thermally stable. Today's various classes of synthetic receptors designed utilize organic macrocycles (cyclodextrins, crown ethers), metal coordination complexes, aptamers and dendrimers [1]. One of the state-of-the-art techniques to generate synthetic receptors is "molecular imprinting", which can be defined as the process of template-induced formation of specific molecular recognition sites in a polymer matrix material [2]. The most common form of imprinting consists in polymerization of a mixture of functional monomers in the presence of a target molecule that acts as a template. During polymerization, the template induces binding sites in the reticulated polymer that are capable of selectively recognizing the target molecules or similar structures after removal of the templates from the polymer (Fig. 1.1). The main benefits of these polymers, so-called Molecularly Imprinted Polymers (MIPs), are related to their synthetic nature, i.e., excellent chemical and thermal stability associated with reproducible, cost-effective fabrication. Therefore, MIPs are considered as very prospective materials for application in various fields such as chemical analysis and detection [3], separation and purification [4], drug delivery [5], and catalysis [6].

MIP-based receptors have been shown to be promising alternatives to natural biological receptors (e.g. Enzymes, DNA, antibodies) in biosensing applications, providing more stable and low-cost recognition elements [7, 8]. However, there remain many unsolved issues in the development of MIP-based biosensors, which can be categorized into the following three aspects: imprinting of high molecular weight templates such as proteins, transformation of the binding event into a measurable signal and miniaturization of the resulting MIP structures aiming at high throughput applications.

The main obstacles in molecular imprinting of proteins are caused by restricted mobility of the large molecular structures within the highly cross-linked polymer networks, resulting in limited rebinding efficiency as well as the need to perform MIP synthesis and the following rebinding study in aqueous media where water molecules can significantly reduce the binding strength of the non-covalent template—monomer interactions. Nevertheless, a number of promising synthetic approaches were developed in order to overcome the above limitations in macromolecular imprinting [9]. It is believed that the use of a more relaxed polymeric network having a significant part of the imprinted binding sites on its surface is more feasible for protein recognition since the mass transfer and the binding kinetics in such surface imprinted polymers are essentially faster. Thus, success was attributed to realizing surface imprinted polymers exhibiting highly selective recognition for a variety of template proteins such as albumin, hemoglobin and cytochrome C [10], lysozyme [11], avidin [12, 13].

Immunoglobulin G (IgG) is a macromolecule of high molecular mass and the most plentiful class of antibodies present in human serum protecting humans against bacterial and viral infections. Analysis of the presence of specific IgG molecules in the body fluids can be extremely useful in diagnosing infections or certain illnesses [14]. Therefore, the realization of a MIP capable of highly selective capture of IgG is of great importance in immunological research and clinical diagnostics. However, to date only a few attempts have been made to imprint IgG [15-18].

Robust interfacing of a MIP uniform thin film with a sensor platform capable of responding to relevant sensitivity levels upon interaction between the MIP film and a binding analyte is a key aspect in the design of a MIP-based biosensor. Electrochemical polymerization seems to be a suitable method for an in-situ synthesis of the MIP film providing a good control for both its thicknesses (down to the nanometer range) and inner morphology (porosity, optical properties) and the ability of the reaction to be carried out at room temperature [19, 20]. Moreover, the electrochemical approach could be feasible to prepare MIPs in a microarray format with a capability of multiplexed readout that would offer an opportunity to explore a sample/samples in a high throughput manner [21].

In addition, label-free detection of proteins is a preferable method since their chemical labeling can influence the interfacial activity of the resulting protein-dye complexes, and consequently the accuracy of measurement results [22]. Thus, the use of label-free sensing platforms for integration with MIPs can provide relevant information on the binding events on the MIP surfaces and has to be considered in the first place in developing protein-MIP-based biosensors. Label-free detection can be implemented with the help of various transduction mechanisms, including, but not limited to, optical, electrochemical or piezoelectric, where the biochemical interaction between an analyte and a recognition element of the sensor is recorded as a change in, e.g., refractive index (Surface Plasmon Resonance, SPR), electrochemical impedance (electrochemical sensors) or resonant frequency (Quartz Crystal Microbalance, QCM), respectively.

It is worth mentioning that in most of the reported work using protein-MIPs for sensing applications QCM, SPR or electrochemical sensor platforms predominate over other ones. Meanwhile, Surface Acoustic Waves (SAW) may provide advances in the fabrication of MIP-based sensors over those platforms. SAW offers about an order of magnitude higher mass resolution than QCMs while keeping low sensor cost. In addition, it is fully compatible with large-scale fabrication and multiplexing technologies [23, 24]. As compared to the SPR, SAW technology is not limited to detecting only mass loading onto the surface, but it is also useful in following structural insights of sensing layers through the use of the dissipation factor of the acoustic wave propagating along the sensor surface.

The research described in the current thesis seeks to develop a synthesis method that generates a polymer film with macromolecular imprints capable of selectively rebinding IgG (the IgG-MIP). The method was expected to be compatible with various label-free detection techniques, providing facile and robust integration of the resulting IgG-MIP films with the sensing surface of

transducers. QCM and SAW piezoelectric transducers were selected as tools allowing the study of the IgG-MIPs and understanding of the factors improving their performance. Eventually, the optimized IgG-capturing materials interfaced with the SAW technology allowed observation of the real-time binding events of the target protein at relevant sensitivity levels, making the realized concept potentially suitable for cost-effective fabrication of protein specific biosensors for the analysis of biological samples in a multiplexed manner.

1. THEORY AND LITERATURE REVIEW

1.1. Introduction to molecular imprinting technology

1.1.1. Principle of molecular imprinting

In general, the term "molecular imprinting" refers to the technique that allows the preparation of robust polymeric materials capable of selectively recognizing a targeted molecule by its shape, size and functional groups. Such type of molecular recognition is based on the availability of specific binding sites occurring as template-shaped cavities in a highly reticulated polymeric network [25]. The general principle of the molecular imprinting process is summarized in Fig. 1.1.

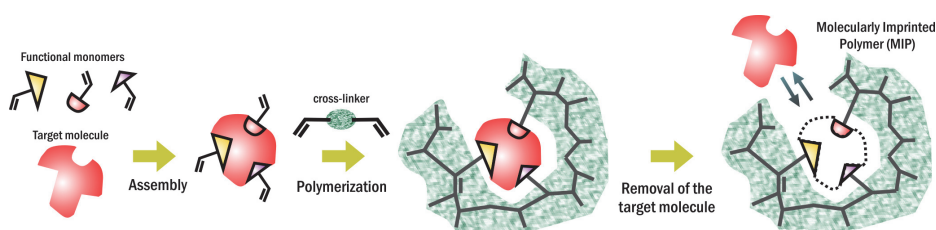


Figure 1.1. Scheme of Molecular Imprinting.

The process starts with the dissolution of a target molecule acting as a template, functional monomers, a polymerization initiator and a cross-linking agent in a suitable solvent. The selection of the functional monomer, cross-linking degree and the format of resulting MIP is based on the type of the chosen template. The functional monomers interact with the template molecules generating a stable, self-assembled or pre-organized pre-polymerization complex subsequently followed by its polymerization. The pre-polymerization complex could be evaluated with the help of spectroscopic techniques such as NMR, UV-vis and several different computational simulation methods. As a result of polymerization with a commonly high cross-linking degree, the functional groups of a synthesized polymer become fixed in a well defined position and have complementary dependence with the available groups on the template as well as a strong affinity for the latter. Subsequent removal of the incorporated molecules by washing with solvent(s) leaves specific cavities that are complementary in shape and size to the template, thus allowing its reversible rebinding to the MIP structure [26].

Essentially, strategies for molecular imprinting can be grouped on the basis of the type of the monomer-template interaction into a covalent and a non-covalent imprinting approach.

Covalent imprinting

Molecular imprinting in the modern sense of the term was established by Wulff and Sarhan in the early 1970s. Studies of Wulff's group showed that molecular templates could be incorporated within the organic polymer matrix and

leave their imprinted binding sites after subsequent washing steps [27]. At that moment, Wulff prepared an organic MIP capable of discriminating between the enantiomers of glyceric acid and used an approach for the formation of a pre-polymerization complex, which was based on reversible covalent bonding. Later on, this covalent monomer–template or covalent polymer–template attachment strategy was referred to as the covalent imprinting. The advantage of such approach comes from defined stoichiometry between the functional monomer and the template. Nonetheless, this strategy is rarely used nowadays since the choice of reversible covalent interactions and the number of potential templates are essentially limited. Furthermore, the need for the harsh acid hydrolysis procedure to cleave the covalent bonds between the template and the functional monomer narrows down potentialities of such method substantially.

Non-covalent imprinting

The second major achievement in the area of organic polymer imprinting was made in 1981 by Mosbach and Arshady who reported on the synthesis of an organic MIP using the non-covalent interactions approach [28]. In contrast to covalent imprinting, the non-covalent approach involves the formation of ionic, hydrophobic, π - π , Van der Waals forces or hydrogen bonds between the template and the monomer. In this approach, functional monomers are self-organized around the template assembling a pre-polymerization complex and interact during the cross-linked co-polymerization procedure. This simple methodology encouraged attention to the MIP development field, causing incredible growth in the articles related to the topic during the decade of the 1990s.

Semi-covalent imprinting

In addition to the concepts above, Whitcombe's group has made an attempt to combine the benefits of these two main approaches by presenting the intermediate approach that was based on covalent interactions in polymerization and non-covalent in the rebinding stage [29]. The limitations of the non-covalent approach in molecular recognition mostly come from the necessity of using hydrophobic environments to stabilize the interactions between monomers and the template, since polar environments such as aqueous media can easily disrupt them. The other major restriction of this approach is that MIP with high molecular recognition properties can be achieved if multiple distinct points of interaction between the monomer and the template molecules are available. Otherwise, using molecules with a single interacting group far less specific binding sites are obtained.

Nonetheless, nowadays non-covalent imprinting is still the most commonly used approach for MIP synthesis. This is because the non-covalent approach is far easier than the covalent analogue and has more potential for further development of molecular imprinting due to the practically unlimited selection of compounds, including bioanalytes, which can also non-covalently interact with functional monomers. The nature of monomers and the availability of functional groups determine the mechanism of polymerization and interaction with template

molecules, thus having direct influence on the quality and performance of the MIP polymeric product.

The main benefits of MIPs are related to their synthetic nature, i.e., excellent chemical and thermal stability associated with reproducible, cost-effective fabrication. All of these make MIP a versatile material that is able to recognize a wide range of analytes including small molecules (e.g., drugs, pesticides, peptides, hormones, sugars and etc.), large organic molecules, and bioanalytes (e.g., immunoglobulins, erythrocytes, viruses or cells). Recent advances in the field of molecular imprinting have shown a great promise of using MIPs in such applications as preparation of artificial antibodies [30], chemical- and biosensors [31, 32], materials separation [33, 34] and drug delivery [35]. MIPs can also be applied as tailor-made receptors even if biological analogues are unavailable. In contrast to selective and affinity properties of antibodies, several authors declare MIPs as synthetic antibodies and suggest that these artificial receptors will potentially replace the natural ones in numerous areas. The main driving forces for the substitution of antibodies with MIPs in sensors may result from their preparation simplicity, low cost and the high stability of these polymers.

However, to obtain optimum parameters for use in practical applications, MIP polymers should reach a number of desirable binding properties, including 'K_D' values similar to those of natural receptors, high affinity and selectivity towards a target molecule as well as appropriate physical properties in combination with readily available methods of synthesis.

1.2. MIP formats

The area where MIPs are supposed to be applied specifies the format in which they are prepared. Certain applications require specific morphologies and properties, such as micron size beads for more efficient packing into chromatographic columns [11], core-shell MIP particles suspended in solution for binding assays [36], or membranes and films for coating of sensor devices [37, 38]. Advantages and limitations together with a brief description of each direction are discussed in the following.

MIP nanoparticles

MIP nanoparticles are synthesized in the form of small beads of precisely controlled shape and diameter ranging from a nanometer to a micrometer-size. As opposed to bulk monoliths, MIP nanoparticles have significantly higher surface area-to-volume ratios, allowing an improved removal of the templates along with easily accessible binding sites and faster binding kinetics. This particular feature makes it possible to achieve highly reproducible results on a large scale for applications, such as drug delivery systems, capillary electrophoresis and chromatography columns. Moreover, MIP nanoparticles have been used as enzyme and antibody substitutes [39]. The most widely used strategies for producing MIP nanoparticles are precipitation polymerization, emulsion polymerization and core-shell emulsion polymerization [40].

Besides the classical MIP nanoparticles format, a variety of nanosized MIPs, such as MIP-nanogels, MIP-nanocapsules, MIP-nanowires, MIP-nanotubes have been developed and promised to have a great future potential [41]. Furthermore, it might be possible to combine nanosized-MIP fabrication methodologies with sophisticated materials, such as polymer nanocomposites containing carbon materials or a stimuli-responsive (sensitive to changes in pH, temperature, incident light, ionic strength) polymers, which will result in the fabrication of a new class of MIPs able to respond to external stimuli during the modulation of their affinity for the target molecules and hence provide an adjustable capacity of the target releasing and binding processes [42-44].

Thin MIP layers

Another very promising direction is the preparation of thin MIP-layers directly on the surface of various substrates. Generally, polymeric layers could be designed in the form of polymer films and brushes, block-copolymer films, layer-by-layer films, hybrid (polymer and particles) films, and membranes [45]. In terms of chemical sensing, MIP-layers could be integrated with appropriate transducers in order to transform the binding events into an analytical signal. Integration of MIP-layers with the sensor could be achieved by a variety of methods, such as in-situ photo- [46] or electropolymerization [38] as well as drop-casting, spray- or spin coating of a pre-polymerization mixture onto the surface [47].

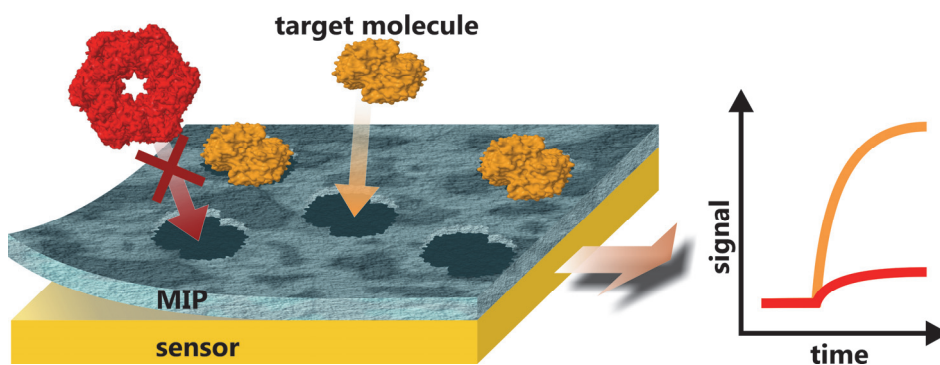


Figure 1.2. A schematic representation of a MIP-based sensor where a MIP film is assembled on the sensing surface of a transducer and provides selectivity to the whole sensor system.

Nowadays, MIP thin films and membranes are widely used as convenient platforms for fundamental studies and practical applications due to the inherent number of advantages, including appropriate macroscopic shape, variable conditions for synthesis (adjustable polymerization rate, temperature, pH, light flux for photoinitiation), and simplicity of preparation. Moreover, the film platform perfectly fits for sensor applications and can be characterized by a wide range of analytical methods [48] (Fig. 1.2).

1.3. MIPs for biosensing applications

Chemical and biosensors have attracted considerable attention in the area of analytical chemistry due to the increasing demand for fast and reliable devices with low detection limits and appropriate selectivity in such fields as clinical analysis, environmental monitoring and other areas. A biosensor combines a physicochemical detector with a recognition element (e.g., DNA, enzyme, antibody) that binds or recognizes the target analyte [49]. However, despite significant progress in biological recognition elements based biosensors, there are several limitations associated with them. While the poor chemical and physical stability together with the labile nature of biomolecules restrict further development of robust and reusable natural recognition elements, as MIP is a completely synthetic material with the possibility of smart response to the target molecules presents a valid alternative to the biological receptors [50]. The main advantages of MIPs over natural receptors are material robustness, resistance to extreme temperatures and pressures, an improved inertness to harsh chemical conditions, as well as low cost production, ease of preparation procedures, long shelf-life, and reproducibility [7].

Though MIPs can be applied as tailor-made receptors to an almost unlimited number of targets, even those whose biological receptors are unavailable, the production of high-effective MIPs against such large structures as proteins, cells and viruses is still quite a novel and fast-evolving area that should overcome a number of limitations.

1.3.1. Protein-MIPs

In the last few decades, interest in the field of macromolecular imprinting has considerably increased due to the wide possibilities of using such MIPs to design a new class of robust diagnostic tools [51].

However, the main drawback related to imprinting of such structures is their large size and complex shape that restrict their mobility within the highly cross-linked polymeric matrix; hence, the poor efficiency in rebinding [52]. Moreover, imprinting of large biomacromolecules involves using of their native medium conditions to eliminate template conformational changes during MIP formation procedures and ensure proper washing out from highly reticulated polymeric networks. While the classical MIP technology relies on the use of organic solvents, water-soluble proteins as specific templates demand development of new, highly-controlled preparation methods compatible with the use of aqueous medium to preserve their native conformation. Moreover, according to the thermodynamic considerations relevant for MIPs, Nicholls assumed that it would be difficult to develop high-effective imprints for such large molecules as proteins [53]. Therefore, high affinity and selectivity under physiological conditions are the main desirable properties of protein-MIPs.

Essentially, the template recognition principle in protein-MIPs can be divided into the recognition of polypeptide or a fragment sequence and the recognition of a protein shape. Considerable success was achieved by realizing surface imprinted polymers exhibiting highly selective recognition for a variety of

template proteins such as albumin, hemoglobin and cytochrome C [10], lysozyme [11], avidin [12, 13]. However, to date, only a few attempts have been made to imprint more complex macromolecules such as antibodies [15-18]. With regard to the above, the preparation of MIPs for selective recognition of proteins is an emerging field of molecular imprinting involving macromolecular templates.

1.3.2. Surface molecular imprinting

One of the perspective solutions to the problem of protein imprinting involves the fabrication of tailor-made materials with more relaxed polymeric networks having high surface-to-volume ratio. The technique of surface molecular imprinting allows the formation of polymers with the selective binding sites located at or close to their surface. Such sites are more accessible, hence the mass transfer and the binding kinetics are faster. Significant results in this area were achieved by protein imprinting of polymer nanowires [54], nanoparticles [55] and thin films [56, 57]. Currently, the field of macromolecular, in particular protein-MIPs preparation, has been highly influenced by the surface imprinting technique, covering up to 60% of all published papers describing the considered approach [58].

Imprinted sites exclusively located on the surface of MIPs could be formed and the binding site density and homogeneity could be better controlled in a variety of ways, including microcontact printing with protein modified stamps [59], and taking advantage of the immobilized templates on sacrificial materials [10, 13].

1.3.3. Immobilization of proteins on a surface

The surface molecular imprinting methods involve the immobilization of protein templates on a solid support that acts either as a sacrificial or a transfer material [60]. Since protein imprinting is rendered more difficult by the thermodynamic motion of proteins in the solution, the quality of the imprints is expected to be improved by using immobilized templates [12].

Elaboration on the appropriate strategies for protein immobilization on the surface is a key point for the successful development of a surface imprinted MIP format. Consequently, the immobilization procedure should comply with the conditions that provide:

- insignificant effect on the protein structure
- subsequent polymerization around the immobilized molecules
- easy subsequent release of the immobilized molecules from the polymer matrix.

As an example, the choice of an immobilization method for such widespread biorecognition elements as antibodies greatly affects their activity, conformation and geometrical orientation on a solid support. Antibody immobilization methods can be conditionally divided into the following categories: antibody direct adsorption; antibody covalent immobilization and modification; utilization of antigen epitopes or antibody binding proteins, and other alternative methods. While simple adsorption of an antibody to a gold surface results in non-desirable

effects, such as random orientation, high level of antibody denaturation and loss of binding properties, immobilization of an antibody to the specific epitope of an antigen provides its proper orientation and potentially could be applied for further preparation of the antibody molecular imprints. Another approach that is more stable and thus highly compatible with the surface molecular imprinting technique is covalent cross-linking of an antibody on a chemically-activated surface [61, 62]. Amino groups on the antibody can be readily coupled with aldehyde, epoxy, imidoester, carboxylic or dithiocarboxylic reactive groups, thereby providing a possibility for application of various surface functionalization methods.

1.3.4. Electrosynthesis approach for protein-MIPs

Electropolymerization is mainly used for the deposition of polymer films on conducting substrates, thus allowing a robust interfacing of a uniform polymer film with a sensor platform and has attracted considerable interest in the industry of chemical- and biosensors [63].

Electrochemical polymerization seems to be a suitable method for an in-situ synthesis of the MIP film since it provides good control for both its thicknesses (down to the nanometer range) and inner morphology as well as the possibility to carry out the reaction at room temperature [19, 64]. Moreover, the electrochemical approach could be feasible to prepare MIPs in a microarray format with the capability of multiplexed readout that would offer an opportunity to explore a sample/samples in a high throughput manner [21]. Nowadays, polymers synthesized by the electrochemical method are successfully applied for the preparation of MIP-based sensors [20]. Promising results on the application of electropolymerization with protein imprinting were shown for a number of different polymers like p(o-phenylenediamine) [65], poly (3, 4-ethylenedioxythiophene) [13, 66], polypyrrole [67, 68] and other polymers.

In this work, the electrosynthesized polydopamine and poly(m-phenylenediamine) were used to prepare protein-MIP films on the surface of QCM and SAW sensors.

Polydopamine

Dopamine (DA) is an organic chemical that contains catechol and amine functional groups. This catecholic compound synthesized in the brain and kidneys plays an important role in human body as a hormone and neurotransmitter. In nature, DA is synthesized in plants and most multicellular animals, e.g., DA similar structures are found in adhesive proteins secreted by mussels. This particular feature has led to an approach for the surface modification based on DA polymerization resulting in the formation of adherent polymeric films on the surface of a wide range of inorganic and organic substrates [69].

The most widely used method to achieve such adherent coatings is a spontaneous self-polymerization of DA under weak alkaline conditions, where catechol groups are oxidized to the quinone form. A more elegant way is

electrochemical polymerization where resulting film thickness is precisely controlled by accurate dosage of the applied charge [70]. It should be noted that this method has the limitation for a maximum thickness of up to several tens of nanometers due to the PDA layer insulating nature. The mechanism of DA polymerization presents the sum of complex redox processes with a series of intermediates that have been synthesized during the reaction period. The chemical structure of DA and a simplified structural unit of PDA are presented in Fig. 1.3.

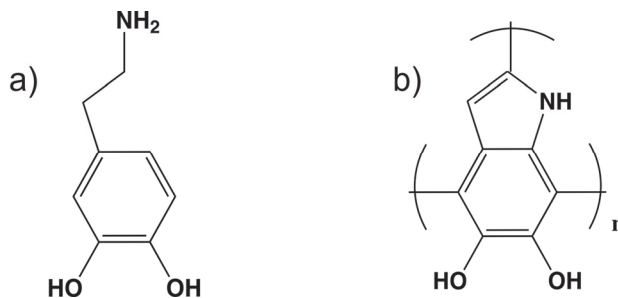


Figure 1.3. Chemical structure of DA (a) and a simplified structural unit of PDA (b).

PDA is successfully applied to prepare MIP thin films due to several attractive properties, such as availability of multiple functional groups (amino-, hydroxy-, π - π bonds), adherent nature of coatings, high hydrophilicity and high biocompatibility, compatibility with aqueous solutions, the possibility to obtain ultrathin films by the precisely controlled process [71].

Poly (*m*-phenylenediamine)

m-Phenylenediamine (*m*-PD), an organic compound classified as aromatic diamine, has attracted considerable attention in recent years due to its good water solubility, multifunctionality as well as possibility of fast and simple polymerization by multiple methods. Essentially, aromatic diamines may be considered as derivatives of the parent aniline. In particular, phenylenediamine has an additional amino group in its ortho-, para- and meta-positions. Notwithstanding the structural similarity of these three isomers, the polymerization process of each leads to different properties of the resulting products [72].

Among other isomers, polymer films from *m*-PD demonstrate remarkably high solvent resistance in organic and aqueous solutions. This particular feature is especially important in terms of MIP quality, indicating that the polymeric matrix could easily withstand both preparation and regeneration procedures. Although only limited information is available about the polymerization mechanism and the structure of PmPD, it is suggested that PmPD chains have benzenoid containing structure with secondary amine groups (Fig. 1.4) [73].

The most common methods for *m*-PD polymerization are chemical-, enzyme catalysed-, photocatalyzed-, and electrochemical oxidation. As compared to other methods, electropolymerization of *m*-PD has a number of attractive features,

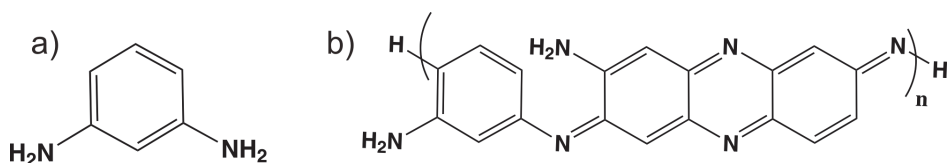


Figure 1.4. Chemical structure of *m*-PD (a) and a simplified structural unit of PmPD (b).

including direct synthesis on the surface, precise monitoring of experimental parameters and significant decrease in synthesis time along with controlled thickness. Accurate selection of the synthesis conditions results in the formation of homogeneous and dense non-conducting films.

The areas of PmPD application range from coatings for corrosion protection [74] to the preparation of nanostructures for biosensing purposes [75-77]. However, to the best of our knowledge, the utilization of PmPD as a matrix for MIP has not been reported until now.

1.4. Immunoglobulin G as a template protein

Immunoglobulins or antibodies are the type of proteins synthesized in animals as a response to the presence of a foreign item (antigens) to protect the animal from the development of infection [78]. Analysis of the presence of specific antibodies or their quantification can provide important data for diagnosis and management of a whole range of infectious, allergic and autoimmune diseases. This fact makes immunoglobulins one of the most widespread biorecognition elements used in biosensing.

The major antibody found in human serum is Immunoglobulin G (IgG). IgG is a large heterotetrameric molecule composed of two heavy and two light polypeptide chains. Geometrically, this macromolecule presents a flexible Y-shaped structure with the total molecular weight of approximately 150 kDa (Fig. 1.5). Each chain has a variable region, which supplies a function of antigen-binding, and a constant region that determines the antibody isotype. The isotype of the heavy chains arranges the functional properties of the antibody. The light chains are bound to the heavy chains by multiple non-covalent as well as disulfide bonds. The variable regions of both chains are joined together with corresponding constant regions, thus generating two identical antigen-binding sites also known as Fab fragments. These allow antibody molecules to cross-link antigens with the aim of strong and stable binding. The crystallizable fragment region or Fc fragment in the function of immune system activation is composed of the carboxy-terminal domains of the heavy chains. The places where Fab fragments are joined with Fc fragments form the flexible Hinge regions. While the overall organization of the domains is identical in all isotypes, the Fc fragment and hinge regions may vary in the antibodies of different isotypes, thus determining their functional properties [79].

Despite the numerous successful reports on imprinting of different proteins, the imprinting of IgG is quite a novel and problematic area. Only several attempts have been made to imprint IgG, including the work of Sellergren's group [16]

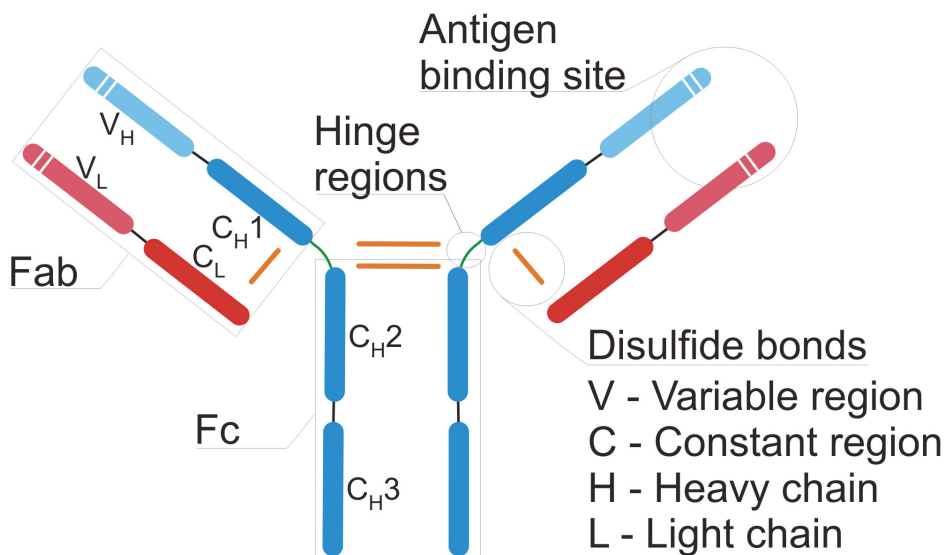


Figure 1.5. Schematic structure of IgG basic units.

and Dickert's group concept of artificial antibody replicas [80]. The main difficulties were attributed to the complex Y-shape structure and large amount of chemically identical groups.

The facts presented appeal to the elaboration of fast, simple and relevant technique for IgG imprinting. Thus, in this work IgG was used as a target protein for the imprinting strategy.

1.5. Label-free biosensor platforms

Label-free detection techniques allow the monitoring of biomolecular interactions with non-labeled analytes [81]. Generally, this method is more preferred since labeling can influence the interfacial activity of the resulting protein-dye complexes, and consequently the accuracy of measured results [22]. The use of label-free sensing platforms for integration with MIPs can provide relevant information on the binding events occurring on MIP surfaces and has to be considered in the first place in the development of protein-MIP-based biosensors. Label-free detection can be implemented with the help of various transduction mechanisms, including, but not limited to, optical, electrochemical or piezoelectric, where the biochemical interaction between an analyte and a recognition element of the sensor is recorded as a change, e.g., in refractive index (SPR sensors), impedance (electrochemical sensors) or resonance frequency (QCM sensors), respectively.

SPR is the most widely used optical system to study molecular interactions. It has an extreme sensitivity for refractive index changes near a metal film on a glass substrate (sensor surface), therefore it can monitor interactions between a receptor and a target analyte [82]. Since SPR is very efficient in detecting the interactions at very short distances from the sensor surface, the only way to

combine this type of instrument with MIPs is to modify the sensor with an ultra thin MIP film. Such thin films would be preferential for recognizing large molecules like proteins, since their mobility is highly hindered in highly cross-linked polymeric networks.

As molecular recognition is a mass exchange process, mass-sensitive acoustic wave devices, in particular the quartz crystal microbalance (QCM) and the surface acoustic wave sensor (SAW), are especially suitable in-situ techniques to study both the preparation and selectivity of MIPs. Acoustic wave devices are based on the use of piezoelectric materials to generate acoustic (mechanical) waves in order to sense various phenomena from the device's environment, which can be registered as changes in the wave properties. They can be classified based on the mode of the wave propagation as a surface acoustic wave (SAW) or a bulk acoustic wave device (BAW).

In surface acoustic wave (SAW) sensors, the acoustic wave travels on the surface of the substrate. In BAW sensors, the acoustic wave travels through the interior of the piezoelectric substrate. Examples of most frequently used BAWs are thickness shear mode (TSM) resonators or shear-horizontal acoustic plate mode (SH-APM) sensors.

1.5.1. Quartz Crystal Microbalance sensor

Quartz Crystal Microbalance (QCM) is a BAW sensor, also known as a thickness shear mode resonator, where the acoustic waves propagate in the complete piezoelectric substrate. This piezoelectric device is capable of extremely sensitive mass measurements ($\text{ng}\cdot\text{cm}^{-2}$) in both air and liquid. QCM uses thickness shear mode vibration with the vibration of the complete substrate by the application of an alternating high frequency electric field using electrode metallic layers, which are usually deposited onto both sides of the disc (Fig. 1.6).

The consequent mass change causes a change in the resonant frequency of the oscillator. The mass sensitivity arises from a dependence of the oscillation frequency on the total mass of the crystal, its electrodes, and any materials present on the electrode surface. The increased mass associated with the binding processes results in a decrease of the oscillating frequency. An increase in the fundamental frequency of the crystal and, thus, the QCM sensitivity, is limited by the thickness of the piezoelectric substrate. More sensitive QCMs involve using of extremely thin and consequently fragile substrate; thus, quartz crystals with fundamental frequencies typically between 5 and 10 MHz are commonly used in manufacturing of commercial devices [83]. In this work, quartz crystals with a fundamental frequency of 5 MHz were used. Common equipment allows device resolution down to 1 Hz on such type of QCMs. For films that are sufficiently rigid and/or thin (termed acoustically thin), a simplified conversion of the resonant frequency change into mass change described by the Sauerbray equation is defined as:

$$\Delta f = -(f_0^2 \Delta m) / N \rho = -C_f \Delta m \quad (1)$$

where Δf – resonant frequency change (Hz), f_0 – fundamental frequency of the crystal (Hz), Δm – mass change ($\text{g}\cdot\text{cm}^{-2}$), N – frequency constant for quartz ($167 \text{ kHz}\cdot\text{cm}$), ρ – density of quartz ($2.65 \text{ g}\cdot\text{cm}^{-3}$), C_f – sensitivity factor (for 5 MHz quartz crystal, $56.6 \text{ Hz}\cdot\mu\text{g}^{-1}\cdot\text{cm}^2$). The equation is derived by considering the coupled mass as though it were an extension of the thickness of the underlying quartz and therefore, the mass to frequency correlation is largely independent of electrode geometry. As a result, mass can be determined without calibration, making the set-up desirable from a cost and time investment standpoint [84].

Due to its high mass sensitivity, QCM has been known as a valuable tool for real-time in-situ monitoring of receptor-analyte interactions [85]. The particular advantages of QCM are: rapid and stable measurements, possibility of integration with various layers and combination with different surface-analytical instruments. As an example, the electrochemical QCM (EQCM) can be used to investigate electropolymerization processes or redox behaviour of electroactive polymers [84, 86] while QCM combined with flow injection analysis (QCM-FIA) can be applied as a biosensor [87]. In view of this, QCM is widely applied for

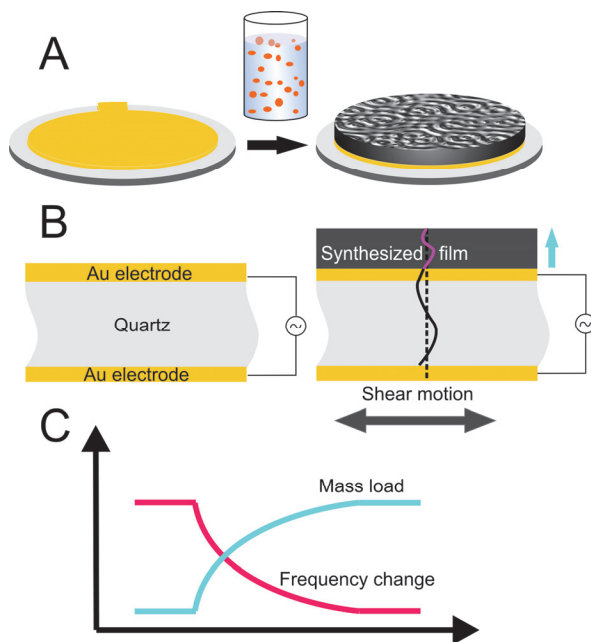


Figure 1.6. Schematic of the QCM operation principle. A) A typical view of a bare (left) and a film-loaded (right) QCM sensor. The film is shown intentionally thicker for clarity reasons. B) Schematic side view of the QCM sensor. Alternating electric field imposed on the electrodes causes oscillation of the quartz, where top and bottom surface move in opposite directions. C) Frequency change is a typical response of a QCM sensor upon mass load on its electrode. The mass load is directly proportional to the resonant frequency decrease.

biosensing purposes, including such areas as protein adsorption [88], antibody-antigen binding [89], various biomolecules immobilization and investigation of their properties [90, 91].

In this work, the combination of QCM with electrochemistry (EQCM) was used to follow electroactive monomers redox behaviour as well as to control precisely synthesized layer thickness during polymerization. Moreover, QCM sensor was integrated with the method of Flow Injection Analysis (FIA) for on-line monitoring of the IgG binding events on the IgG-MIP.

1.5.2. Surface Acoustic Wave sensor

Surface acoustic wave (SAW) sensors are a class of sensing platforms that rely on the modulation of surface acoustic waves to sense a physical phenomenon. SAW sensors can be classified by the propagation mode of the acoustic wave into Rayleigh-SAW sensors and shear-horizontal SAW (SH-SAW) sensors.

Rayleigh SAW sensors have a vertical shear component that increases sensitivity to the device's external environment, however, it undergoes severe damping when displaced in a liquid medium, thus narrowing the use of Rayleigh SAW devices to gas and vacuum environments [23].

SH-SAW sensors use acoustic waves with shear horizontal component that have a displacement, which is perpendicular to the wave propagation direction and parallel to the substrate surface.

Although SH-SAW sensors already have comparatively low attenuation values when operated in liquids, another type of SH-SAW sensors benefits from the so-called Love wave effect. In these sensors, acoustic energy is concentrated exclusively within the guiding layer of a foreign material deposited on top of the substrate and the acoustic losses into the bulk of the substrate and into the liquid above the sensor surface are minimized. Therefore, these so-called Love-wave SAW sensors were found to be even more suitable for operation in contact with liquid [92]. Currently, Love-wave SAW sensors are the most sensitive acoustic sensors [23]. The Love-wave SAW sensor (hereafter simply referred to as SAW sensor) was used in this work.

As compared to the traditional QCMs, in Love-wave SAW sensors, the surface acoustic waves propagate only in a guiding layer at the surface of the substrate, thus excluding the influence of the substrate thickness on the behaviour

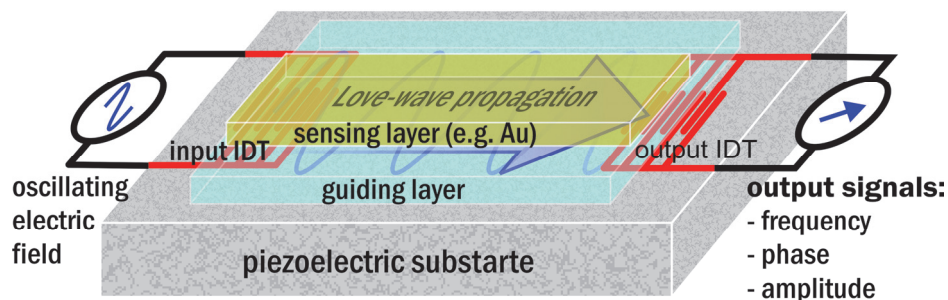


Figure 1.7. A schematic drawing of a Love-wave SAW sensor.

of the sensor. Being an advanced device with higher operating frequencies, SAW sensors surpass QCMs in sensitivity to mass changes, density, viscosity and electrical conductivity as well as offer significant advantages regarding the damping in liquids [93].

A typical Love-wave SAW sensor consists of three basic components: a piezoelectric substrate, interdigital transducers (IDTs) and an area of acoustic wave propagation (Fig. 1.7). The substrate-deforming mechanical waves generated in the input IDT by applying the oscillating electrical field are travelling across the area of propagation and thus their velocity and/or amplitude are altered by a contact with any medium associated with the surface. By reaching the output IDT, the wave is converted back into an electrical signal. Input and output electrical signals are then translated to the resulting frequency and amplitude changes. Using both the phase shift and the amplitude shift of the surface acoustic wave allows discrimination of changes in the corresponding mass and mechanical properties from viscoelastic effects [24].

Although SPR and QCM remain to be widely used sensor platforms for the on-line label-free detection of binding events in the aqueous media, Love-wave SAW may provide advances in the fabrication of MIP-based sensors over those platforms. Love-wave SAW offers about an order of magnitude higher mass resolution than QCMs while keeping low sensor cost. In addition, it is fully compatible with large-scale fabrication and multiplexing technologies [23, 24]. As compared to SPR, SAW technology is not limited to detecting only mass loading onto the surface, but also useful in the following structural insights of sensing layers through the use of the dissipation factor of the acoustic wave propagating along the sensor surface.

1.6. Characterization of MIP recognition properties

A systematic approach allowing assessment of the quality of the synthesized MIPs is crucial to describe the resulting MIPs as well as to understand the factors improving their performance. The following sections summarize the criteria and the evaluation methods associated.

1.6.1. Binding kinetics

Kinetic analysis is based on the investigation of receptor (MIP) and ligand (analyte molecules) interaction, in which complexes are formed by reversible association and dissociation of molecules. Thus, kinetic measurements provide a way to determine both kinetic (e.g., rate constant) and equilibrium (e.g., K_D) constants of the binding process between MIP and analyte molecules [94].

Monitoring the MIP-analyte binding interactions and analyzing them as a function of time vs. response signal provide data for subsequent fitting to a mathematical model assumed to describe the interactions (Fig. 1.8). The analyte injection period or so called association phase consists of both association and dissociation processes between MIP and analyte molecules, while the dissociation phase is related only to the dissociation of analyte from the MIP surface. By fitting the association phase to an appropriate kinetic model, the rate

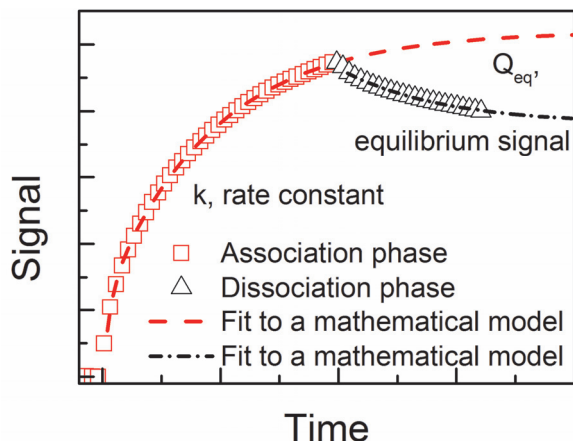


Figure 1.8. The principle of binding kinetics analysis.

constant of the process (k), and the response upon analyte rebinding at equilibrium (Q_{eq}) can be obtained. Q_{eq} values can be subsequently used in plotting the adsorption isotherm (Section 1.6.2).

The kinetic evaluation of the MIP rebinding behavior is especially important for using MIPs in time-dependent applications such as MIP-based sensors [95]. In addition, the equilibrium dissociation constant or K_D , which can be determined from kinetic measurements, is commonly used to describe the affinity between a ligand and a receptor, i.e., how tightly analyte molecules bind to a particular MIP. A small K_D means that the MIP has a high affinity for analyte molecules. K_D is measured in the dimensions of concentration, and equals the concentration of ligand at which half of the receptor binding sites are occupied. In this work, K_D was used to assess the affinity of the prepared IgG-MIP films to the template protein.

Binding kinetics models

The first- and second-order rate models have been widely used to describe the adsorption data obtained under non-equilibrium conditions [96, 97]. The pseudo-first and second order rate equations (2) and (3) in the integrated form are expressed as follows:

$$Q = Q_{eq}[1 - e^{-k_1 t}] \quad (2)$$

$$Q = [Q_{eq}^2 k_2 t] / [1 + Q_{eq} k_2 t] \quad (3)$$

where Q is the response upon analyte rebinding at time t , Q_{eq} is its value at equilibrium, k_1 is a pseudo-first rate constant, k_2 is a pseudo-second order rate constant. A detailed analysis of these rate equations was performed by S. Azizian [98].

According to the first-order kinetics model, the analyte binds only to a single active site on the MIP surface and the interactions of analyte and MIP are of physical nature; the rate of occupation of adsorption sites is proportional to the

number of unoccupied sites [99]. The pseudo-second order model recognizes that the rate-limiting step is chemisorption, involving sharing or exchange of electrons between MIP and analyte and the rate of occupation of adsorption sites is proportional to the square of the number of unoccupied sites [100]. Both models have been successfully applied to describe the adsorption kinetics on the MIP surfaces [101-103].

1.6.2. Adsorption isotherms

The relation between the volume concentration of an analyte and its concentration on the surface of MIP when binding is performed at a constant temperature can be represented by an adsorption isotherm. A mathematical analysis of the adsorption isotherm with different adsorption models, e.g. Langmuir, Langmuir-Freundlich, provides insight into the nature of the binding process.

Adsorption models

The Langmuir isotherm derived by I. Langmuir in 1918 is the most widely used semi-empirical isotherm model with a kinetic basis that is able to fit various adsorption data. The main assumptions used in this model are: equivalence of adsorption sites (accommodation of one molecule per one site), homogeneity of the surface and non-interacting with each other analyte molecules, absence of phase transitions as well as formation of a single monolayer without adsorption to other analyte molecules. However, all these assumptions are rarely observed in practice, which leads to the necessity of the model appropriate modifications [104]. The Langmuir isotherm is defined as:

$$Q = Q_{\max}C/(C+K_D) \quad (4)$$

where C is the concentration of the analyte in the solution, K_D is the equilibrium dissociation constant and Q and Q_{\max} are the fractions of bound analyte and its saturation value, respectively.

Preparation of MIP introduces different variations of adsorption sites (imprinted cavities) [105]. Such models as Bi-Langmuir (the sum of two Langmuir isotherms) can take into account a situation when two types of adsorption sites are presented on the surface [99] (Table 1.1). Since MIPs are usually described as materials with a higher degree of heterogeneity, Freundlich and combined Langmuir-Freundlich models have been applied to take into account such issues as surface roughness, heterogeneity, and analyte-analyte interactions [106, 107]. Langmuir-Freundlich isotherm is defined as:

$$Q = Q_{\max}C^m/(C^m+K_D) \quad (5)$$

where C is the concentration of the analyte in the solution, K_D is the equilibrium dissociation constant and Q and Q_{\max} are the fraction of the bound analyte and its saturation value, and m is the surface heterogeneity index.

Imprinting factor

Imprinting factor (IF) indicates the capacity of a MIP towards an analyte molecule, but normalized to that of NIP. Thus, when a MIP and the respective NIP surfaces are completely saturated and found at equilibrium conditions, IF can be calculated according to the following equation:

$$IF = Q_{\max}(\text{MIP})/Q_{\max}(\text{NIP}) \quad (6)$$

where $Q_{\max}(\text{MIP})$ is the maximum adsorption capacity of MIP and $Q_{\max}(\text{NIP})$ is the maximum adsorption capacity of NIP. Sometimes, when the complete saturation is rather difficult to achieve, it is acceptable to calculate IF at the equilibrium achieved at a particular concentration:

$$IF = Q_{\text{eq}}(\text{MIP})/Q_{\text{eq}}(\text{NIP}) \quad (7)$$

where $Q_{\text{eq}}(\text{MIP})$ is the response value upon analyte binding at equilibrium onto MIP and $Q_{\text{eq}}(\text{NIP})$ is the response value upon analyte binding at equilibrium onto NIP.

Table 1.1 Langmuir and Freundlich isotherms and their several variations used to describe the behaviour of MIP materials

Isotherm model	Equation
Langmuir isotherm	$Q = (Q_{\max}C)/(C+K_D)$
Freundlich isotherm	$Q = \alpha C^m$
Langmuir-Freundlich isotherm	$Q = (Q_{\max}C^m)/(C^m+K_D)$
Bi-Langmuir isotherm	$Q = Q_1 + Q_2$, where $Q_1 = (Q_{\max 1}C)/(C+K_{D1})$; $Q_2 = (Q_{\max 2}C)/(C+K_{D2})$

Binding selectivity

Binding selectivity is the ability of a MIP material to discriminate between the template molecule and other analyte molecules with different or similar chemical structures (i.e., structural analogs). Selectivity factor S, which is the ratio of IF of an interfering substance to that toward the template molecule, can be used to assess the cross-reactivity of MIP:

$$S = IF_{(\text{interf})}/IF_{(\text{template})} \quad (8)$$

where $IF_{(\text{template})}$ is the imprinting factor of a MIP for the template and $IF_{(\text{interf})}$ is the imprinting factor of MIP for interfering analyte. $IF_{(\text{interf})}$ values for interfering analytes can be calculated according to Eq. (6), where the values of Q_{eq} upon interfering analytes adsorption onto MIP and NIP are determined from the kinetics data using the appropriate binding kinetic model (Eqs. (2)-(3)).

1.7. Summary of the literature review and objectives of the study

Molecular imprinting technique, which can be defined as the process of template-induced formation of specific molecular recognition sites in a polymer matrix, has become one of the state-of-the-art techniques to generate MIP-based synthetic receptors. The main benefits of MIPs are related to their synthetic nature, i.e., excellent chemical and thermal stability associated with reproducible, cost-effective fabrication. Thus, MIP-based receptors have been shown to be promising alternatives to natural biological receptors (e.g., enzymes, DNA, antibodies) in biosensing applications, providing more stable and low-cost recognition elements. However, there remain many unsolved issues in the development of MIP-based biosensors, including the limitations in macromolecular imprinting and robust interfacing of MIP with a sensor transducer.

The preparation of a polymer film with macromolecular imprints capable of selective rebinding of macromolecules, e.g. proteins (protein-MIP film) by combining the surface imprinting method and the electropolymerization technique seems to be a prospective solution to address the above-mentioned issues.

The use of label-free sensing platforms for integration with MIPs can provide relevant information on binding events on MIP surfaces and has to be considered in the first place in developing protein-MIP-based biosensors. Among the label-free sensor technique acoustic wave devices, such as QCM and SAW, are cost-effective sensor platforms capable of monitoring molecular binding events in thin films in real-time and label-free manner, and thus are especially suitable for the study of preparation and selectivity of MIPs.

Since IgG is widely used for diagnostic purposes, the realization of a MIP material capable of highly selective capture of IgG, but interfaced with a label-free platform, allows us to follow in real time the respective molecular binding events and thus, is of great importance in immunological research and clinical diagnostics.

The overall objective of this thesis was to explore molecular surface imprinting of the synthetic polymer prepared by a controlled electropolymerization, but integrated with a label-free sensor platform for real-time detection of macromolecules such as proteins (IgG) to create a selective, robust and multiplexed MIP-based biosensor.

The aims of this doctoral thesis were as follows:

- To develop a reliable strategy for immobilization of IgG molecules on a sensing surface of QCM and SAW;
- To develop an electrosynthesis method allowing direct fabrication of the IgG-MIP films on the sensing surface of QCM and SAW;
- To validate the recognition capability and selectivity of the prepared IgG-MIPs through the analysis of the responses of the IgG-MIP modified QCM and SAW sensors upon interaction with target and interfering proteins;
- To understand the factors improving the performance of the IgG-MIPs in terms of their recognition capability towards IgG.

2. EXPERIMENTAL PART

2.1. A macromolecular imprinting approach for the protein-MIP film fabrication

In this thesis, a method for the preparation of surface imprinted protein-MIP films directly on a sensor surface was developed. The method includes the sequence of (a) the macromolecular template immobilization, (b) electrochemical deposition of a nanometer thin polymer film, and (c) template removal procedures resulting in the complementary binding sites confined in the surface of the polymer film (Fig. 2.1). Every stage of the sequence is described in detail in Sections 2.2 -2.4.

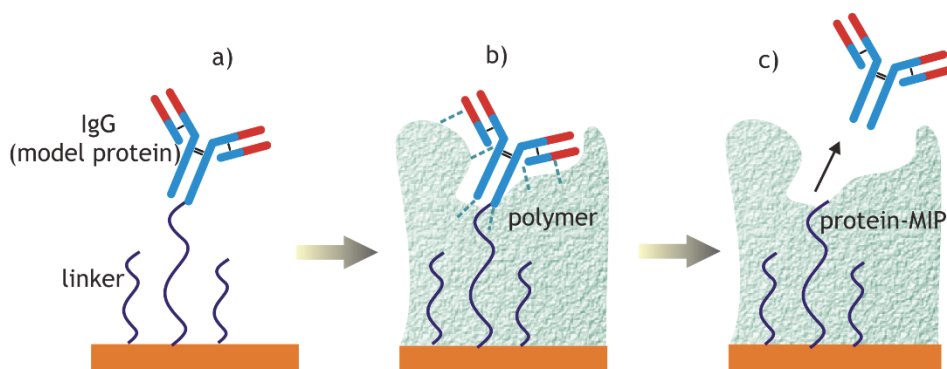


Figure 2.1. A macromolecular imprinting approach for the protein-MIP film fabrication: (a) immobilization of a protein via a linker system to a gold surface; (b) electrodeposition of a polymer film; (c) washing out the protein.

2.2. Protein immobilization on a gold electrode surface

An attempt was made to immobilize macromolecules by two principal strategies. In the first strategy, a specially synthesized peptide modified with cysteine (Cys-peptide) was immobilized on the para-maleimidophenyl grafted surfaces by cross-linking between the maleimide groups and the sulfhydryl group of the Cys residues. Accordingly, the Cys-peptide was supposed to work as an antigen able to bind specifically an antibody served as a macromolecular template. The other strategy relied on the immobilization of the macromolecular template on a surface via a DTSSP cleavable linker, allowing an easy detaching of the template afterwards. Each immobilization strategy is described in detail in Sections 2.2.1–2.2.2.

2.2.1. Surface functionalization via the *p*-MP/Cys-peptide linker system

p-MP functional groups were electrochemically grafted on gold and silicon surfaces from solutions of the *p*-maleimidophenyl diazonium tetrafluoroborate. A specially synthesized peptide modified with cysteine (Cys-peptide) was then immobilized on the *p*-MP grafted substrates by cross-linking between the maleimide groups and the sulfhydryl group of the cysteine residues. Accordingly, the Cys-peptide worked as an antigen that was able to bind specifically the target antibody (anti-GST antibody), while it was non-sensitive to a negative contrast antibody (i.e., anti-Flag b) (Fig. 2.2).

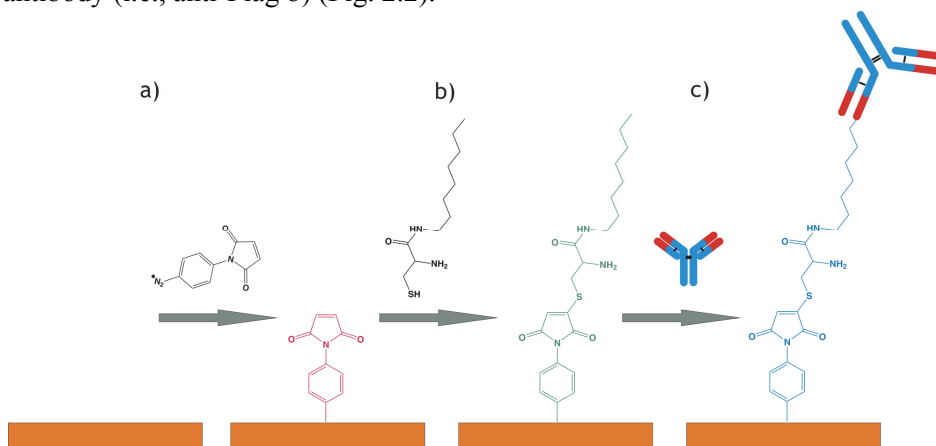


Figure 2.2. A strategy for protein immobilization via the *p*-MP/Cys-peptide linker system: (a) *p*-MP layer formation on a gold electrode; (b) attachment of Cys-peptide; (c) protein immobilization.

2.2.2. Surface functionalization via 4-aminophenol/DTSSP linker system

The gold electrode surface was modified with amino-groups by the formation of a self-assembled monolayer of 4-ATP. Then, the homobifunctional crosslinker with a cleavable disulfide bond and a suitable spacer unit (i.e. DTSSP) was attached to the amino-modified surface. The template protein (IgG) was immobilized by the formation of a covalent amide bond between the succinimide group of DTSSP and the amino-group of lysine residues of IgG (Fig. 2.3).

2.3. Polymer matrix formation by electropolymerization

Polymer matrix was formed by the electrochemical polymerization of *m*-PD or DA around the immobilized IgG. The in-situ polymerization of *m*-PD and DA was carried out in specially designed electrochemical cells. The electrochemical cells accommodated three electrodes, i.e., the gold electrode of QCM or the sensing surface of SAW chip as a working electrode, a spiral shaped platinum wire or a rectangular shaped platinum plate as a counter electrode, and a

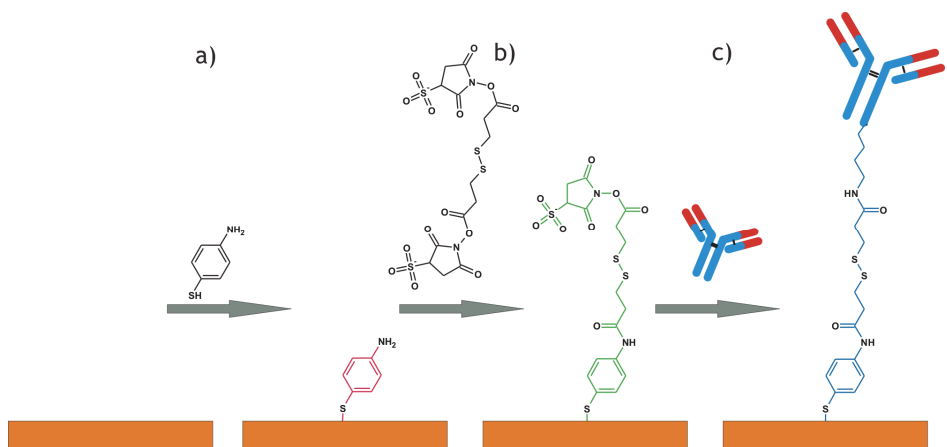


Figure 2.3. A strategy for protein immobilization via 4-aminophenol/DTSSP linker system: (a) 4-ATP self-assembled monolayer formation on a gold electrode; (b) attachment of a DTSSP cleavable linker; (c) protein covalent immobilization.

Ag/AgCl/ KCl_{Sat}. as a reference electrode, all connected to an electrochemical workstation (Reference 600TM, Gamry Instruments, Inc., USA).

2.3.1. Electrodeposition of PDA films

DA electrochemical polymerization on the IgG-modified electrode was monitored by the Electrochemical Quartz Crystal Microbalance (EQCM). EQCM measurements were performed using the QCM100 system (Stanford Research Systems, Inc., Sunnyvale, CA, USA) connected to an electrochemical workstation (Reference 600TM, Gamry Instruments, Inc., USA) and PM 6680B counter (Fluke Corporation), as described in [38]. Electropolymerization was carried out on the IgG-modified QCM sensors by cycling the potential between -0.45 and $+0.55$ V at a scan rate of $50 \text{ mV}\cdot\text{s}^{-1}$ in PBS buffer solution containing 5 mM of DA until the resonant frequency dropped to a designated value.

Thickness of the deposited PDA film was believed to be uniform and estimated by dividing the corresponding mass provided by the Sauerbrey equation (Section 1.5.1, Eq. (1)) and the polymer's density. After polymer film electrochemical deposition, the electrode was rinsed with distilled water and dried in a nitrogen stream. When not in use, the IgG-PDA modified QCM sensors were stored under nitrogen atmosphere in the refrigerator.

2.3.2. Electrodeposition of PmPD films

The protein-modified SAW chip was placed into the 5-mL electrochemical cell designed to expose the modified sensing surface to the synthesis solution. *m*-PD electropolymerization on the IgG-modified surface was carried out in the PBS buffer solution containing 10 mM of *m*-PD by imposing the constant potential of 0.9 V to the working electrode.

To yield the polymeric structures of a defined thickness, their growth was controlled by the charge passed through the working electrode. Thicknesses were determined by a spectroscopic ellipsometer (SE 850 DUV, Sentech Instruments GmbH, Berlin, Germany). Ellipsometric parameters ψ and Δ were measured from three spots for each sample in ambient air, confining to the wavelength range between 380 and 850 nm at the angle of incidence of 70°. The spectra were fitted (SpectraRay 3 software) with the optical model containing a one-layer Cauchy layer on top of gold and the thicknesses were determined.

2.4. IgG removal from polymeric matrix

IgG was removed from polymeric matrix of the electrodeposited PDA film in order to form the IgG-MIP films. For this purpose, the IgG-PDA modified electrode was immersed in 0.1 M solution of 2-mercaptoethanol in ethanol, and heated in a water bath up to 100 °C. The reaction was maintained under stirring for 15 minutes. After rinsing with ethanol and distilled water, the electrode was immersed into 3M NaCl aqueous solution containing 0.1% SDS and the same parameters of heating were applied. The washing out procedure of protein was maintained under stirring for 15 minutes, repeated twice. Finally, the resulting IgG-MIP sensor was washed thoroughly with distilled water and subjected to protein rebinding studies. In addition to the procedure implemented with PDA matrix, the SAW sensor with a synthesized PmPD film was additionally immersed into DMSO for 30 minutes in order to disrupt multiple hydrogen bonds.

To compare the IgG-MIPs in terms of their affinity to IgG molecule, a non-imprinted polymer (NIP) structure was also created. The NIP was formed under the same conditions as the IgG-MIP, excluding the protein removal stage. In this case, polymer film still contains the target protein, but has no cavities on its surface.

2.5. Characterization of the IgG-MIP film

2.5.1. Rebinding study by QCM

IgG rebinding on the prepared IgG-MIP films modified QCM sensors was studied by Quartz Crystal Microbalance-Flow Injection Analysis (QCM-FIA) combined technique, allowing real-time monitoring of molecular interactions on the surface of the QCM sensor. The analysis was carried out in a QCM-FIA system comprising two programmable precision syringe pumps (Cavro® XLP 6000, Tecan Nordic AB, Mölndal, Sweden), a motorized six-way port injection valve (C22-3186EH, VICI® Valco Instruments Company Inc., USA) controlled by a microelectric actuator and a small volume (150 μ l) axial flow cell attached to the QCM sensor holder (Stanford Research Systems, Inc.) (Fig 2.4). All elements of the system were connected to a PC and controlled by software written in Labview. A constant flow of degassed PBS buffer solution (pH=7.4) flew over the sensor at a flow rate of 12 μ l·min⁻¹ until a constant baseline of QCM sensor resonance frequency was reached. Subsequently, various concentrations of analyte samples (IgG solution in PBS buffer) were injected into the flow stream

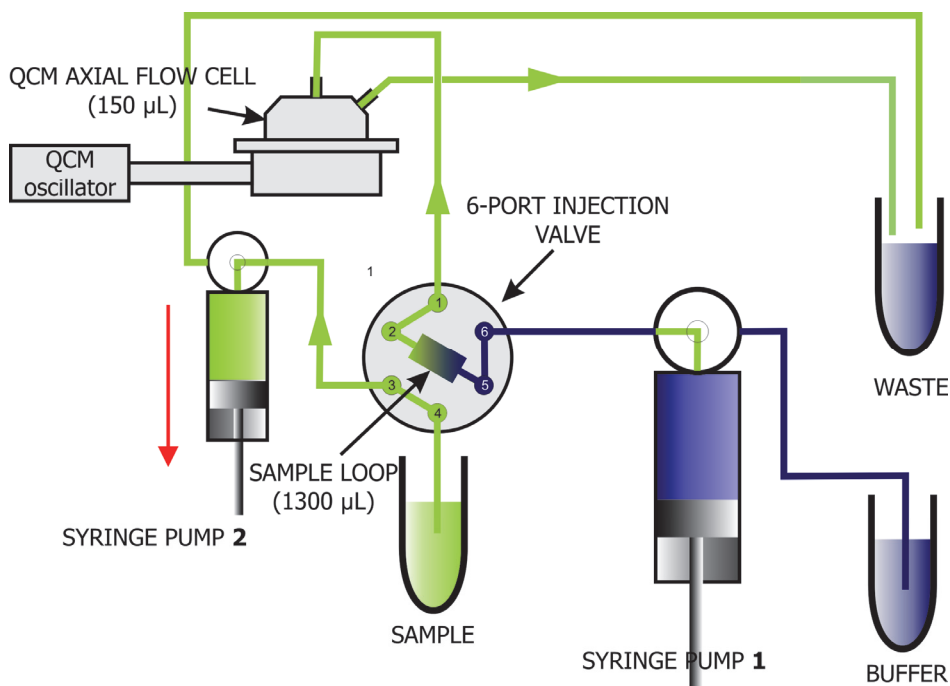


Figure 2.4. Schematic diagram of the FIA-QCM system consisting of two programmable precision syringe pumps, a motorized six-way port injection valve for switching between the solutions and an axial flow cell attached to the QCM holder.

via an injection loop (250 µL), allowing interaction with the IgG-MIP or NIP modified sensor for 2500 s.

2.5.2. Rebinding study by SAW

Real-time rebinding of IgG on the prepared IgG-MIP-modified SAW chips was performed using a SAW biosensor system (SamX®, NanoTemper Technologies GmbH, München, Germany) capable of handling two SAW chips having four separate sensor elements each (Fig. 2.5). The main components of the fluidic system were: autosampler, syringe pump, bottle holder with fluidic interconnects, internal valves, and two fluidic cells with the volume of 2.3 µl per sensor element. The internal valves of the system provided an option to deliver analyte solutions to the modified sensor elements either individually or in serial fashion.

The sensor elements were preconditioned at constant flow ($25 \mu\text{l}\cdot\text{min}^{-1}$) of the degassed PBS buffer solution (pH=7.4) until a constant baseline was reached. Subsequently, various concentrations (from 0.4 nM to 53 nM) of analytes prepared from the same buffer were injected into the flow stream via an autosampler using a 430 µL injection loop and allowed interaction with the IgG-MIP or NIP modified SAW chip.

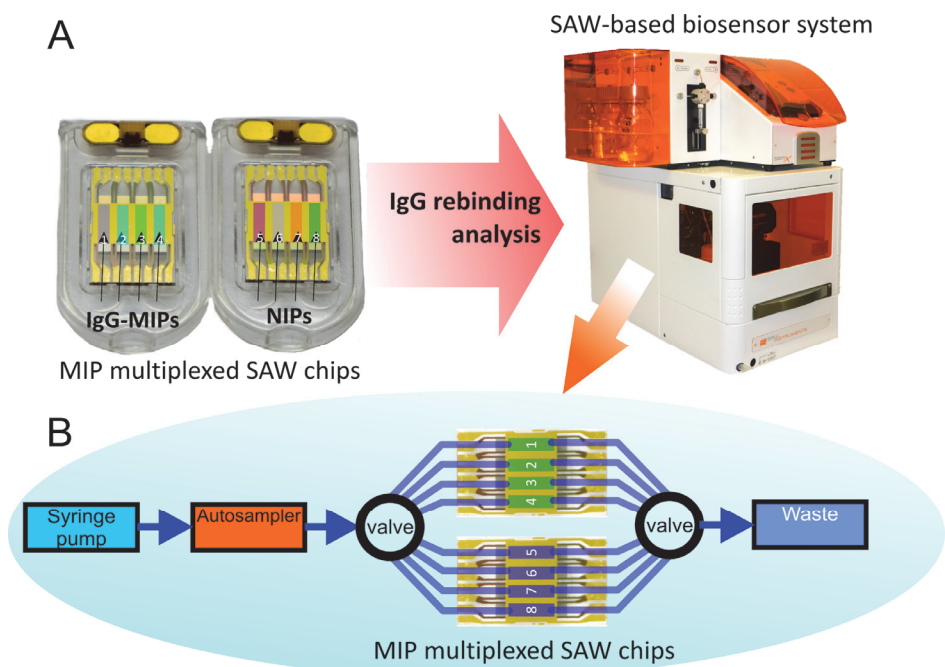


Figure 2.5. (A) A layout of the IgG-MIP/NIP films on the SAW chips and the SAW biosensor system. (B) The flow paths over the SAW chips in the sensor system.

The SAW sensor system is capable of both phase and amplitude signal measurement, reflecting changes in mass and in viscoelastic properties of a material at the sensor surface, respectively. In this work, phase-shift response was analyzed to evaluate rebinding properties of the IgG-MIPs.

Data were analyzed using Origin 9.1 (Northampton, MA). Raw data were exported, cut and analyzed by individual fits using two kinetic models for sorption from a liquid solution represented by the first- and second-order equations, as will be described in the Results and Discussion section. Affinity constants and K_D values were determined from the plot of the equilibrium signal (Q_{eq}) versus analyte concentration using the Langmuir-Freundlich equation for the data fitting. The film-modified chips were regenerated by their immersion in the 3M NaCl aqueous solution for 2 hours with stirring and heating up to 100 °C.

3. RESULTS AND DISCUSSION

3.1. Immobilization of IgG on a gold surface

3.1.1. Immobilization through the *p*-MP/Cys-peptide linker system

The first elaborated strategy for antibody immobilization involved electrochemical grafting of the *p*-MP layer with subsequent attachment of Cys-peptide. The electrochemical deposition of maleimidobenzene on the Au surface led to an ultra thin layer with a thickness of about two monolayers after five potential scans. *p*-MP is a very favourable reactive group in the cross-linking process and reacts specifically with sulfhydryl (–HS) groups in aqueous solution at a pH value between 6.5 and 7.5 to form a stable and non-reversible thioether linkage. HS-groups could be introduced into a chosen target peptide (antigen) by chemical modification at its N-terminus with cysteine, so that the obtained Cys-peptide could be covalently immobilized on a maleimide-modified surface by cross-linking (Article I, Section 2).

Since the Cys-peptide works as a specific epitope to the target anti-GST antibody, the above-mentioned Cys-peptide modified surface was investigated for its biosensing capabilities with respect to the selective antibody-antigen interaction. The performance evaluation with the QCM-FIA technique demonstrated the preferential binding of a specific anti-GST IgG on the Cys-peptide modified surface rather than a non-specific (anti-flag b), respectively, thus indicating the potential analytical efficiency of such Cys-peptide-modified surfaces for the development of biochemical sensors feasible for label-free detection in antigen-antibody immunoassays. However, further application of that immobilization approach for the development of an antibody-MIP sensor encountered several issues associated with antibody conformational changes during immunoreaction with epitope, which, as compared to a non-coupled template, may give a different shape and arrangement of functional groups in the prepared imprints. Moreover, as shown in Fig. 3.1, insulating nature of the chosen *p*-MP monolayer showed that it is impossible to form an appropriate polymer matrix by the electropolymerization method.

3.1.2. Immobilization via 4-aminothiophenol/DTSSP

To address the drawbacks of the first method, an alternative strategy with an antibody covalent immobilization principle was proposed. This strategy is based on 4-aminothiophenol (4-ATP), a small aromatic thiol derivative that is able to form stable self-assembled monolayers with available amino-groups on gold surface. The terminal function of the amino-group has been employed for the covalent attachment of different substances including DNA [108]; peptide [109] and IgG [110]. Then, a homobifunctional crosslinker with a cleavable disulfide bond and a suitable spacer unit (i.e. DTSSP) was covalently attached to the amino-modified surface. DTSSP or 3,3'-Dithiobis(sulfosuccinimidylpropionate) is a water-soluble crosslinker that contains amine-reactive sulfo-NHS ester ends around an 8-atom spacer arm, with disulfide bond in the center that can be readily

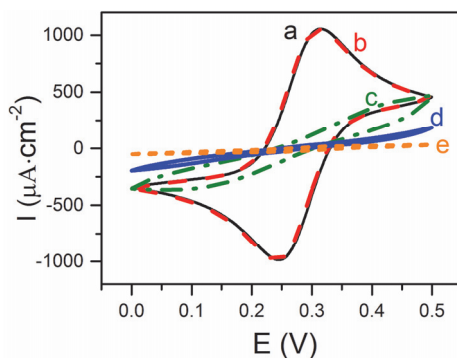


Figure 3.1. Cyclic voltammograms of a gold electrode: bare gold (a); 4-ATP coated (b); Au/4-ATP/DTSSP coated (c); Au/4-ATP/DTSSP/IgG coated (d); *p*-MP coated (e) in 1M KCl aqueous solution containing 4 mM $K_3[Fe(CN)_6]/K_4[Fe(CN)_6]$, scan rate $50\text{ mV}\cdot\text{s}^{-1}$.

cleaved with such reducing agents as Mercaptoethanol. Finally, the target protein - human IgG was immobilized on the surface by the formation of a covalent amide bond between the succinimide group of DTSSP and the amino-group of lysine residues of IgG (Article II). According to the structure of IgG taken from Protein Data Bank (PDB), the highest amount of steric accessible lysine groups is concentrated in the Fc fragment, thus suggesting partially oriented coupling with the DTSSP linker.

Fig. 3.1 compares the insulating properties of *p*-MP vs. 4-ATP. It can be seen that the bare Au electrode shows a reversible peak for the redox couple, indicating that the electron transfer reaction is diffusion-controlled. The reversibility of the reaction at Au/4-ATP is almost the same as that at the bare electrode, indicating that the 4-ATP monolayer exhibits rather poor blocking ability. This could be explained by the chemical properties of the 4-ATP monolayer as well as existence of pinholes and defects allowing application of further electropolymerization of the selected monomer even after final attachment of IgG. In the case of the Au/*p*-MP surface, no well-defined current peaks were observed on the voltammogram, thus composing a significant barrier to the charge-transfer reaction involving the redox couple due to the surface blocking and the insulating layer formation (Fig. 3.1e).

Thus, the IgG covalent immobilization via the DTSSP cleavable crosslinker was chosen for further formation of the IgG-MIPs discussed in Section 3.2.

3.2. Fabrication of the IgG-MIP films

The IgG-MIP was generated by the highly controlled electrodeposition of a polymer film onto a gold electrode preliminarily modified with the IgG via the DTSSP crosslinker. It is expected that the multiple non-covalent interactions (hydrogen bond, van der Waals forces, electrostatic and hydrophobic interactions) between chosen polymer matrices and the IgG molecule ensure the formation of complementary cavities in the prepared IgG-MIP films. Subsequent

cleavage of this linker and removal of the protein resulted in the formation of complementary binding sites on the surface of the polymer film.

For the surface imprinting strategy used in this study, the deposition of a polymer film with an appropriate thickness is one of the most important tasks in order to eliminate the complete entrapment of IgG molecules in the polymeric matrix and produce the IgG-MIP film with specific binding sites located on the surface. To evaluate the appropriate thickness of the electrodeposited polymer layer, the length of the immobilized structure- 4-ATP/DTSSP/IgG - was theoretically estimated using geometric analysis by RasMol software (Article II, Fig. 1). The theoretically estimated height of the whole immobilized structure can vary from approx. 10.5 to 20 nm. As a result, the thickness of the electrodeposited polymer film can be chosen proceeding from an assumption of this structure dimensions. Thus, in this particular work, to evaluate the varying extent of polymer coverage on the IgG-modified surface, the polymer films with thicknesses ranging from approx. 4 to 27 nm were applied.

3.2.1. Formation of the polymer matrix by electropolymerization

Electrosynthesized polymers, PDA and PmPD, were chosen for polymeric matrix formation to obtain the IgG-MIP films on QCM and SAW sensor surfaces, respectively (Article II and III).

Due to the insulating nature of PDA and PmPD layers, their electrochemical growth has the limitation for maximum thickness achievable. In order to obtain appropriate PDA film thickness, two electropolymerization techniques, chronoamperometry and cyclic voltammetry, were studied. It was observed that PDA film growth is non-linear, characterized by a higher thickness increase at the beginning of the process and its gradual slowing-down until a constant thickness value is reached, indicating self-limiting polymerization. As can be seen from Fig. 3.2 (a and b), chronoamperometry at 0.9 V resulted in the maximal polymer thickness of 8 nm, which does not comply with the estimation theoretically made for the optimal polymer thickness. Cyclic voltammetry with the potential range from -0.45 to + 0.55 V allowed us to obtain the PDA thickness of ca 22 nm. Thus, cyclic voltammetry was applied for PDA film electrodeposition in order to prepare the IgG-MIP on QCM sensor surface.

The PmPD film was formed on the IgG modified SAW sensor surface by chronoamperometry at 0.9 V. This polymerization method allowed us to synthesize PmPD films in a wide thickness range up to one hundred nm, providing extremely fast synthesis as compared to an analogous procedure with PDA. To prepare the IgG-MIP, the PmPD films with thicknesses in the range of 6 nm and 27 nm were synthesized on the IgG-modified SAW chips.

The clear advantage of using PmPD for the IgG-MIP film synthesis is the faster electropolymerization of *m*-PD over that of DA. Consequently, a lower exposure of surface-immobilized IgG to the synthesis solution and to the applied potential significantly reduces the possibility of conformational changes of IgG.

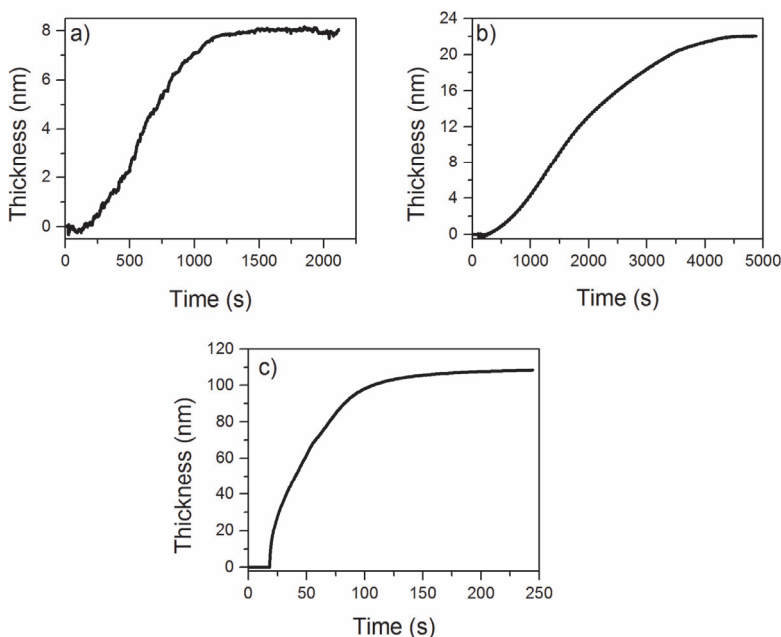


Figure 3.2. The time dependence of the polymer thickness deposited on the IgG-modified gold electrode of the QCM sensor during: (a) electropolymerization by chronoamperometry at 0.9 V in the PBS buffer solution containing 5 mM of DA; (b) electropolymerization by potential cycling between -0.45 and $+0.55$ V at a scan rate of $50 \text{ mV}\cdot\text{s}^{-1}$ in PBS buffer solution containing 5 mM of DA; (c) electropolymerization by chronoamperometry at 0.9 V in the PBS buffer solution containing 10 mM of *m-pD*.

3.2.2. Removal of IgG from the polymeric matrix

IgG was removed from the polymeric matrix of the electrodeposited PDA and PmPD films to form the IgG-MIP films. The washing out procedure was elaborated taking into account the types of possible interactions between the polymer and the IgG. The procedure of IgG removal from the polymer matrix included mercaptoethanolic treatment at approximately $100 \text{ }^\circ\text{C}$ to disrupt the disulfide bond of the DTSSP linker as well as treatment with 3M NaCl solution and DMSO for non-covalent bonds disruption. Protein denaturation has also high probability of occurrence at such washing conditions.

In order to evaluate the influence of the washing out procedure on the stability of polymeric films, the cyclic voltammograms of the polymer coated gold electrode in the presence of $\text{K}_3[\text{Fe}(\text{CN})_6]/\text{K}_4[\text{Fe}(\text{CN})_6]$ redox probe before and after treatment were recorded and compared with cyclic voltammograms of a bare gold electrode. Fig. 3.3 demonstrates that a pair of $\text{K}_3[\text{Fe}(\text{CN})_6]/\text{K}_4[\text{Fe}(\text{CN})_6]$ redox peaks completely disappears on the cyclic voltammograms of PmPD and PDA covered gold surfaces, confirming the insulating character of the deposited films. Moreover, there is no significant difference between voltammogram

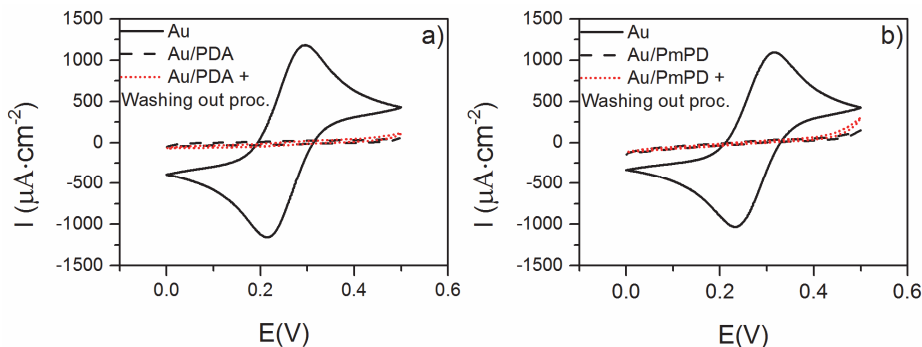


Figure 3.3. Effect of the washing out procedure on PDA (a) and PmPD (b) thin film stability.

recordings before and after the washing out procedure, suggesting that both polymer films were stable in the conditions applied for IgG removal.

3.3. Characterization of the IgG-MIP films

The IgG-MIP films were characterized in terms of their affinity and selectivity towards IgG by monitoring the binding events with the QCM and SAW systems. To ascertain that the interaction between the IgG and the IgG-MIP surface was specific, a control experiment was performed with the NIP-modified sensor for each tested polymer film. The influence of the electrodeposited polymer thickness on the recognition properties of the IgG-MIP was also explored.

3.3.1. Rebinding study by QCM

IgG rebinding on the prepared the IgG-MIP films was studied by the QCM-FIA combined system (Article II). A series of the IgG-MIPs having different thicknesses of PDA were fabricated directly on the sensing surface of the QCM. Fig. 3.4 shows the sensorgrams and additive calibration curves for the thickness-optimized (18 nm) IgG-MIP and the respective NIP upon consecutive injections of the solutions with increasing concentration of IgG in PBS buffer.

A frequency drop associated with the IgG binding is observed for the IgG-MIP modified QCM sensor already after the injection of 2 nM IgG concentration, while the NIP modified sensor shows the non-significant frequency change (Fig. 3.4a). With the increasing concentration of IgG, the frequency drop becomes more pronounced for both the IgG-MIP and NIP films but at the same time, a noticeable difference between the frequency responses of the IgG-MIP and NIP modified sensors is still observed. However, there is also evidence that a significant non-specific adsorption appeared as a considerable frequency decrease recorded by the NIP modified QCM sensor at IgG concentrations exceeding 53 nM. Nevertheless, the binding capacity of the IgG-MIP is always higher than that of the respective NIP, which is most likely caused by the presence of the complementary cavities on the surface of the IgG-MIP films due to the imprinting phenomenon (Fig. 3.4b). Among the IgG-MIPs prepared, those with

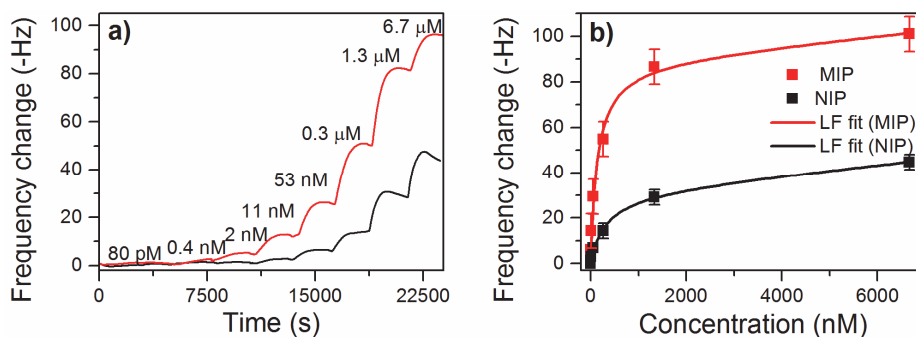


Figure 3.4. (a) Resonant frequency responses of the IgG-MIP and NIP modified QCMs. The data were obtained from the thickness-optimized films (18 nm) and upon successive injections of the different concentrations of IgG in 10 mM PBS buffer; (b) the respective cumulative binding isotherms fitted with the Langmuir–Freundlich (LF) isotherm model.

PDA film thicknesses of ca 18 nm demonstrated the most pronounced imprinting effect (IF 1.66) as well as the submicromolar range binding affinity (K_D 296 nM) that was approximately one order of magnitude higher than that for the respective NIP (Article II, Table 1). It is believed that at such PDA film thickness, the immobilized IgG molecules were appropriately confined in the polymer and the more specific binding sites were formed at the polymer surface after the subsequent IgG removal procedure.

3.3.2. Rebinding study by SAW

The IgG-MIPs with different PmPD film thicknesses were tested for IgG rebinding capabilities by the SAW sensor platform (Article III). The thickness of synthesized films was additionally verified by spectroscopic ellipsometry measurements and the calibration plot for accurate dosage of applied charge was generated (Article III, Fig. 2).

The binding kinetic analysis with the pseudo second-order rate model allowed to determine equilibrium binding response and thus, to calculate and compare the imprinting factors for the IgG-MIP of different polymer thicknesses. It was found that the IgG-MIP films with the thickness of 11 nm had higher specific recognition ability towards IgG than the other IgG-MIP counterparts studied. The analysis of the isotherm data by fitting them to the Langmuir–Freundlich adsorption model suggested a certain degree of heterogeneity of the binding sites in the IgG-MIP films (Fig. 3.5). Although the binding capacity of the IgG-MIP was about three times higher than that of NIP, their dissociation constants were somewhat comparable. It is more likely to be attributed to the disproportionately low contribution of the high affinity binding sites to the increased binding capacity of the IgG-MIP (Article III, Fig. 3).

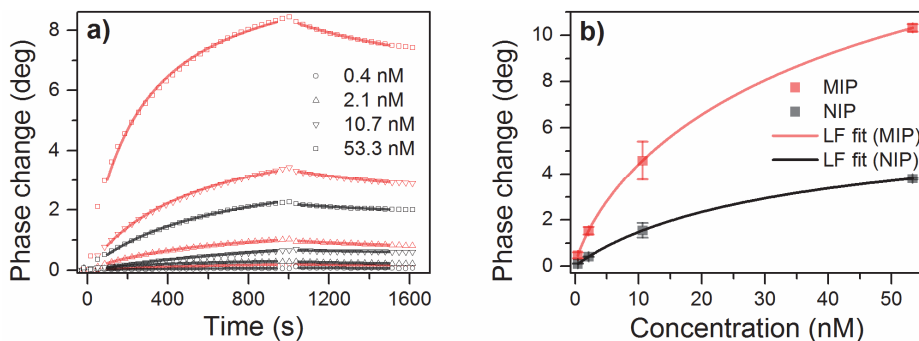


Figure 3.5. (a) Typical phase-shift responses of the IgG-MIP and NIP modified SAW chips upon consecutive injection of IgG in PBS. The binding isotherms (b) obtained using Q_{eq} determined from fitting of the kinetic data (a) fitted with pseudo-second rate model. The solid lines represent fits of the data to the Langmuir–Freundlich (LF) isotherm model.

3.3.3. Comparison of QCM and SAW devices

Although a SAW and a QCM share a similar principle of operation, its benefits over QCM were clearly revealed in this thesis. Both QCM and SAW allowed observing the real-time binding events of the target protein on the IgG-MIP modified surfaces, however owing to the low-volume flow cell (2.3 μL), the SAW system made it possible to analyze the binding events once the kinetic responses were acquired. The analysis predicted the values of Q_{eq} for every concentration applied, allowing, in turn, to generate more precisely the binding isotherm for every variation of the IgG-MIP film studied in the thesis. The presence of the multiple sensor elements in one experiment delivers some extra benefits. The SAW sensing platform used in this study could manage two SAW chips having four sensor elements whereas each one was employed. This property enabled us to characterize in parallel various IgG-MIP and in particular, respective NIP films, thus, reducing experimental time and errors derived from differences in the properties of the chips and reproducibility of the films.

3.3.4. Selectivity of the IgG-MIP

Selectivity of IgG imprinted films towards the template was studied by injecting 8 $\mu\text{g}\cdot\text{mL}^{-1}$ solutions of other serum proteins: HSA and IgA that may cause serious interference when analyzing real samples. The IgG-MIP demonstrated the preferential binding to the original template molecule (IgG) over the IgA and HSA with the S values of 0.3 and 0.09, respectively. The data suggest that both of the interfering proteins have lower binding affinity to the IgG-MIP than IgG, even though the molecular size and shape of IgG and IgA are similar. Thus, the IgG-MIP can recognize the target protein, confirming the presence of IgG imprints in the polymer matrix that can be discriminated on the basis of molecular shape and size as well as functional group arrangement (Article III, Fig. 6).

4. CONCLUSIONS

In this thesis, a novel method was developed that allows generation of a synthetic polymer film with macromolecular imprints (MIP) capable of selective rebinding of macromolecular substances such as proteins. Immunoglobulin G (IgG) was chosen as a model macromolecular template to form the respective IgG molecular cavities in the polymer matrix after its removal. The main advantage of the method is that it provides facile and robust integration of the films with various label-free detection techniques (QCM, SAW), thus making it possible to understand the underlying processes in biomacromolecular recognition by MIPs and offering a premise for fabrication of MIP-based biosensors.

The main results of the present study are as follows:

1. IgG immobilization on the gold surface via the DTSSP cleavable linker was found not to restrict electron transfer processes on the surface, allowing subsequent electrogeneration of the polymer matrix.
2. The advantage of the electrosynthesis approach was demonstrated. The approach allowed the highly controllable growth of the PDA and PmPD matrices at the nanoscale (4-27 nm) through the electrical charge dosage that was confirmed with the ellipsometry measurements.
3. The PmPD and PDA films appeared to be reliable at all stages of the IgG-MIP film formation, however, the PmPD was found to be more preferable since it had substantially shorter time of the synthesis, thus being less harmful to IgG native conformation.
4. The capability of the IgG-MIP to recognize the target protein specifically was found to be in strong dependence on the polymer matrix thickness. The optimal thickness of the polymer matrix for the IgG-MIP was determined to be 18 nm and 11 nm for PDA and PmPD-based films, respectively. It is believed that at these thickness values of the polymer matrix, IgG molecules are appropriately confined in the polymer, avoiding their irreversible entrapment and the more selective binding sites were formed at the polymer surface after the subsequent IgG removal procedure.
5. The thickness-optimized IgG-MIPs demonstrated the imprinting factors in the range of 1.7 – 4.0, as well as bound IgG, template protein, with dissociation constants, K_D , in the submicromolar range (17 nM), proving the feasibility of the developed method for the IgG imprinting.
6. The IgG-MIP demonstrated higher selectivity of the original template molecule (IgG) over interfering proteins, IgA and HSA. Their selectivity factors were found to be about 3.4 and 10 times lower than those for IgG, respectively.
7. The IgG-MIP preserved its capability to recognize selectively the template after up to four regeneration cycles.
8. Langmuir–Freundlich adsorption model proved more suitable to describe the binding isotherm of IgG toward the IgG-MIP. This indicated the presence of a certain degree of heterogeneity of the binding sites in the IgG-MIP films.

The integration of the IgG-MIPs with SAW and QCM detection techniques allowed observing the real-time binding events of the target protein, whereas SAW offered an enormous benefit over QCM in terms of its multiplexing capability, considerably reducing experimental time and errors.

ABSTRACT

Chemical and biosensors have attracted considerable attention in the area of analytical chemistry to meet an increasing demand for fast and reliable devices having low detection limits and appropriate selectivity to resolve the analytes of interest in clinical analysis, environmental monitoring and in other areas.

However, despite the significant progress in modern biosensors, there is a significant limitation mostly associated with a labile nature of biological recognition elements, i.e., their poor chemical and physical stability restricts further development of robust and reusable natural recognition elements. Therefore, it is required to develop alternative synthetic receptors to overcome that disadvantage.

One of the state-of-the-art techniques allowing generation of synthetic receptors is “molecular imprinting”, which can be defined as the process of template-induced formation of specific molecular recognition sites in a polymer matrix material. In general, the molecular imprinting consists in the polymerization of a mixture of functional monomers in the presence of a target molecule that acts as a template. During polymerization, the template induces binding sites in the reticulated polymer that are capable of selective recognition of the target molecules or similar structures after removal of the templates from the polymer. The main benefits of these polymers, so-called Molecularly Imprinted Polymers (MIPs), are related to their synthetic nature, i.e., excellent chemical and thermal stability associated with reproducible, cost-effective fabrication. Therefore, MIPs are considered very prospective materials for application in various fields, such as chemical analysis and detection, separation and purification, drug delivery.

The overall objective of this thesis was to explore molecular surface imprinting of the synthetic polymer prepared by a controlled polymerization technique, but integrated with a sensor transducer for label-free detection of macromolecules such as proteins, to create highly selective, robust and multiplexed MIP-based biosensors. Acoustic wave devices such as QCM and SAW were chosen as cost-effective sensor platforms capable of monitoring molecular binding events in a real-time and label-free manner.

To attach the tailored protein recognition function to the QCM and SAW, a method interfacing the protein-MIP films with the sensor chips was developed. The method includes the sequence of (i) the macromolecular template immobilization, (ii) electropolymerization and (iii) template removal procedures applied directly to the sensing surfaces of the chips.

An attempt was made to immobilize macromolecules by two principal strategies. In the first strategy, a specially synthesized peptide modified with cysteine (Cys-peptide) was immobilized on the para-maleimidophenyl grafted surfaces by cross-linking between the maleimide groups and the sulfhydryl group of the Cys residues. Accordingly, the Cys-peptide was supposed to work as an antigen able to bind specifically an antibody served as a macromolecular template. The other strategy relied on the immobilization of the macromolecular template on a surface via a DTSSP cleavable linker, allowing an easy detaching of the template afterwards.

Although the first strategy seemed to be potentially suitable for the oriented fixation of an antibody, the origin conductivity of the modified surface was substantially degraded, making the subsequent electropolymerization procedure severely limited. Vice versa, the second template immobilization strategy did not restrict electron transfer processes on the surface, allowing the subsequent controlled electropolymerization of the monomer to yield the ultrathin polymeric matrix. Thus, the DTSSP linker system was selected and used hereinafter as a base for the immobilization of the macromolecular template on the surface of a transducer.

Immunoglobulin G (IgG) is a macromolecule and the most plentiful class of antibodies present in human serum, and it protects an organism against bacterial and viral infections. Analysis of the presence of specific IgG molecules in the body fluids can be useful in diagnosing infections or certain illnesses. For that reason, IgG was chosen as a model macromolecular template to form the respective IgG molecular cavities in the polymer matrix after its removal.

A highly controlled method for the polymerization process is indispensable to ensure that immobilized IgG is confined to the surface of the growing polymer matrix rather than completely entrapped. Therefore, the electrochemical approach was utilized to generate the ultrathin (4-27 nm) polymeric films of either PDA or PmPD with the required precision. Subsequently, the films were subjected to the template removal procedure to yield the IgG-MIPs. During that procedure, the DTSSP linker system holding covalently the template was disrupted by reducing the linker sulfide-sulfide bond and additional solutions breaking down the hydrogen, electrostatic and hydrophobic bonds were applied to facilitate the template removal process.

It was revealed that the IgG-MIPs generated in the course of the stages mentioned are capable of recognizing strong dependence of IgG on the polymer film thickness that could be easily optimized by the amount of the electrical charge consumed during the electrodeposition. The thickness-optimized IgG-MIPs demonstrated the imprinting factors towards IgG in the range of 1.7–4 and dissociation constants in the submicromolar range (17 nM) as well as 3.4 and 10 times higher selectivity for IgG over the interfering proteins, IgA and HSA, respectively. It was found that the IgG-MIP preserved its capability to recognize selectively the template after up to four regeneration cycles.

The presented method of the facile integration of the protein-MIP sensing layer with the SAW technology allowed observing the real-time binding events of the target protein at the relevant sensitivity levels and could be potentially suitable for cost-effective fabrication of a biosensor for the analysis of biological samples in a multiplexed manner.

KOKKUVÕTE

Keemilised sensorid, sealhulgas biosensorid, on omandanud analüütilises keemias kindla koha tänu pidevalt kasvavale nõudlusele kiirete, suure tundlikkuse ja selektiivsusega usaldusväärsete analüüsimeetodite järele. Selliste meetodite järele on suur nõudlus kiiresti arenevas kliinilises analüüsis, keskkonna seisundi jälgimisel ning paljudes teistes valdkondades.

Vaatamata edusammudele moodsate biosensorite väljatöötamisel, on täna siiski veel probleemiks looduslike bioloogiliste retseptorite füüsikaliste ja keemiliste omaduste ebastabiilsus. Üheks selle probleemi võimalikuks lahenduseks on bioloogiliste retseptorite asemel omadustelt oluliselt stabiilsemate sünteetiliste retseptorite väljatöötamine.

Sünteetiliste retseptorite loomise võimaluseks on „molekulaarse jäljendamise“ tehnoloogia kasutamine. Molekulaarse jäljendamise tehnoloogia võimaldab polümeeri maatriksis tekitada spetsiifiliste sihtmolekulide „jäljendid“. Sellised „jäljendid“ valmistatakse polümerisatsiooni teel sihtmolekuli ja funktsionaalse monomeeri juuresolekul ning sellele järgneva sihtmolekuli eemaldamisega polümeeri maatriksist. Protsessi tulemusena tekivad polümeeri maatriksis tühjad mälupesad, mis järgnevalt kohtudes uuesti sihtmolekulidega on võimelised neid efektiivselt siduma.

Molekulaarselt jäljendatud polümeere (MIP) iseloomustab erinevalt looduslikest retseptoritest nende hea keemiline ja termiline stabiilsus, omaduste reprodutseeritavus ja valmistamistehnoloogia odavus. Tänu sellistele omadustele loetakse molekulaarselt jäljendatud polümeere väga perspektiivseteks materjalideks analüütilises keemias, keskkonna puhastamisel ja näiteks ravimite suunatud viimiseks ravitavasse keskkonda ja seal nende efektiivseks juhtimiseks.

Doktoritöö eesmärgiks oli molekulaarse jäljendamise tehnoloogia arendamine pindmiste mälupesadega materjalide loomise teel ja nende ühildamine märgisevabade määramise meetoditega suurte biomolekulide nagu proteiinide sidumiseks.

Jäljendatud polümeeri ja sihtmolekuli sidumisel tekkiva füüsikalise muutuse kirjeldamiseks kasutati piesoelektrilise kvartskristalli resonantssageduse muutuse (QCM) ja pinna akustilise laine muutuse (SAW) põhimõttel töötavaid muundureid, mis võimaldavad nn. märgisevabalt registreerida sihtmolekulide sidumisel tekkivaid signaale. Saadud signaale töödeldi sihtmolekuli sidumise efektiivsuse iseloomustamiseks, arvestades sidumisprotsessi kui adsorptsiooni-protsessi kineetikat ja iseloomu.

Proteiini suhtes jäljendatud polümeerid valmistati vahetult signaali muunduri pinnal elektropolümerisatsiooni abil, millele eelnes sihtmolekuli immobiliseerimine ja järgnes sihtmolekuli eemaldamine polümeeri maatriksist.

Proteiini sidumiseks muunduri aluspinnaga kasutati kahte strateegiat. Esimese strateegia kohaselt immobiliseeriti Cys-peptiid para-malemiinofenüülga kaetud muunduri pinnale nii, et Cys-peptiid käituks kui antigeen sihtmolekuli suhtes.

Teise strateegia kohaselt kasutati muunduri aluspinna ja sihtmolekuli sidumiseks DTSSP silda, mis seob edukalt sihtmolekuli, kuid võimaldab samal ajal ka silda katkestada, et tekitada proteiini kui sihtmolekuli jäljendit polümeer-maatriksis.

Esimese strateegia positiivseks omaduseks oli antikeha sobilik orientatsioon muunduri pinnal, kuid samal ajal pinna elektri juhtivus vähenes ja elektropolümeerisatsioon oli raskendatud.

Seevastu teine immobilisatsiooni strateegia DTSSP silla abil ei kahandanud elektri juhtivust, elektropolümeerisatsiooni protsess oli juhitav ja see võimaldas ka edukalt kontrollida polümeermaatriksi paksust.

Immunoglobuliin G (IgG) on üks enim esindatud antikehi inimese seerumis ja põhiline immuunsuse garant viirushaiguste vastu. Immunoglobuliini kiire ja täpne määramine inimese organismis on äärmiselt tähtis erinevate haiguste varasel diagnoosimisel. Seepärast on ka käesoleva väitekirja peamiseks eesmärgiks kiire, efektiivse ja odava tehnoloogia väljatöötamine IgG määramiseks, kasutades molekulaarse jäljendamise tehnoloogiat.

Immunoglobuliini edukaks jäljendamiseks on vajalik polümeerisatsiooni protsessi efektiivne kontrollimine, mis on hästi teostatav elektropolümeerisatsiooni abil. Monomeeridena kasutati polüdopamiini (PDA) ja polüfenüleendiamiini (PmPD), sillana IgG ja polümeeri maatriksi vahel DTSSP-d, mis elektropolümeerisatsioonil koos sihtmolekuliga moodustasid polümeeri üliõhukese (4-27 nm) kile, millest oli kerge väljapesemisega eraldada sihtmolekuli IgG. Elektropolümeerisatsioon võimaldas ka efektiivselt kontrollida polümeerkile paksust, millel on oluline roll efektiivsel sihtmolekuli uuesti sidumisel.

Optimaalse paksusega IgG suhtes jäljendatud polümeerisid olid IgG spetsiifilise sidumise efektiivsust väljendavad IF (Imprinting factor) väärtused vahemikus 1,7–4,0 ja IgG dissotsiatsiooni konstandi K_D väärtus 17 nM ning selektiivsus konkureerivate proteiinide IgA ja HSA suhtes vastavalt 3,4 ja 10 korda kõrgem. Molekulaarselt jäljendatud IgG reprodutseeritavus ja määramise efektiivsus säilis vähemalt nelja regenererimise tsükli järel.

Kokkuvõttes võib käesoleva väitekirja tulemusena järeldada, et immunoglobuliini molekulaarne jäljendamine mitmekanalilise SAW muunduri pinnal loob eeldused efektiivse ja odava biosensori valmistamiseks, mis võimaldab reaajas määrata piisava täpsusega erinevaid bioloogilisi sihtmolekule.

ACKNOWLEDGMENTS

I am extremely thankful to my supervisor **Dr. Vitali Syritski** for his patient guidance, encouragement and advice throughout my time as his student. I have been very lucky to have a supervisor who cared so much about my work, enabled me to develop an understanding of the subject and responded to my questions and queries so promptly.

I would like to express my sincere gratitude to my co-supervisor **Prof. Andres Öpik** for providing an excellent opportunity for my studies and research at the Chair of Physical Chemistry of Tallinn University of Technology, for his support and supervision.

Also, I would like to express my deepest gratitude to my co-supervisor **Dr. Jekaterina Reut** for all her help, support, interest and valuable advice.

I wish to thank **Prof. Enn Mellikov**, Head of the Department of Materials Science up to 2015, for the opportunity to use high-end research equipment.

I thank **Dr. Jörg Rappich** for the opportunity to perform ellipsometry measurements at Helmholtz-Zentrum Berlin für Materialien und Energie GmbH.

In addition, I would like to thank my colleagues **Roman Boroznjak**, **Akinrinade George Ayankojo** and everybody who I have worked with in the Department of Materials Science.

Finally, I am grateful to my family and all the people who have supported me during my doctoral studies.

This research was conducted at the Chair of Physical Chemistry, Department of Materials Science. The work was financially supported by Estonian Science Foundation (**PUT150**), Estonian Ministry of Education and Research (**SF0140033s12**), European Social Fund's Doctoral Studies and Internationalization Program (**DoRa8**), FMTDK graduate school "Functional materials and technologies" (**European Social Fund under Project 1.2.0401.09-0079 in Estonia**).

REFERENCES

- [1] E.M. Peck, B.D. Smith, Applications of Synthetic Receptors for Biomolecules, in: B.D. Smith (Ed.) Synthetic Receptors for Biomolecules: Design Principles and Applications, The Royal Society of Chemistry 2015, pp. 1-38.
- [2] L. Ye, K. Haupt, Molecularly imprinted polymers as antibody and receptor mimics for assays, sensors and drug discovery, *Analytical and Bioanalytical Chemistry*, 378 (2004) 1887-1897.
- [3] E.L. Holthoff, F.V. Bright, Molecularly templated materials in chemical sensing, *Analytica chimica acta*, 594 (2007) 147-161.
- [4] F.G. Tamayo, E. Turiel, A. Martin-Esteban, Molecularly imprinted polymers for solid-phase extraction and solid-phase microextraction: recent developments and future trends, *Journal of chromatography. A*, 1152 (2007) 32-40.
- [5] C. Alvarez-Lorenzo, A. Concheiro, Molecularly imprinted polymers for drug delivery, *Journal of chromatography. B, Analytical technologies in the biomedical and life sciences*, 804 (2004) 231-245.
- [6] G. Wulff, Enzyme-like catalysis by molecularly imprinted polymers, *Chemical Reviews*, 102 (2002) 1-27.
- [7] K.M. Haupt, K., Molecularly Imprinted Polymers and Their Use in Biomimetic Sensors, *Chemical Reviews*, 100 (2000) 2495-2504.
- [8] L. Ye, K. Mosbach, Molecular Imprinting: Synthetic Materials As Substitutes for Biological Antibodies and Receptors, *Chemistry of Materials*, 20 (2008) 859-868.
- [9] A. Bossi, F. Bonini, A.P. Turner, S.A. Piletsky, Molecularly imprinted polymers for the recognition of proteins: the state of the art, *Biosensors & bioelectronics*, 22 (2007) 1131-1137.
- [10] Y. Li, H.H. Yang, Q.H. You, Z.X. Zhuang, X.R. Wang, Protein recognition via surface molecularly imprinted polymer nanowires, *Analytical chemistry*, 78 (2006) 317-320.
- [11] L.H. Qin, X.; Li, W.; Zhang, Y., Surface-modified polystyrene beads as photografting imprinted polymer matrix for chromatographic separation of proteins, *Journal of Chromatography A*, 1216 (2009) 807-814.
- [12] G. Lautner, J. Kaev, J. Reut, A. Öpik, J. Rappich, V. Syritski, G.R. E., Selective Artificial Receptors Based on Micropatterned Surface-Imprinted Polymers for Label-Free Detection of Proteins by SPR Imaging, *Advanced Functional Materials*, 21 (2010) 591-597.
- [13] A. Menaker, V. Syritski, J. Reut, A. Öpik, V. Horváth, G.R. E., Electrosynthesized Surface-Imprinted Conducting Polymer Microrods for Selective Protein Recognition, *Advanced Materials*, 21 (2009) 2271 - 2275.
- [14] G. Lakos, L. Soós, A. Fekete, Z. Szabó, M. Zeher, I. Horváth, K. Dankó, A. Kapitány, A. Gyetvai, G. Szegedi, Anti-cyclic citrullinated peptide antibody isotypes in rheumatoid arthritis: association with disease duration, rheumatoid factor production and the presence of shared epitope, *Clinical and experimental rheumatology*, 26 (2008) 253.

- [15] G. Erturk, L. Uzun, M.A. Tumer, R. Say, A. Denizli, Fab fragments imprinted SPR biosensor for real-time human immunoglobulin G detection, *Biosensors & bioelectronics*, 28 (2011) 97-104.
- [16] A. Nematollahzadeh, W. Sun, C.S.A. Aureliano, D. Lütkemeyer, J. Stute, M. Abdekhodaie, J., A. Shojaei, B. Sellergren, High-Capacity Hierarchically Imprinted Polymer Beads for Protein Recognition and Capture, *Angew. Chem.*, 123 (2010) 515-518.
- [17] R. Schirhagl, P.A. Lieberzeit, D. Blaas, F.L. Dickert, Chemosensors for viruses based on artificial immunoglobulin copies, *Advanced materials*, 22 (2010) 2078-2081.
- [18] D. Yin, M. Ulbricht, Antibody-imprinted membrane adsorber via two-step surface grafting, *Biomacromolecules*, 14 (2013) 4489-4496.
- [19] C. Malitesta, L. I., Z.P. G., Molecularly Imprinted Electrosynthesized Polymers: New Materials for Biomimetic Sensors, *Analytical Chemistry*, 71 (1999) 1366-1370.
- [20] P.S. Sharma, A. Pietrzyk-Le, F. D'Souza, W. Kutner, Electrochemically synthesized polymers in molecular imprinting for chemical sensing, *Analytical and bioanalytical chemistry*, 402 (2012) 3177-3204.
- [21] M. Bossert, J. Erdössy, G. Lautner, J. Witt, K. Köhler, N. Gajovic-Eichelmann, A. Yarman, G. Wittstock, F.W. Scheller, R.E. Gyurcsányi, Microelectrospotting as a new method for electrosynthesis of surface-imprinted polymer microarrays for protein recognition, *Biosensors and Bioelectronics*, 73 (2015) 123-129.
- [22] E. Kolodziejczyk, V. Petkova, J.J. Benattar, M.E. Leser, M. Michel, Effect of fluorescent labeling of β -lactoglobulin on film and interfacial properties in relation to confocal fluorescence microscopy, *Colloids and Surfaces A: Physicochemical and Engineering Aspects*, 279 (2006) 159-166.
- [23] T.M.A. Gronewold, Surface acoustic wave sensors in the bioanalytical field: Recent trends and challenges, *Analytica Chimica Acta*, 603 (2007) 119-128.
- [24] K. Länge, B.E. Rapp, M. Rapp, Surface acoustic wave biosensors: a review, *Analytical and Bioanalytical Chemistry*, 391 (2008) 1509-1519.
- [25] G. Vlatakis, L.I. Andersson, R. Müller, K. Mosbach, Drug assay using antibody mimics made by molecular imprinting, *Nature*, 361 (1993) 645-647.
- [26] G. Vasapollo, R.D. Sole, L. Mergola, M.R. Lazzoi, A. Scardino, S. Scorrano, G. Mele, Molecularly imprinted polymers: present and future prospective, *International journal of molecular sciences*, 12 (2011) 5908-5945.
- [27] G. Wulff, A. Sarhan, Über die Anwendung von enzymanalog gebauten Polymeren zur Racemattrennung, *Angew. Chem.*, 84 (1972) 364.
- [28] R. Arshady, K. Mosbach, Synthesis of substrate-selective polymers by host-guest polymerization, *Die Makromolekulare Chemie* 182 (1981) 687-692.
- [29] M.J. Whitcombe, M.E. Rodriguez, P. Villar, E.N. Vulfson, A new method for the introduction of recognition site functionality into polymers prepared by molecular imprinting—synthesis and characterization of polymeric receptors for cholesterol, *Journal of the American Chemical Society*, 117 (1995) 7105-7111.
- [30] O. Ramstrom, L. Ye, K. Mosbach, Artificial antibodies to corticosteroids prepared by molecular imprinting, *Chemistry & biology*, 3 (1996) 471-477.

- [31] Y. Fuchs, O. Soppera, A.G. Mayes, K. Haupt, Holographic molecularly imprinted polymers for label-free chemical sensing, *Advanced materials*, 25 (2013) 566-570.
- [32] K. Haupt, K. Mosbach, Molecularly imprinted polymers in chemical and biological sensing, *Biochemical Society transactions*, 27 (1999) 344-350.
- [33] M. Szumski, B. Buszewski, Molecularly imprinted polymers: a new tool for separation of steroid isomers, *Journal of separation science*, 27 (2004) 837-842.
- [34] T. Takeuchi, J. Haginaka, Separation and sensing based on molecular recognition using molecularly imprinted polymers, *Journal of chromatography. B, Biomedical sciences and applications*, 728 (1999) 1-20.
- [35] B. Sellergren, C.J. Allender, Molecularly imprinted polymers: a bridge to advanced drug delivery, *Advanced drug delivery reviews*, 57 (2005) 1733-1741.
- [36] M. Bompant, Y. De Wilde, K. Haupt, Chemical nanosensors based on composite molecularly imprinted polymer particles and surface-enhanced Raman scattering, *Advanced materials*, 22 (2010) 2343-2348.
- [37] T.A. Sergeeva, O.A. Slinchenko, L.A. Gorbach, V.F. Matyushov, O.O. Brovko, S.A. Piletsky, L.M. Sergeeva, G.V. Elska, Catalytic molecularly imprinted polymer membranes: development of the biomimetic sensor for phenols detection, *Analytica chimica acta*, 659 (2010) 274-279.
- [38] V. Syritski, J. Reut, A. Menaker, G.R. E., A. Öpik, Electrosynthesized molecularly imprinted polypyrrole films for enantioselective recognition of l-aspartic acid, *Electrochimica Acta*, 53 (2008) 2729-2736.
- [39] A. Poma, A.P. Turner, S.A. Piletsky, Advances in the manufacture of MIP nanoparticles, *Trends in biotechnology*, 28 (2010) 629-637.
- [40] H. Yan, K.H. Row, Characteristic and Synthetic Approach of Molecularly Imprinted Polymer, *International Journal of Molecular Sciences*, 7 (2006) 155-178.
- [41] S. Tokonami, H. Shiigi, T. Nagaoka, Review: micro- and nanosized molecularly imprinted polymers for high-throughput analytical applications, *Analytica chimica acta*, 641 (2009) 7-13.
- [42] W.M. Chen, Y.; Pan J.; Meng, Z.; Pan, G.; Sellergren, B., Molecularly Imprinted Polymers with Stimuli-Responsive Affinity: Progress and Perspectives, *Polymers*, 7 (2015) 1689-1715.
- [43] Y. Liu, L. Zhu, Y. Zhang, H. Tang, Electrochemical sensing of 2,4-dinitrophenol by using composites of graphene oxide with surface molecular imprinted polymer Sensors and Actuators, B: Chemical, 171-172 (2012) 1151-1158.
- [44] G. Pan, Y. Zhang, X. Guo, C. Li, H. Zhang, An efficient approach to obtaining water-compatible and stimuli-responsive molecularly imprinted polymers by the facile surface-grafting of functional polymer brushes via RAFT polymerization, *Biosensors & bioelectronics*, 26 (2010) 976-982.
- [45] I. Tokarev, M. Motornov, S. Minko, Molecular-engineered stimuli-responsive thin polymer film: a platform for the development of integrated multifunctional intelligent materials, *Journal of Materials Chemistry*, 19 (2009) 6932-6948.

- [46] Y. Fuchs, O. Soppera, K. Haupt, Photopolymerization and photostructuring of molecularly imprinted polymers for sensor applications—A review, *Analytica Chimica Acta*, 717 (2012) 7-20.
- [47] S. Li, S. Cao, M.J. Whitcombe, S.A. Piletsky, Size matters: Challenges in imprinting macromolecules, *Progress in Polymer Science*, 39 (2014).
- [48] D.J. Duffy, K. Das, S.L. Hsu, J. Penelle, V.M. Rotello, H.D. Stidham, Binding efficiency and transport properties of molecularly imprinted polymer thin films, *Journal of the American Chemical Society*, 124 (2002) 8290-8296.
- [49] F.G. Banica, *Chemical sensors and biosensors: fundamentals and applications*, John Wiley & Sons 2012.
- [50] A.P.F. Turner, Biosensors--sense and sensitivity, *Science*, 290 (2000) 1315-1317.
- [51] M.J. Whitcombe, I. Chianella, L. Larcombe, S.A. Piletsky, J. Noble, R. Porter, A. Horgan, The rational development of molecularly imprinted polymer-based sensors for protein detection, *Chemical Society Reviews*, 40 (2011) 1547-1571.
- [52] E. Verheyen, J.P. Schillemans, M. van Wijk, M.-A. Demeniex, W.E. Hennink, C.F. van Nostrum, Challenges for the effective molecular imprinting of proteins, *Biomaterials*, 32 (2011) 3008-3020.
- [53] I.A. Nicholls, Thermodynamic Considerations for the Design of and Ligand Recognition by Molecularly Imprinted Polymers, *Chemistry Letters*, 24 (1995) 1035-1036.
- [54] M.M. Titirici, A.J. Hall, B. Sellergren, Hierarchically imprinted stationary phases: Mesoporous polymer beads containing surface-confined binding sites for adenine, *Chemistry of Materials*, 14 (2002) 21-23.
- [55] M.M. Titirici, B. Sellergren, Peptide recognition via hierarchical imprinting, *Analytical and bioanalytical chemistry*, 378 (2004) 1913-1921.
- [56] Z. Zhang, Y. Long, L. Nie, S. Yao, Molecularly imprinted thin film self-assembled on piezoelectric quartz crystal surface by the sol-gel process for protein recognition, *Biosensors and Bioelectronics*, 21 (2006) 1244-1251.
- [57] T. Shiomi, M. Matsui, F. Mizukami, K. Sakaguchi, A method for the molecular imprinting of hemoglobin on silica surfaces using silanes, *Biomaterials*, 26 (2005) 5564-5571.
- [58] D.R. Kryscio, N.A. Peppas, Critical review and perspective of macromolecularly imprinted polymers, *Acta biomaterialia*, 8 (2012) 461-473.
- [59] H.-Y. Lin, C.-Y. Hsu, J.L. Thomas, S.-E. Wang, H.-C. Chen, T.-C. Chou, The microcontact imprinting of proteins: The effect of cross-linking monomers for lysozyme, ribonuclease A and myoglobin, *Biosensors and Bioelectronics*, 22 (2006) 534-543.
- [60] E. Yilmaz, K. Haupt, K. Mosbach, The use of immobilized templates—A new approach in molecular imprinting, *Angewandte Chemie International Edition*, 39 (2000) 2115-2118.
- [61] Y. Jung, J.Y. Jeong, B.H. Chung, Recent advances in immobilization methods of antibodies on solid supports, *The Analyst*, 133 (2008) 697-701.
- [62] A. Makaraviciute, T. Ruzgas, A. Ramanavicius, A. Ramanaviciene, Antibody fragment immobilization on planar gold and gold nanoparticle

modified quartz crystal microbalance with dissipation sensor surfaces for immunosensor applications, *Analytical Methods*, 6 (2014) 2134-2140.

[63] S. Cosnier, M. Holzinger, Electrosynthesized polymers for biosensing, *Chemical Society Reviews*, 40 (2011) 2146-2156.

[64] C. Malitesta, E. Mazzotta, R.A. Picca, A. Poma, I. Chianella, S.A. Piletsky, MIP sensors—the electrochemical approach, *Analytical and Bioanalytical Chemistry*, 402 (2012) 1827-1846.

[65] Y. Wang, T.-X. Wei, Surface plasmon resonance sensor chips for the recognition of bovine serum albumin via electropolymerized molecularly imprinted polymers, *Chinese Chemical Letters*, 24 (2013) 813-816.

[66] J. Orozco, A. Cortés, G. Cheng, S. Sattayasamitsathit, W. Gao, X. Feng, Y. Shen, J. Wang, Molecularly imprinted polymer-based catalytic micromotors for selective protein transport, *Journal of the American Chemical Society*, 135 (2013) 5336-5339.

[67] X. Kan, Z. Xing, A. Zhu, Z. Zhao, G. Xu, C. Li, H. Zhou, Molecularly imprinted polymers based electrochemical sensor for bovine hemoglobin recognition, *Sensors and Actuators B: Chemical*, 168 (2012) 395-401.

[68] A. Ramanaviciene, A. Ramanavicius, Molecularly imprinted polypyrrole-based synthetic receptor for direct detection of bovine leukemia virus glycoproteins, *Biosensors and Bioelectronics*, 20 (2004) 1076-1082.

[69] H. Lee, S.M. Dellatore, W.M. Miller, P.B. Messersmith, Mussel-inspired surface chemistry for multifunctional coatings, *Science*, 318 (2007) 426-430.

[70] B. Stöckle, D.Y.W. Ng, C. Meier, T. Paust, F. Bischoff, T. Diemant, R.J. Behm, K.E. Gottschalk, U. Ziener, T. Weil, Precise control of polydopamine film formation by electropolymerization, *Macromolecular Symposia*, Wiley Online Library, 2014, pp. 73-81.

[71] K. Liu, W.Z. Wei, J.X. Zeng, X.Y. Liu, Y.P. Gao, Application of a novel electrosynthesized polydopamine-imprinted film to the capacitive sensing of nicotine, *Analytical and bioanalytical chemistry*, 385 (2006) 724-729.

[72] X.G. Li, M.R. Huang, W. Duan, Y.L. Yang, Novel multifunctional polymers from aromatic diamines by oxidative polymerizations, *Chemical reviews*, 102 (2002) 2925-3030.

[73] X.G. Li, W. Duan, M.R. Huang, L.N.J. Rodriguez, Electrocopolymerization of meta-phenylenediamine and ortho-phenetidine, *Reactive & Functional Polymers*, 62 (2005) 261-270.

[74] B. Duran, G. Bereket, M. Duran, Electrochemical synthesis and characterization of poly(m-phenylenediamine) films on copper for corrosion protection, *Progress in Organic Coatings*, 73 (2012) 162-168.

[75] Z. Wang, X. Li, D. Feng, L. Li, W. Shi, H. Ma, Poly(m-phenylenediamine)-based fluorescent nanoprobe for ultrasensitive detection of matrix metalloproteinase 2, *Analytical chemistry*, 86 (2014) 7719-7725.

[76] T. Wang, L. Zhang, C. Li, W. Yang, T. Song, C. Tang, Y. Meng, S. Dai, H. Wang, L. Chai, J. Luo, Synthesis of Core-Shell Magnetic Fe₃O₄@poly(m-Phenylenediamine) Particles for Chromium Reduction and Adsorption, *Environmental science & technology*, 49 (2015) 5654-5662.

- [77] Y. Zhang, H. Li, Y. Luo, X. Shi, J. Tian, X. Sun, Poly(m-phenylenediamine) nanospheres and nanorods: selective synthesis and their application for multiplex nucleic acid detection, *PloS one*, 6 (2011) e20569.
- [78] P.J. Conroy, S. Hearty, P. Leonard, R.J. O'Kennedy, Antibody production, design and use for biosensor-based applications, *Seminars in cell & developmental biology*, Elsevier, 2009, pp. 10-26.
- [79] J.M. Berg, J.L. Tymoczko, L. Stryer, *Biochemistry*, Fifth Edition, W.H. Freeman, New York, 2002.
- [80] R. Schirhagl, A. Seifner, F.T. Husain, M. Cichna-Markl, P.A. Lieberzeit, F.L. Dickert, Antibodies and Their Replicaes in Microfluidic Sensor Systems — Labelfree Quality Assessment in Food Chemistry and Medicine, *Sensor Letters*, 8 (2010) 399-404.
- [81] S. Ray, G. Mehta, S. Srivastava, Label-free detection techniques for protein microarrays: Prospects, merits and challenges, *Proteomics*, 10 (2010) 731-748.
- [82] J. Homola, Present and future of surface plasmon resonance biosensors, *Analytical and Bioanalytical Chemistry*, 377 (2003) 528-539.
- [83] K.A. Marx, Quartz crystal microbalance: a useful tool for studying thin polymer films and complex biomolecular systems at the solution-surface interface, *Biomacromolecules*, 4 (2003) 1099-1120.
- [84] D.A. Buttry, M.D. Ward, Measurement of interfacial processes at electrode surfaces with the electrochemical quartz crystal microbalance, *Chemical Reviews*, 92 (1992) 1355-1379.
- [85] R. Schumacher, *The Quartz Microbalance: A Novel Approach to the In-Situ Investigation of Interfacial Phenomena at the Solid/Liquid Junction [New Analytical Methods (40)]*, *Angewandte Chemie International Edition in English*, 29 (1990) 329-343.
- [86] V. Syritski, A. Öpik, O. Forsen, Ion transport investigations of polypyrroles doped with different anions by EQCM and CER techniques, *Electrochimica Acta*, 48 (2003) 1409-1417.
- [87] M.A. Cooper, V.T. Singleton, A survey of the 2001 to 2005 quartz crystal microbalance biosensor literature: applications of acoustic physics to the analysis of biomolecular interactions, *Journal of Molecular Recognition*, 20 (2007) 154-184.
- [88] K. Glasmästar, C. Larsson, F. Höök, B. Kasemo, Protein adsorption on supported phospholipid bilayers, *Journal of Colloid and Interface Science*, 246 (2002) 40-47.
- [89] C. Ayela, F. Roquet, L. Valera, C. Granier, L. Nicu, M. Pugnère, Antibody-antigenic peptide interactions monitored by SPR and QCM-D: A model for SPR detection of IA-2 autoantibodies in human serum, *Biosensors and Bioelectronics*, 22 (2007) 3113-3119.
- [90] F. Caruso, E. Rodda, D.N. Furlong, K. Niikura, Y. Okahata, Quartz crystal microbalance study of DNA immobilization and hybridization for nucleic acid sensor development, *Analytical Chemistry*, 69 (1997) 2043-2049.
- [91] Y. Okahata, Y. Matsunobu, K. Ijio, M. Mukae, A. Murakami, K. Makino, Hybridization of nucleic acids immobilized on a quartz crystal microbalance, *Journal of the American Chemical Society*, 114 (1992) 8299-8300.

- [92] M.I. Rocha-Gaso, Y. Jimenez, L. Francis, A. Arnau, Love Wave Biosensors: A Review, in: T. Rinken (Ed.) State of the Art in Biosensors - General Aspects 2013.
- [93] J. Cui, J. Iturri, U. Götz, M. Jimenez, A. del Campo, Analysis of responsive polymer films using surface acoustic waves, *Langmuir*, 29 (2013) 6582-6587.
- [94] V.M. Mirsky, A. Yatsimirsky, Artificial receptors for chemical sensors, John Wiley & Sons 2010.
- [95] J.A. García-Calzón, M.E. Díaz-García, Characterization of binding sites in molecularly imprinted polymers, *Sensors and Actuators B: Chemical*, 123 (2007) 1180-1194.
- [96] Y.-S. Ho, Review of second-order models for adsorption systems, *Journal of hazardous materials*, 136 (2006) 681-689.
- [97] Y. Liu, L. Shen, From Langmuir kinetics to first-and second-order rate equations for adsorption, *Langmuir*, 24 (2008) 11625-11630.
- [98] S. Azizian, Kinetic models of sorption: a theoretical analysis, *Journal of Colloid and Interface Science*, 276 (2004) 47-52.
- [99] X. Li, S.M. Husson, Adsorption of dansylated amino acids on molecularly imprinted surfaces: a surface plasmon resonance study, *Biosensors and Bioelectronics*, 22 (2006) 336-348.
- [100] Y.-S. Ho, G. McKay, Pseudo-second order model for sorption processes, *Process biochemistry*, 34 (1999) 451-465.
- [101] E. Corton, J.A. García-Calzón, M.E. Díaz-García, Kinetics and binding properties of chloramphenicol imprinted polymers, *Journal of Non-Crystalline Solids*, 353 (2007) 974-980.
- [102] K. da Mata, M.Z. Corazza, F.M. de Oliveira, A.L. de Toffoli, C.R.T. Tarley, A.B. Moreira, Synthesis and characterization of cross-linked molecularly imprinted polyacrylamide for the extraction/preconcentration of glyphosate and aminomethylphosphonic acid from water samples, *Reactive and Functional Polymers*, 83 (2014) 76-83.
- [103] Q. You, Y. Zhang, Q. Zhang, J. Guo, W. Huang, S. Shi, X. Chen, High-capacity thermo-responsive magnetic molecularly imprinted polymers for selective extraction of curcuminoids, *Journal of Chromatography A*, 1354 (2014) 1-8.
- [104] R.I. Masel, Principles of Adsorption and Reaction on Solid Surfaces, Wiley & Sons Ltd 1996.
- [105] H.J. Butt, K. Graf, M. Kappl, Adsorption, 2 ed., Wiley-VCH, Federal Republic of Germany, 2006.
- [106] R.J. Umpleby, 2nd, S.C. Baxter, Y. Chen, R.N. Shah, K.D. Shimizu, Characterization of molecularly imprinted polymers with the Langmuir-Freundlich isotherm, *Analytical chemistry*, 73 (2001) 4584-4591.
- [107] G.T. Rushton, C.L. Karns, K.D. Shimizu, A critical examination of the use of the Freundlich isotherm in characterizing molecularly imprinted polymers (MIPs), *Analytica Chimica Acta*, 528 (2005) 107-113.
- [108] E. Vale'rio, L.M. Abrantes, V.A. S., 4-Aminothiophenol Self-Assembled Monolayer for the Development of a DNA Biosensor Aiming the Detection of Cylindrospermopsin Producing Cyanobacteria, *Electroanalysis*, 20 (2008) 2467-2474.

- [109] S.-J. Xiao, M. Wieland, S. Brunner, Surface reactions of 4-aminothiophenol with heterobifunctional crosslinkers bearing both succinimidyl ester and maleimide for biomolecular immobilization, *Journal of Colloid and Interface Science*, 290 (2005) 172-183.
- [110] D.M. Disley, D.C. Cullen, H.-X. You, L.C. R., Covalent coupling of immunoglobulin G to self-assembled monolayers as a method for immobilizing the interfacial-recognition layer of a surface plasmon resonance immunosensor, *Biosensors and Bioelectronics*, 13 (1998) 1213-1225.

APPENDIX A

PAPER I

Xin Zhang, **Aleksei Tretjakov**, Marc Hovestaedt, Guoguang Sun, Vitali Syritski, Jekaterina Reut, Rudolf Volkmer, Karsten Hinrichs, Joerg Rappich, Electrochemical functionalization of gold and silicon surfaces by a maleimide group as a biosensor for immunological application, *Acta Biomaterialia*, 9(3) (2013) 5838–5844.



Electrochemical functionalization of gold and silicon surfaces by a maleimide group as a biosensor for immunological application

Xin Zhang^a, Aleksei Tretjakov^b, Marc Hovestaedt^{c,d}, Guoguang Sun^e, Vitali Syritski^b, Jekaterina Reut^b, Rudolf Volkmer^c, Karsten Hinrichs^e, Joerg Rappich^{a,*}

^a Helmholtz-Zentrum Berlin für Materialien und Energie GmbH, Institut für Silizium-Photovoltaik, Kekuléstr. 5, 12489 Berlin, Germany

^b Department of Materials Science, Tallinn University of Technology, Ehitajate tee 5, Tallinn 19086, Estonia

^c Charité Universitätsmedizin Berlin, Institut für Medizinische Immunologie, Abteilung Molekulare Bibliotheken, Hessische Str. 3-4, 10115 Berlin, Germany

^d Charité Universitätsmedizin Berlin, Institute of Biochemistry 18, Reinickendorfer Str. 61, Haus 10, D-13347 Berlin, Germany

^e Leibniz-Institut für Analytische Wissenschaften – ISAS – e.V., Department Berlin, Albert-Einstein-Str. 9, 12489 Berlin, Germany

ARTICLE INFO

Article history:

Received 2 May 2012

Received in revised form 11 September 2012

Accepted 18 October 2012

Available online 29 October 2012

Keywords:

Biosensor

Au and Si surfaces

Maleimidophenyl

Cys-peptide

Antibody

ABSTRACT

In the present study we investigated the preparation of biofunctionalized surfaces using the direct electrochemical grafting of maleimidophenyl molecules with subsequent covalent immobilization of specific peptide to detect target antibody, thereby extending the application of the biosensing systems towards immunodiagnostics. *Para*-maleimidophenyl (*p*-MP) functional groups were electrochemically grafted on gold and silicon surfaces from solutions of the corresponding diazonium salt. A specially synthesized peptide modified with cysteine (Cys-peptide) was then immobilized on the *p*-MP grafted substrates by cross-linking between the maleimide groups and the sulfhydryl group of the cysteine residues. Accordingly, the Cys-peptide worked as an antigen that was able to bind specifically the target antibody (anti-GST antibody), while it was non-sensitive to a negative contrast antibody (i.e. anti-Flag β). The immobilization of both specific and non-specific antibodies on the Cys-peptide-modified surfaces was monitored by infrared spectroscopic ellipsometry, a quartz crystal microbalance integrated in flow injection analysis system and potentiometric response. The results obtained clearly demonstrated that the direct modification of a surface with maleimidophenyl provides a very simple and reliable way of preparing biofunctionalized surfaces suitable for the construction of immunological biosensors.

© 2012 Acta Materialia Inc. Published by Elsevier Ltd. All rights reserved.

1. Introduction

In the materials and life sciences there is a great demand for biofunctionalized surfaces, which offer a variety of innovative biotechnological applications in the field of bioelectronics, biosensors and drug delivery. A great number of surface modification techniques have been developed, providing the possibility of specifically attaching biomolecules. The functionalization of metal and glass surfaces with self-assembled monolayers (SAMs) [1,2] is used extensively for the physical and chemical attachment of proteins [3]. SAMs of alkenethiols are widely employed for the modification of gold metal surfaces [4]. One drawback of this method is the instability of the gold–thiolate bond at reductive potentials, which causes the desorption of the layer [5]. Aryl diazonium salts are a possible alternative to SAMs that has considerable promise due to the high stability of the layers produced and the versatility of the chemistry. Nowadays, electrochemical reduction of organic diazonium salt is a well-known technique to graft organic

molecules [6–8], especially aromatic rings, onto metal [9–11], carbon [9,12] and semiconductor surfaces [13–15]. The organic layer formed is covalently attached to a substrate, providing a stable functionalized surface suitable for application in different research areas, such as microelectronics [16] and sensors [10,17]. Different functional groups can be introduced to the surface depending on the substituent on the *para*-position of the aryl diazonium salt. For this, electrochemical grafting of 4-carboxyphenyldiazonium [10], 4-nitrophenyldiazonium [18] and 4-aminophenyldiazonium salts [19] have been used. However, for the immobilization of biomolecules on carboxy-, nitro- and amino-derivatized surfaces, further functionalization is needed, including: the activation of carboxyl function through a carbodiimide route to allow subsequent covalent coupling with an amino group of the biomolecule [20,21]; and chemical coupling reactions with a biomolecule-reactive group, such as *N*-hydroxysuccinimide (NHS) or maleimide. Considering that biomolecular coupling through the amino groups of lysine residues in the case of NHS-modified surfaces leads to additional heterogeneities in the population of molecules, the site-specific immobilization of a biomolecule through thiol groups (i.e. cysteines) on maleimide functionalities is the preferred

* Corresponding author. Tel.: +49 30806241386.

E-mail address: rappich@helmholtz-berlin.de (J. Rappich).

method [22]. Surface modification with maleimide is usually a multistep process that includes the functionalization of the surface with amino groups followed by the attachment of some heterobifunctional crosslinker containing amine-reactive group on the one end and thiol-reactive maleimide on the other [23,24]. Recently, Harper et al. [9] reported the direct grafting of maleimide on Au and glassy carbon electrodes from *para*-maleimidophenyl diazonium tetrafluoroborate (*p*-MPDT). They showed the possibility of immobilizing biomolecules such as ferrocene and the redox-active protein cytochrome *c* on the maleimidophenyl-modified surface for the development of bioelectronic devices, including biofuel cells, biosensors, and DNA and protein microarrays.

In the present study we investigated the possibility of preparing biofunctionalized surfaces using the direct electrochemical grafting of maleimidophenyl molecules with subsequent covalent immobilization of specific peptide to detect a target antibody, thereby extending the application of the biosensing systems towards immunodiagnosics. Fig. 1 presents the method used to construct an immunological biosensor.

The first step is the modification of the electrode surfaces with *p*-MP by the electrochemical reduction of *p*-MPDT (step 1 in Fig. 1). *p*-MP is a very favourable reactive group in the cross-linking process and reacts specifically with sulphhydryl (–HS) groups in aqueous solution at a pH value between 6.5 and 7.5 to form a stable and non-reversible thioether linkage [25]. An HS group could be introduced into a target peptide (antigen) by chemical modification at its N-terminus with cysteine, so that the obtained Cys-peptide could be covalently immobilized on a maleimide-modified surface by cross-linking (as sketched for *p*-MP at step 2 in Fig. 1). We prepared biofunctionalized electrodes by the covalent immobilization of Cys-peptide on *p*-MP modified Au and/or Si substrates and investigated their specificity to interact with the target antibody (anti-GST antibody) (step 3 in Fig. 1), identifying both the specific infrared vibrational signature of amide bonds by infrared spectroscopic ellipsometry (IRSE) [26] and the mass change upon the antibody binding by the quartz crystal microbalance integrated in flow injection analysis (QCM-FIA) technique [27]. IRSE was used to characterize all the steps of the electrode modification process, including the grafting of the maleimide group, Cys-peptide and target antibodies immobilization by their specific vibrational signature. Additionally, the interaction between Cys-peptide and the

antibody was monitored by zero current potential (U_2) measurements between the biofunctionalized electrode (as a working electrode) and the reference electrode during the anti-GST antibody binding. Thus, the biosensing process was displayed in real time via a simple electrochemical response.

2. Experimental section

2.1. Substrates

A 200 nm polycrystalline Au film deposited on the glass with a 3 nm Ti coadhesive layer and *p*-Si(111) substrates were used as electrodes for the electrochemical grafting process. The Au surfaces were cleaned using fresh piranha solution (97% H_2SO_4 :30% $\text{H}_2\text{O}_2 = 1:1$) for 20 s, then rinsed copiously with deionized water. *p*-Si(111) wafers (0.5–2.5 Ω cm), covered by a 100 nm thick oxide layer and polished on one side, were purchased from the Leibniz Institute for Crystal Growth (IKZ). Before any modification, the SiO_2/Si samples were treated ultrasonically in 2-propanol for 10 min before being washed with deionized water. Then hydrogenated *p*-Si(111) surfaces were prepared in three steps. First, the Si samples were immersed in 5% HF for 10 min to remove the oxide layer. Second, the samples were reoxidized for 10 min in freshly prepared piranha solution. Next, the Si samples were rinsed by water and immersed in 40% NH_4F for 6–8 min to obtain a flat and hydrogen-terminated Si surface [15]. Finally, the samples were washed with deionized water and dried by nitrogen. The HF, NH_4F , H_2SO_4 and H_2O_2 solutions used were supplied by Aldrich® with grade Selectipure® (VLSI grade). The water used was purified by a PURELAB® Ultra water system ($\leq 18 \text{ M}\Omega$ cm at 25 °C).

2.2. Chemicals and materials

The *p*-MPDT used in this work was synthesized from *N*-(4-aminophenyl)maleimide (TCI Europa) and identified by nuclear magnetic resonance spectroscopy in $\text{CD}_3\text{-CN}$ (8.55 dbt, 2H; 8.12 dbt, 2H; 7.07 singlet, 2H). The reagents and solvents employed were used as received, and were as follows: anhydrous acetonitrile (ACN, 99.8%, Sigma–Aldrich) and electrochemical grade tetrabutylammonium tetrafluoroborate (Bu_4NBF_4 , $\geq 99.0\%$, Fluka). Phosphate-buffered saline powder (PBS, pH 7.4), and Tris-buffered saline powder (TBS, pH 8.0) were bought from Sigma and dissolved in deionized water to obtained 0.05 M buffer solution.

The specific peptide with the amino acid sequence LAKDLIVPRR was specially synthesized for immobilization of the target antibody – a murine anti-GST IgG (Sigma–Aldrich). The selectivity and sensitivity of the synthesized peptides was verified by complete substitution analysis and affinity determinations with surface plasmon resonance spectroscopy. These binding of these peptides to other antibodies was also tested, including anti-p24 (HIV) CB 4-1 IgG, anti-TGF α -IgG, anti-Flag β antibody and anti-mouse IgG. None of the antibodies showed any interaction with the peptide used. Thus, the LAKDLIVPRR peptide and anti-GST IgG interaction is very specific, and is very well suited as a model reaction for the biosensor study. Anti-Flag β antibody was taken as the negative contrast. A variant of peptide LAKDLIVPRR was produced then with an N-terminal cysteine (Cys)-linker β Ala in milligram amounts by solid-phase synthesis.

2.3. Electrochemical grafting

The *p*-MP layers were electrochemically grafted onto either Au or Si surfaces via the appropriate procedures described below. For the Au surface grafting process, an electrochemical cell accommodating three electrodes, i.e. a gold-coated glass slide as the working

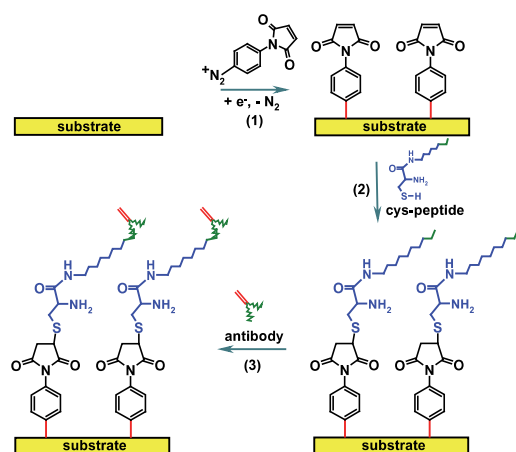


Fig. 1. Scheme of an antibody immobilization onto *p*-MP modified substrate: (1) electrochemical modification by *p*-MP functional groups; (2) coupling of Cys-peptide; and (3) target antibody immobilization.

electrode, a gold wire counter electrode and an Ag/AgCl (3 M KCl) reference electrode, was used. All the electrodes were connected to a potentiostat/galvanostat (Ivium Technologies, CompactStat™) and the deposition of the *p*-MP layers was carried out from ACN solution containing 2 mM *p*-MPDT and 0.1 M Bu₄NBF₄ by cyclic voltammetry, ramping the potential between +0.75 V and –0.6 V at a rate of 50 mV s^{–1} several times. After the deposition, the *p*-MP-functionalized Au surface was cleaned ultrasonically in ACN for 2 min and dried in N₂ stream.

For electrochemical grafting of the *p*-MP layer onto the Si surface, chronoamperometry in combination with the injection technique was used [15]. The hydrogenated p-Si(111) surfaces were immersed in 4 units of volume of the acetonitrile solution with 0.1 M tetrabutylammonium salt. The solution was stirred using a magnet bar and a potential of –2 V was applied to prevent the Si surface from oxidizing and to ensure the reduction of the diazonium ions. After a short time period (about 20 s), 1 unit of volume of 10 mM *p*-MPDT solution was injected into the electrochemical cell. The total concentration of the diazonium ions in the cell was quickly changed to 2 mM under stirring.

2.4. Biofunctionalization of the *p*-MP modified surfaces

The specific synthesized Cys-peptide was immobilized on the maleimide-modified surface at room temperature by a cross-linking reaction performed in PBS solution containing 0.5 mg ml^{–1} of Cys-peptide for several hours. The Cys-peptide-modified surfaces were then tested for biological recognition ability by immersing them in the TBS solution containing 0.08–50 μg ml^{–1} of either specific (anti-GST) or non-specific (anti-Flag β) antibodies. The biosensing process was monitored by IRSE, QCM-FIA and potentiometric response, as described below.

2.5. IRSE measurements

The IR ellipsometric measurements were performed with a photometric ellipsometer attached to a Bruker 55 or Vertex 70 Fourier transform spectrometer as described in detail elsewhere [26,28]. The Kramers–Kronig-related ellipsometric parameters tanψ and Δ, which are defined through $\tan\psi/e^{i\Delta} = r_p/r_s$, where r_p and r_s are the complex reflection coefficients polarized in parallel and perpendicularly, respectively, with respect to the plane of incidence. The spectra were obtained at an angle of incidence of 65° with a resolution of 4 cm^{–1} using a mercury cadmium telluride detector (KV104-1, Kolmar Technologies, Newburyport, MA, USA). All samples were purged for 0.5 h in a dry air environment before starting the measurements to eliminate the influence of H₂O and CO₂. IRSE was established recently for the characterization of electrochemically prepared organic films on Au and Si [29,30].

2.6. Electrochemical quartz crystal microbalance (EQCM)

The EQCM measurements were performed using the QCM100 system (Stanford Research Systems, Inc., Sunnyvale, CA, USA) connected to a potentiostat/galvanostat (Reference 600™, Gamry Instruments, Inc, Warminster, PA, USA) and a counter (PM6680B, Fluke Corporation, Everett, WA, USA), as described in Ref. [27]. A custom-made 8 ml Teflon electrochemical cell accommodated three electrodes, where the liquid face of a one inch diameter, polished, gold-coated 5 MHz crystal (Maxtek, Inc.) served as the working electrode, a rectangular shaped platinum plate (4 × 1.5 cm²) was used as the counter electrode and Ag/AgCl (3 M KCl) was used as the reference electrode, respectively.

2.7. QCM-FIA measurements

The antibody binding to the Cys-peptide functionalized Au surface was studied in a QCM-FIA system comprising two programmable precision syringe pumps (Cavro® XLP 6000, Tecan Nordic AB, Mölndal, Sweden), a motorized six-way port injection valve (C22-3186EH, VICI® Valco Instruments Company Inc., USA) controlled by a microelectric actuator, and a small volume (150 μl) axial flow cell attached to the QCM sensor holder (Stanford Research Systems, Inc.) [27]. All elements of the system were connected to a PC and controlled by software written in Labview.

For the QCM-FIA measurements, the Cys-peptide functionalized QCM sensor was placed into the flow cell and the working buffer (TBS, pH 8.0) was pumped at 62.5 μl min^{–1} by the syringe pump until a constant baseline of the QCM sensor resonant frequency was reached. Subsequently, various concentrations of either anti-GST IgG antibody (specific) or anti-Flag β antibody (non-specific) (8 × 10^{–5}–5 × 10^{–2} mg ml^{–1}) prepared in the same buffer were injected into the flow stream via an injection loop (250 μl). The amount of the antibodies adsorbed was calculated from the recorded resonant frequency change using the Sauerbrey equation.

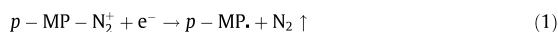
2.8. Immuno-electrode potentiometric response measurement

The change in the potential difference between the immuno-electrode and a reference electrode, U_Z , was determined during galvanostatic control so that no net current flow ($I = 0$) was observed, thereby avoiding any electrochemical reduction/oxidation of the solvent or surface molecules. Any change in potential should then be due to the change in the surface potential caused by the adsorbed and/or bonded surface species (i.e. antibodies). Thus, the behaviour of U_Z should follow the trend observed for the QCM-FIA measurement.

3. Results and discussion

3.1. Electrochemical grafting of the *p*-MP layer

Fig. 2a shows the cyclic voltammograms of an Au surface in contact with the electrolyte solution containing 2 mM *p*-MPDT and 0.1 M Bu₄NBF₄ in ACN. The current peak, which occurred at about 200 mV during the first potential scan, is attributed to the reduction of the diazonium ions. The diazonium group of the *p*-MPDT is reduced by an electron transfer from the Au electrode followed by the separation of an N₂ molecule from the aryl ring (reaction 1). The aryl radical thus originated reacts with the Au surface to form a stable covalent bond [19], and a *p*-MP layer is formed.



In the second potential scan, the current response is strongly reduced, indicating that the surface is already passivated by *p*-MP groups. Therefore, additional scans show a further weak reduction in current since the *p*-MP layer continues to grow and consequently blocks the electron transfer at the solution/electrode interface. Also, the mass response, recorded by the EQCM, reflects relevant behaviour coincident with the effect of the growing MP layers. The mass increases significantly in the first scan, by about 0.28 μg cm^{–2}; thereafter, the mass increase is reduced by every additional potential scan, from 0.06 down to about 0.03 μg cm^{–2}, respectively (Fig. 2a, top). Thus, the first scan generates a *p*-MP layer with the thickness of about one monolayer, assuming the surface area of maleimidobenzene to be 10.9 Å² and close-packed *p*-MP layer growth. After five potential scans, the *p*-MP layer reaches a nominal thickness of about two monolayers.

The cyclic voltammetry method is not applicable for deposition of *p*-MP layer on Si surfaces, due to the oxidation of the hydrogenated Si(111) surface at potentials that are more anodic than the reduction of the diazonium ion. To avoid the oxidation of Si–H surfaces, another method – the injection technique (chronoamperometry plus the addition of the diazonium salt at a certain time) – was used. The chronoamperometric curves for the electrochemical grafting of *p*-MP molecules onto the hydrogenated p-Si(111) surfaces are shown in Fig. 2b. The cathodic current shows a rapid increase when the diazonium compound is added to the solution, followed by a strong decrease in current flow up to about 60 s and a levelling out of the current at longer times. This sharp current peak shows that the first monolayer of grafted *p*-MP molecules is completed within 60 s, as confirmed by quantitative calculation of the transferred electrons according to reaction (1). The following current decrease after that turning point ($t = 60$ s) is much slower because of the steric hindrance for the further reaction of MP radicals by the organic layer. The thickness of the *p*-MP layer on the Si surface is about two monolayers after 250 s deposition, as calculated from the charge consumed during the deposition considering a two-electron transfer reaction [14]. This very thin layer is one reason for the steric hindrance of *p*-MP in the *ortho* position [31]. Therefore, the typical polymer formation via phenyl radical binding to this *ortho* position [7,8,32] is strongly inhibited for maleimidobenzene due to the size of the maleimido group. This layer thickness is in general agreement with the one found for other thin layers, as obtained for binding of poly(*n*-butyl methacrylate) via a $-C_6H_4-CH(CH_3)-Br$ aryl layer [33], 3,5-bis-*tert*-butyl benzene [31] and nitrophenyl [34].

The steric effect of the *p*-MP group is a crucial point for the whole deposition process, leading to its low efficiency ($\sim 20\%$), as obtained from the in situ EQCM experiment correlating the mass and charge responses.

3.2. IR spectroscopy of the *p*-MP layer

The presence of the *p*-MP layer on the Au and Si surfaces was confirmed by its characteristic molecular vibrational signature as measured by the IRSE technique (Fig. 3). The curves represent the $\tan\Psi$ spectra of the maleimidophenyl-modified Au and Si surfaces, respectively. The strong peak at 1728 cm^{-1} and the weak peak at 1785 cm^{-1} are assigned to the symmetric and antisymmetric stretching vibrations of two C=O groups from the maleimide ring, respectively [35,36]. The peaks at 1418 and 1383 cm^{-1} are assigned to the symmetric vibration of C–N–C from maleimide and the vibration of the aryl C–N bond, respectively [35,36]. The peak

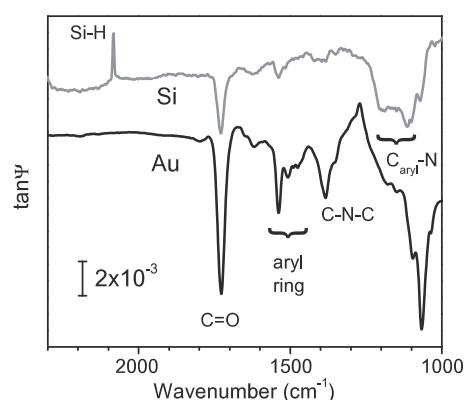


Fig. 3. IRSE spectra of *p*-MP covered Au and Si surfaces. The loss of Si–H (at 2083 cm^{-1}) is clearly seen after the grafting of *p*-MP by the pronounced C=O and N–H bond vibration structure.

at 2083 cm^{-1} for the Si sample is a result of the loss of Si–H bonds by the grafting of the maleimidophenyl group.

3.3. IR spectroscopy for the Cys-peptide and antibody-modified *p*-MP layer

Biofunctionalization of *p*-MP modified surfaces by the covalent attachment of the specially synthesized Cys-peptide and the subsequent affinity binding of the specific (Fig. 4a) or non-specific (Fig. 4b) antibody were also investigated by the IRSE technique. To highlight the changes during every recognition process, the IRSE spectra after modification by Cys-peptide were normalized to the spectra of the surfaces modified with *p*-MP. After coupling with antibodies, the IRSE spectra were normalized to the spectra of the surfaces modified with Cys-peptide. Because all of the peptide and antibodies are identified by the amide I and II bands [37], only the amide bands and C=O vibration are discussed to show the modification process.

The curves 1 in Fig. 4a and b show the *p*-MP modified Si surfaces as identified by C=O vibration at 1728 cm^{-1} and other small bands (discussed above). The successful modification with the Cys-peptide was confirmed by the strong amide I and II peaks at 1676 and 1538 cm^{-1} in curves 2, respectively. The peak upwards at about

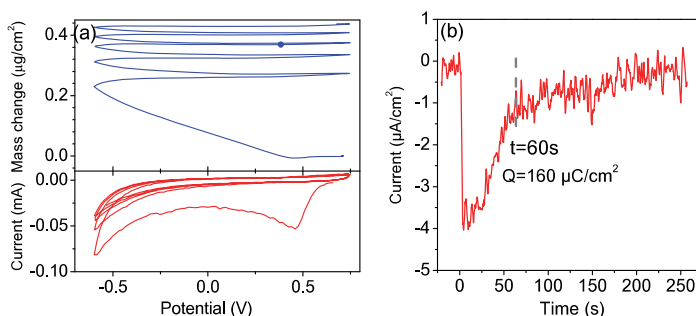


Fig. 2. (a) Cyclic voltammogram (bottom) and respective mass response (top) measured on Au-coated QCM in 2 mM *p*-MPDT with 0.1 M Bu₄NBF₄ in ACN at 50 mV s^{-1} ; (b) chronoamperometry during the electrochemical grafting of *p*-MP molecules on hydrogenated p-Si(111) surface from 2 mM *p*-MPDT in ACN solution. The diazonium salt was injected at time position 0.

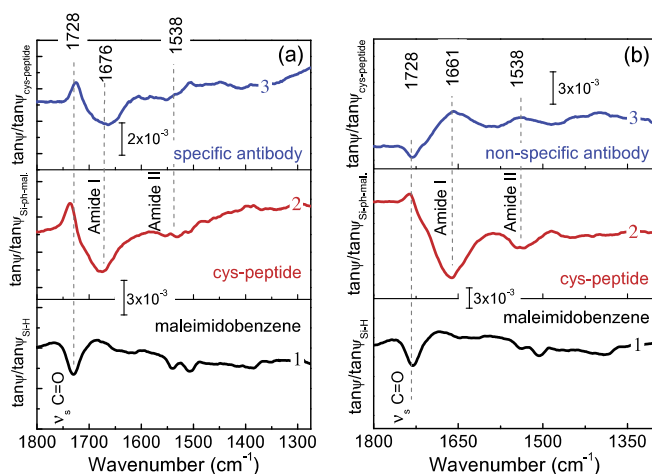


Fig. 4. Tan Ψ spectra of Si surfaces terminated by *p*-MP normalized to bare surface (black line, 1), to a Cys-peptide-modified *p*-MP layer normalized to the *p*-MP terminated surface (red line, 2), and (blue line, 3) after coupling with specific antibody (left, a) and with non-specific antibody (right, b) normalized to the Cys-peptide-modified surface.

1728 cm^{-1} reflects the decoupling of the C=O vibration in the maleimide group by losing the C=C double bond through Cys-peptide binding. The amide peaks in curve 3 of Fig. 4a show the successful binding of specific antibody onto the surface since there is still a strong increase in the amide I and II peaks after the deduction of the peptide signal. The small peaks at 1661 and 1538 cm^{-1} in curve 3 of Fig. 4b indicate that non-specific antibody was not adsorbed on the Cys-peptide surface and a small amount of physically adsorbed peptide was removed. This difference shows the selectivity of the biosensing process. This measurement could also be considered as an ex situ biosensing technique using Si- and Au-based biosensors.

3.4. Application for biological sensors

Because the Cys-peptide could work as a binding site for an antigen, the above-mentioned Cys-peptide-modified surfaces were investigated for their biosensing capabilities with respect to their selective interaction (step 3 in Fig. 1) with the target antibody (anti-GST). We used a QCM-FIA technique to demonstrate the potential analytical efficiency of such Cys-peptide-modified surfaces for the development of biochemical sensors feasible for label-free detection in antigen antibody immunoassays.

Fig. 5a shows the massogram obtained with the Cys-peptide-modified QCM sensors upon consecutive additions of antibody solutions with concentration increasing from 0.08 to 50 $\mu\text{g ml}^{-1}$. In particular, curves 1 and 2 represent cases for solutions containing the specific (anti-GST) and non-specific (anti-flag β) antibodies, respectively. As expected, the Cys-peptide-modified surface clearly demonstrates its significantly higher affinity for anti-GST than for anti-Flag β . Remarkably, the QCM sensor reveals an increase binding activity at anti-GST concentrations exceeding 10 $\mu\text{g ml}^{-1}$, with the greatest mass change occurring at 50 $\mu\text{g ml}^{-1}$. However, in anti-Flag β solutions the sensor reaches the binding saturation value at 10 $\mu\text{g ml}^{-1}$, with no further increase occurring at higher concentrations. Obviously, some non-specific binding sites still exist on the *p*-MP/Cys-peptide-modified Au surface.

Since the interaction between an antigen and an antibody is a pure biochemical reaction that occurs without any electron transfer, the charge of the Cys-peptide-modified electrode will strongly depend on the amount of antibody specifically bound to its surface and thus will shift the Fermi level of the electrode with respect to

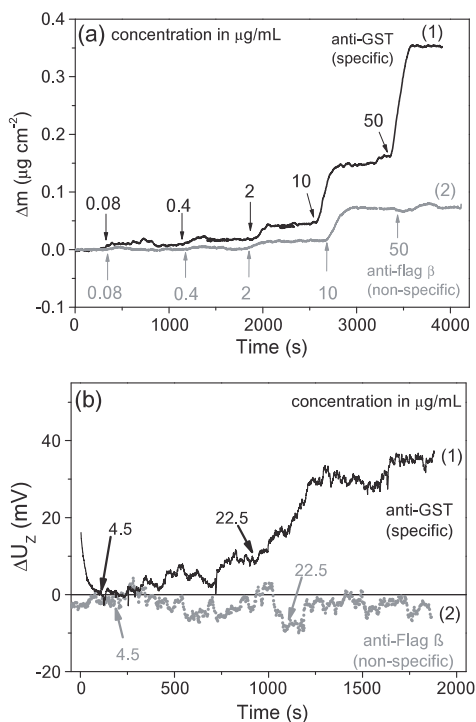


Fig. 5. (a) Frequency response of the Cys-peptide-modified Au electrodes (QCM) as a function of time after the addition of different concentrations (from 0.08 to 50 $\mu\text{g ml}^{-1}$) of solutions of specifically binding anti-GST antibody (1) and non-specific anti-Flag β antibody (2); (b) electrical response of a Cys-peptide-modified Si electrode after the addition of anti-GST antibody (1) and anti-Flag β antibody (2).

the solution. Consequently, potentiometry could be used as a method for detecting antibody [38–40] directly, without the need of labels or indicators. The surface charge caused by immobilized

biological species will be changed after coupling with corresponding species in the sample. Therefore, we measured the changes in the potential at zero current condition (U_z) of the Cys-peptide-modified Si electrode (the so-called immunoelectrode sensor) upon exposing it to the buffer solution with different concentrations of the antibodies. The plots in Fig. 5b show the difference in $\Delta U_z = U_z - U_z(t = 150 \text{ s})$ after the addition of a solution containing either the specific or the non-specific antibody (curves 1 and 2, respectively). In the first 120 s, before the injection of 100 μl of anti-GST antibody, the potential drops down and stabilizes at about $U_z(t = 150 \text{ s}) = -0.4 \text{ V}$. After injection of the specific antibody (to give a concentration in the cell of 4.5 $\mu\text{g ml}^{-1}$), ΔU_z increases slowly and becomes slightly noisy.

The increase in ΔU_z is more pronounced after injection of additional 300 μl of anti-GST antibody (concentration in the cell = 22.5 $\mu\text{g ml}^{-1}$) after about 1000 s. The potential change is caused by the coupling of the antibody to the Cys-peptide and amounts to about 40 mV, as shown by curve 1 in Fig. 5b. As a negative contrast, a second Si sample modified with Cys-peptide was fixed in the same environment ($I = 0$, in 10 ml of TBS buffer). In the first 100 s, no antibody was injected into the cell (curve 2 in Fig. 5b) and the potentiometric response was noisy but did not change as much as observed for the specific antibody in the cell. After injection of 100 and 300 μl of non-specific antibody (concentrations in the cell of 4.5 and 22.5 $\mu\text{g ml}^{-1}$, respectively), the potential changed only slightly. The noise of the electrical response is possibly influenced by the light in the laboratory, which induced a charge carrier in the Si substrate.

4. Conclusions

Biofunctionalization of Au or Si surfaces with the specific Cys-peptide based on the direct electrochemical grafting of maleimide group was demonstrated. The electrochemical deposition of maleimidobenzene led to an ultra thin layer with a thickness of about two monolayers after five scans in the case of the Au electrode and after 250 s of deposition on the Si electrode. IRSE spectra confirmed the multilayer formation on the electrode surface.

Each stage of the surface modification was proved qualitatively by IRSE spectra. The biosensing capabilities of the obtained Cys-peptide functionalized surfaces was clearly demonstrated ex situ by an increase in the absorption due to amide I and II bands in the IRSE spectra, as well as in situ by the identification of target antibody specific binding by the QCM-FIA technique and by potentiometric measurements. It was found that the electrical sensing process at zero current (chronopotentiometry) was very sensitive to the coupling of the target antibody on the modified Si surface, and a change in potential of about 40 mV was observed at a concentration of 22.5 $\mu\text{g ml}^{-1}$ whereas no distinct change in potential was visible for the non-specific antibody. QCM-FIA measurements showed the selectivity of the functionalized Au surface towards the target antibody, while a slight affinity to the non-specific antibody was also observed. More tests are required for this type of sensing system. Nevertheless, the results obtained clearly demonstrate that the direct modification of a surface with maleimidophenyl provides a very simple and reliable way to prepare biofunctionalized surfaces suitable for the construction of immunological biosensors. Furthermore, other kinds of biomolecules (DNA, protein, etc.) could be connected to such an electrochemically modified surface to provide a way to construct biosensing devices.

Acknowledgements

The financial support of the European Union through the EFRE Program (ProFIT Grant, Contract No. 10136530/1/2) is gratefully

acknowledged. V.S. and J.R. thank the Estonian Ministry of Education and Research Grants (SF0140033s12 and ETF8249) for financial support. We thank Ilona Fischer for technical assistance.

Appendix A. Figures with essential colour discrimination

Certain figures in this article, particularly Figs. 1, 2 and 4, are difficult to interpret in black and white. The full colour images can be found in the on-line version, at <http://dx.doi.org/10.1016/j.actbio.2012.10.022>.

References

- [1] Ulman A. Formation and structure of self-assembled monolayers. *Chem Rev* 1996;96:1533.
- [2] Eckermann AL, Feld DJ, Shaw JA, Meade TJ. Electrochemistry of redox-active self-assembled monolayers. *Coord Chem Rev* 2010;254:1769.
- [3] Ferretti S, Paynter S, Russell DA, Sapsford KE, Richardson DJ. Self-assembled monolayers: a versatile tool for the formulation of bio-surfaces. *TrAC Trends Anal Chem* 2000;19:530.
- [4] Nuzzo RG, Zegarski BR, Dubois LH. Fundamental studies of the chemisorption of organosulfur compounds on gold(111). Implications for molecular self-assembly on gold surfaces. *J Am Chem Soc* 1987;109:733.
- [5] Walczak MM, Popenoe DD, Deinhammer RS, Lamp BD, Chung C, Porter MD. Reductive desorption of alkanethiolate monolayers at gold: a measure of surface coverage. *Langmuir* 1991;7:2687.
- [6] Bélanger D, Pinson J. Electrografting: a powerful method for surface modification. *Chem Soc Rev* 2011;40:3995.
- [7] Chehimi MM, editor. Aryl diazonium salts: new coupling agents in polymer and surface science. Weinheim: Wiley-VCH Verlag; 2012.
- [8] Pinson J, Podvorica F. Attachment of organic layers to conductive or semiconductive surfaces by reduction of diazonium salts. *Chem Soc Rev* 2005;34:429.
- [9] Harper JC, Polsky R, Wheeler DR, Brozik SM. Maleimide-activated aryl diazonium salts for electrode surface functionalization with biological and redox-active molecules. *Langmuir* 2008;24:2206.
- [10] Liu GZ, Bocking T, Gooding JJ. Diazonium salts: Stable monolayers on gold electrodes for sensing applications. *J Electroanal Chem* 2007;600:335.
- [11] Zhang X, Sun G, Hinrichs K, Janietz S, Rappich J. Infrared spectroscopic study of the amidation reaction of aminophenyl modified Au surfaces and p-nitrobenzoic acid as model system. *Phys Chem Chem Phys* 2010;12:12427.
- [12] Delamar M, Hitmi R, Pinson J, Saveant JM. Covalent modification of carbon surfaces by grafting of functionalized aryl radicals produced from electrochemical reduction of diazonium salts. *J Am Chem Soc* 1992;114:5883.
- [13] Buriak JM. Organometallic chemistry on silicon and germanium surfaces. *Chem Rev* 2002;102:1271.
- [14] de Villeneuve CH, Pinson J, Bernard MC, Allongue P. Electrochemical formation of close-packed phenyl layers on Si(111). *J Phys Chem B* 1997;101:2415.
- [15] Hartig P, Dittrich T, Rappich J. Surface dipole formation and non-radiative recombination at p-Si(111) surfaces during electrochemical deposition of organic layers. *J Electroanal Chem* 2002;524:120.
- [16] Joyeux X, Mangiagalli P, Pinson J. Localized attachment of carbon nanotubes in microelectronic structures. *Adv Mater* 2009;21:4404.
- [17] Gooding JJ. Advances in interfacial design sensors: aryl diazonium salts for electrochemical biosensors and for modifying carbon and metal electrodes. *Electroanalysis* 2008;20:573.
- [18] Harper JC, Polsky R, Wheeler DR, Lopez DM, Arango DC, Brozik SM. A multifunctional thin film Au electrode surface formed by consecutive electrochemical reduction of aryl diazonium salts. *Langmuir* 2009;25:3282.
- [19] Lyskawa J, Bélanger D. Direct modification of a gold electrode with aminophenyl groups by electrochemical reduction of in situ generated aminophenyl monodiazonium cations. *Chem Mater* 2006;18:4755.
- [20] Mandon CA, Blum LJ, Marquette CA. Aryl diazonium for biomolecules immobilization onto SPRi chips. *Chempophyschem* 2009;10:3273.
- [21] Mahouche-Chergui S, Gam-Deroich S, Mangeney C, Chehimi MM. Aryl diazonium salts: a new class of coupling agents for bonding polymers, biomacromolecules and nanoparticles to surfaces. *Chem Soc Rev* 2011;40:4143.
- [22] Zimmermann JL, Nicolaus T, Neuert G, Blank K. Thiol-based, site-specific and covalent immobilization of biomolecules for single-molecule experiments. *Nat Protoc* 2010;5:975.
- [23] Lee CS, Baker SE, Marcus MS, Yang WS, Eriksson MA, Hamers RJ. Electrically addressable biomolecular functionalization of carbon nanotube and carbon nanofiber electrodes. *Nano Lett* 2004;4:1713.
- [24] Zhang X, Sun GG, Hovestadt M, Syritski V, Esser N, Volkmer R, et al. A new strategy for the preparation of maleimide-functionalised gold surfaces. *Electrochem Commun* 2010;12:1403.
- [25] Hermanson GT. *Bioconjugate techniques*. Elsevier; 2008.
- [26] Hinrichs K, Gensch M, Esser N. Analysis of organic films and interfacial layers by infrared spectroscopic ellipsometry. *Appl Spectrosc* 2005;59:272a.
- [27] Syritski V, Reut J, Menaker A, Gyurcsányi RE, Öpik A. Electrolytically synthesized molecularly imprinted polypyrrole films for enantioselective recognition of L-aspartic acid. *Electrochim Acta* 2008;53:2729.

- [28] Mikhaylova Y, Ionov L, Rappich J, Gensch M, Esser N, Minko S, et al. In situ infrared ellipsometric study of stimuli-responsive mixed polyelectrolyte brushes. *Anal Chem* 2007;79:7676.
- [29] Roodenko K, Mikhaylova Y, Ionov L, Gensch M, Stamm M, Minko S, et al. Ultrathin responsive polyelectrolyte brushes studied by infrared synchrotron mapping ellipsometry. *Appl Phys Lett* 2008;92:103102.
- [30] Rappich J, Hinrichs K. In situ study of nitrobenzene grafting on Si(111)-H surfaces by infrared spectroscopic ellipsometry. *Electrochem Commun* 2009;11:2316.
- [31] Combellas C, Kanoufi F, Pinson J, Podvorica F. Sterically hindered diazonium salts for the grafting of a monolayer on metals. *J Am Chem Soc* 2008;130:8576.
- [32] Bernard M-C, Chaussé A, Cabet-Deliry E, Chehimi MM, Pinson J, Podvorica F, et al. Organic layers bonded to industrial, coinage, and noble metals through electrochemical reduction of aryl diazonium salts. *Chem Mater* 2003;15:3450.
- [33] Matrab T, Save M, Charleux B, Pinson J, Cabet-deliry E, Adenier A, et al. Grafting densely-packed poly(n-butyl methacrylate) chains from an iron substrate by aryl diazonium surface-initiated ATRP: XPS monitoring. *Surf Sci* 2007;601:2357.
- [34] Anariba F, DuVall SH, McCreery RL. Mono- and multilayer formation by diazonium reduction on carbon surfaces monitored with atomic force microscopy "scratching". *Anal Chem* 2003;75:3837.
- [35] Hinrichs K, Gensch M, Esser N, Schade U, Rappich J, Kroning S, et al. Analysis of biosensors by chemically specific optical techniques. Chemiluminescence-imaging and infrared spectroscopic mapping ellipsometry. *Anal Bioanal Chem* 2007;387:1823.
- [36] Parker SF, Mason SM, Williams KPJ. Fourier transform Raman and infrared spectroscopy of N-phenylmaleimide and methylene dianiline bismaleimide. *Spectrochim Acta A Mol Spectrosc* 1990;46:315.
- [37] Onodera K, Hirano-Iwata A, Miyamoto KI, Kimura Y, Kataoka M, Shinohara Y, et al. Label-free detection of protein-protein interactions at the GaAs/water interface through surface infrared spectroscopy: discrimination between specific and nonspecific interactions by using secondary structure analysis. *Langmuir* 2007;23:12287.
- [38] Janata J. Immuno-electrode. *J Am Chem Soc* 1975;97:2914.
- [39] Liang RP, Peng HZ, Qiu JD. Fabrication, characterization, and application of potentiometric immunosensor based on biocompatible and controllable three-dimensional porous chitosan membranes. *J Colloid Interface Sci* 2008;320:125.
- [40] Yuan R, Tang DP, Chai YQ, Zhong X, Liu Y, Dai JY. Ultrasensitive potentiometric immunosensor based on SA and OCA techniques for immobilization of HBsAb with colloidal Au and polyvinyl butyral as matrixes. *Langmuir* 2004;20:7240.

PAPER II

Aleksei Tretjakov, Vitali Syritski, Jekaterina Reut, Roman Boroznjak, Olga Volobujeva, and Andres Öpik, Surface molecularly imprinted polydopamine films for recognition of immunoglobulin G, *Microchimica Acta*, 180(15) (2013) 1433-1442.

Surface molecularly imprinted polydopamine films for recognition of immunoglobulin G

Aleksei Tretjakov · Vitali Syritski · Jekaterina Reut · Roman Boroznjak · Olga Volobujeva · Andres Öpik

Received: 5 November 2012 / Accepted: 30 June 2013 / Published online: 14 July 2013
© Springer-Verlag Wien 2013

Abstract We have prepared a surface imprinted polymer (SIP) film for label-free recognition of immunoglobulin G (IgG). The IgG-SIPs were obtained by covalent immobilization of IgG via a cleavable covalent bond and a suitable spacer unit to a gold electrode, followed by electrodeposition of a nm-thin film of polydopamine (PDA). The IgG was then removed by destruction of the cleavable bond so that complementary binding sites were created on the surface of the film. IgG-SIPs with various thicknesses of the PDA films were compared with respect to their affinity to IgG using a quartz crystal microbalance combined with flow injection analysis. The films were also characterized by cyclic voltammetry and scanning electron microscopy. The IgG-SIPs with a film thickness of around 17 nm showed the most pronounced imprinting effect (IF 1.66) and a binding constant of 296 nM.

Keywords Molecularly imprinted polymers · IgG · Polydopamine · EQCM · QCM · FIA · Electrochemical polymerization

Introduction

Today, the concept of molecular imprinting has been widely recognized as a promising strategy for developing robust

molecular recognition materials with high specificity toward the analyte [1]. Molecular imprinting consists in polymerization of a mixture of functional monomers in the presence of a target molecule that acts as a template. During polymerization, the template induces binding sites in the reticulated polymer that are capable to selectively recognize the target molecules or similar structures after removal of the templates from the polymer. The main benefits of these so-called Molecularly Imprinted Polymers (MIPs), are related to their synthetic nature, i.e., excellent chemical and thermal stability associated with reproducible, cost-effective fabrication. Therefore, MIPs have a substantial potential for application in various fields such as chemical analysis and detection [2], separation and purification [3], drug delivery [4], and catalysis [5]. In addition, MIPs have been shown to be a promising alternative to natural biological receptors (e.g. enzymes, DNA, antibodies) in biosensors providing more stable and low-cost recognition elements [1].

However, there remain many unsolved issues in the development of MIP-based biosensors, especially concerning the imprinting of high molecular weight templates, proteins or whole cells. The main drawbacks in protein imprinting including permanent entrapment, poor mass transfer, denaturation, and heterogeneity in binding sites, are commonly attributed to the inherent properties of proteins such as conformational instability, large size, and complexity. Moreover the need of synthesis in aqueous media can present serious difficulties as aqueous solutions significantly reduce the binding strength of the non-covalent template—monomer interactions. The surface imprinting approach resulting in polymer with the imprinted sites situated at or close to the surface—Surface Imprinted Polymers (SIPs)—as well as introducing new biocompatible monomers are promising ways to overcome these difficulties. SIPs have many advantages such as monoclonal binding sites; faster mass transfer and hence stronger

Electronic supplementary material The online version of this article (doi:10.1007/s00604-013-1039-y) contains supplementary material, which is available to authorized users.

A. Tretjakov · V. Syritski (✉) · J. Reut · R. Boroznjak · O. Volobujeva · A. Öpik
Department of Materials Science, Tallinn University of Technology, Ehitajate tee 5, 19086 Tallinn, Estonia
e-mail: syritski@gmail.com

binding capacity as compared to traditional MIPs [6]. SIPs for selective protein recognition were realized by implementing various protocols based on immobilization of a target protein on different support materials acting either as a sacrificial [7], or a transfer material [6]. Li et al. has prepared the SIP nanowires exhibiting highly selective recognition for a variety of template proteins, including albumin, hemoglobin, and cytochrome *c* [8]. Qin et al. demonstrated a possibility to combine surface initiated living-radical polymerization with a protein SIP and prepared the lysozyme-SIP beads capable of separating the template from competitive proteins in a chromatographic column [9]. Sellergren's group introduced hierarchical imprinting to produce MIP particles with surface-confined binding sites for a small molecule of amino acid [10], as well as for peptide [11] and protein [12]. Recently, we have achieved success in the development of surface imprinted poly(3,4-ethylenedioxythiophene) microstructures for avidin specific recognition [13, 14].

Immunoglobulin G (IgG) is the most plentiful class of antibodies present in human serum, and protects organism against bacterial and viral infections. Analyzing the presence of specific IgG molecules in the body fluids can be useful in diagnosing infections or certain illnesses. Despite the numerous successful reports on molecular imprinting of different kinds of proteins, only a few attempts have been made to imprint IgG [12, 15]. The difficulties in producing of the complementary cavities for IgG in a polymer matrix are mainly attributed to the complex Y-shape structure of an antibody molecule as well as the considerable amount of chemically identical groups in one molecule. A significant progress has been recently achieved by Dickert and co-workers who produced artificial antibody replicas by applying IgG-imprinted nanoparticles as templates in a surface imprinting process to generate SIP thin films directly on the sensor electrodes of a quartz crystal microbalance (QCM) [15].

QCM technique is a widely applied for the investigation of biomolecular interactions allowing the real-time analysis of reactions without labeling requirements [16]. Furthermore, a QCM sensor integrated in a FIA system (QCM-FIA) provides the advantage to monitor on-line the binding events of an analyte and could be applied to analysis of specific interactions such as antigen-antibody [17], protein-drug [18] as well as between MIP films and template molecules [19].

Although the significant achievements were reported for preparation of different protein MIPs formats, the use of thin MIP films seems to be preferred for sensing applications. MIP films can be easily integrated with different sensor transducers (e.g. optical, piezoelectric) allowing real-time label-free monitoring of protein binding events. Electrochemical polymerization is one of the prospective approaches for combining a MIP film with a sensor transducer surface. In this method, the conducting surface of a transducer is used as an electrode, where a polymeric film with well controlled thickness can be easily

formed by varying amount of charge passed during the electrodeposition. There are a number of successful reports on the application of the electropolymerization method in molecular imprinting, where various types of polymer were used, such as overoxidized polypyrrole [19], poly(*o*-phenylenediamine) [20], and polydopamine (PDA) [21]. PDA appears to be especially attractive for protein-SIPs formation due to its high hydrophilicity and high biocompatibility as well as the existence of a wide variety of functional groups (amino-, hydroxy-, and π - π bonds), compatibility with aqueous solutions, the possibility to obtain an ultrathin compact polymer film by the controlled self-limiting growth. Until now there are only a few reports on PDA based MIP films and most of them however concern the PDA prepared by chemical or self-polymerization of dopamine at weak alkaline pH [22, 23]. The application of the electrosynthesized PDA based MIP film as a recognition element for the capacitive sensing of nicotine was firstly reported by Liu et al. [21].

The aim of this work was to elaborate a strategy that gives a possibility to create IgG surface imprinted polymer (IgG-SIP) thin films using PDA controlled electrodeposition on QCM sensor electrodes for real-time label-free IgG recognition. The specific rebinding of IgG to the prepared IgG-SIPs was analyzed by QCM-FIA technique. In order to optimize the strategy a series of the IgG-SIPs based on the various thicknesses of PDA films were compared in terms of their affinity to IgG molecule.

Materials and methods

Materials

IgG from human serum, IgA from human serum, 4-aminothiophenol (4-ATP), 2-mercaptoethanol, phosphate buffer saline tablets (PBS), sodium chloride and sodium dodecyl sulfate were obtained from Sigma-Aldrich (<http://www.sigmaaldrich.com>). 3,3'-dithiobis [sulfosuccinimidylpropionate] (DTSSP) was purchased from ThermoFisher Scientific Inc (<http://www.thermoscientific.com>). 4-(2-aminoethyl)benzene-1,2-diol (dopamine) was supplied from Fluka (<http://www.sigmaaldrich.com>). All chemicals were of analytical grade or higher and were used as received without any further purification. Ultrapure Milli-Q water (resistivity 18.2 M Ω · cm, Millipore, USA) was used for preparation of all aqueous solutions. PBS solution (0.01 M, pH 7.4) was prepared by dissolving one tablet in 200 mL of Milli-Q water.

IgG immobilization on the gold electrode surface

The gold electrode of a 5 MHz quartz crystal microbalance (QCM) sensor (Maxtek, Inc.) served as a substrate for IgG immobilization. The electrode was cleaned by immersion in

fresh piranha solution (97 % H₂SO₄:30 % H₂O₂, 3:1 volume ratio) for 10 min and then rinsed abundantly with Milli-Q water. Then the electrode was electrochemically treated in 0.1 M H₂SO₄ by cycling the potential between -0.2 and +1.5 V (vs Ag/AgCl) until the gold oxide formation region of the voltammograms displayed three distinct peaks and successive scans showed minimal to no change. Finally, the electrode was rinsed with distilled water and dried in a nitrogen stream. The modification of the QCM electrode surface with amino-groups was carried out by immersing the cleaned electrode in ethanolic solution of 0.1 M 4-ATP for 1 h to form the self-assembled monolayer, after which the electrode was thoroughly rinsed with ethanol to remove the unreacted thiols. The attachment of DTSSP crosslinker to the 4-ATP- modified electrode was achieved by subsequent incubation in PBS buffer (pH 7.4) containing 10 mM of DTSSP for 30 min followed by rinsing with PBS buffer. Then, 100 μ L of PBS containing 1 mg mL⁻¹ of IgG was dropped onto the modified electrode surface and allowed to react for 30 min, following which the unbound IgG was washed out from the electrode surface by additional rinsing with PBS buffer.

Electrochemical measurements

Gold electrode modification steps were characterized electrochemically by cyclic voltammetry (CV) and electrochemical impedance spectroscopy (EIS). Electrochemical measurements were made in a custom-made 8 mL Teflon electrochemical cell connected with Reference 600 Potentiostat (Gamry Instruments, USA). A conventional three-electrode system was used with QCM sensor electrode as working electrode, a rectangular shaped platinum plate (4 \times 1.5 cm²) as counter electrode, and a Ag/AgCl/KCl_{sat} reference electrode. Also, gold disk electrodes with diameter either 2 mm or 7 mm were used as working electrodes for CV and EIS studies (see experimental details in ESM).

Electrochemical deposition of PDA film

Dopamine electrochemical polymerization on the IgG-modified electrode was monitored by the Electrochemical Quartz Crystal Microbalance (EQCM). EQCM measurements were performed using the QCM100 system (Stanford Research Systems, Inc., Sunnyvale, CA, USA) connected to the Reference 600TM potentiostat (Gamry Instruments, Inc.) and PM 6680B counter (Fluke Corporation) as described [19]. Electropolymerization was carried out on the IgG-modified QCM sensors by cycling the potential between -0.45 and +0.55 V at a scan rate of 50 mV \cdot s⁻¹ in PBS buffer solution containing 5 mM of dopamine until the resonant frequency dropped a designated value. The thickness of the deposited PDA film T_f was believed to be uniform and

estimated from the resonant frequency shift Δf according to the equation Eq. 1:

$$T_f = -\frac{\Delta f}{C_f \cdot \rho} \quad (1)$$

where C_f is the sensitivity factor for a 5 MHz quartz crystal resonator, $C_f=56.6$ Hz cm² μ g⁻¹; the PDA film density ρ is assumed to be 1.2 g cm⁻³ as polyaniline density [24].

After polymer film electrochemical deposition, the electrode was rinsed with distilled water and dried in a nitrogen stream. When not in use, the IgG-PDA modified QCM sensors were stored under nitrogen atmosphere in the refrigerator.

Template protein removal

Removal of the template protein, IgG, from polymeric matrix of the electrodeposited PDA film was carried out in order to create IgG-SIP films. For this purpose the IgG-PDA modified electrode was immersed in 0.1 M solution of 2-mercaptoethanol in ethanol, and heated in water bath up to 100 $^{\circ}$ C. The reaction was maintained under stirring for 15 min. After rinsing with ethanol and distilled water, the electrode was immersed into 3 M NaCl aqueous solution containing 0.1 % sodium dodecyl sulfate and the same parameters of heating were applied. The protein washing out procedure was maintained under stirring for 15 min and repeated twice. Finally, the resulting IgG-SIP sensor was washed thoroughly with distilled water and subjected to protein rebinding studies. To compare the IgG-SIPs in terms of their affinity to IgG molecule, a non-imprinted polymer (NIP) structure was also created. The NIP was formed under very same conditions as the IgG-SIP, excluding protein subsequent removal. In this case the PDA film still contains the target protein, but has no cavities on its surface.

IgG rebinding studies by QCM-FIA technique

Template protein rebinding on the prepared IgG-SIP films modified QCM sensors was studied by a QCM-FIA technique. The analysis was carried out in a QCM-FIA system comprising programmable precision pump (M6, VICI[®] Valco Instruments Company Inc., USA), a motorized six-way port injection valve controlled by a microelectric actuator (C22-3186EH, VICI[®] Valco Instruments Company Inc., USA) and a small volume (150 μ L) axial flow cell attached to the QCM sensor holder (Stanford Research Systems, Inc.) [19]. All elements of the system were connected to a PC and controlled by software written in Labview. A constant flow of degassed PBS buffer solution (pH=7.4) flowed over the sensor at a flow rate of 12 μ L \cdot min⁻¹ until a constant baseline of the QCM sensor resonance frequency was reached. Subsequently, various concentrations of analyte samples (IgG solution in PBS buffer) was injected into the flow stream via an injection loop (250 μ L) and allowed to interact with the IgG-SIP or NIP modified QCM sensor for 2,500 s.

Scanning electron microscopy

Scanning Electron Microscope Zeiss Ultra 55 (Carl Zeiss AG, Germany, Oberkochen) with ultra high resolution imaging was used for the surface investigation of the IgG-SIP and NIP modified as well as bare Au electrodes. A series of images at 100,000 \times magnification were obtained and analyzed.

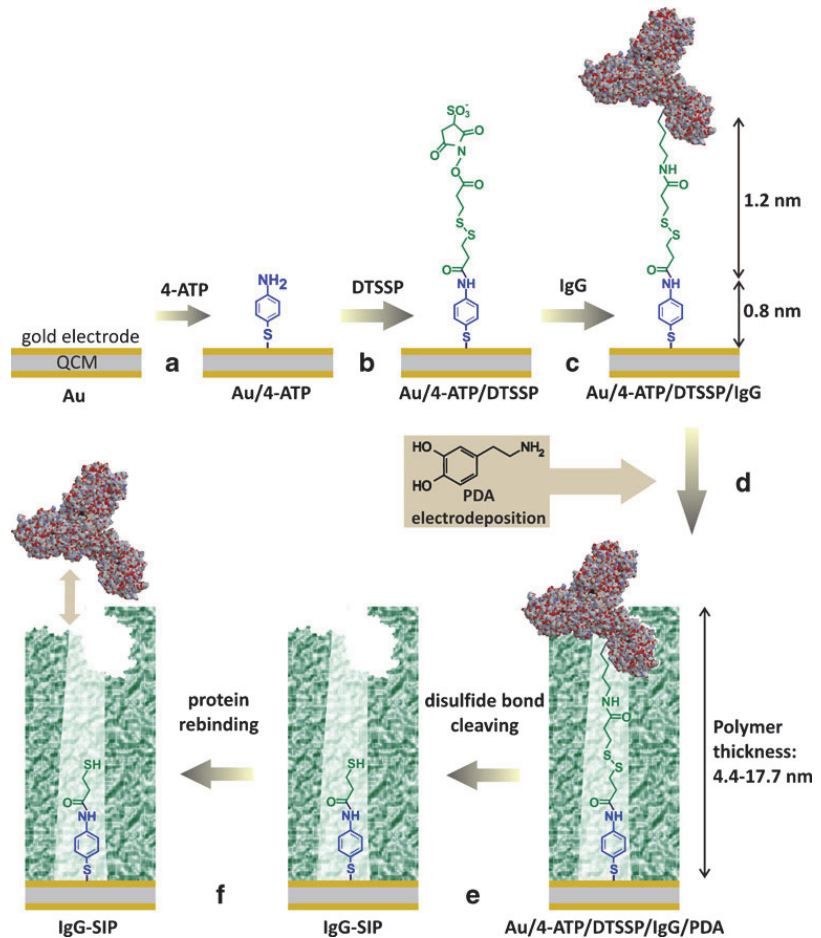
Results and discussion

Strategy for preparation of IgG-SIP thin films

Our approach for an IgG-SIP thin film formation is based on covalent immobilization of the target protein using a cleavable cross-linker to a gold electrode surface followed by electrochemical deposition of a nanometer thin PDA film. Figure 1 sketches

the concept of the strategy and gives theoretically estimated values of attached layers thicknesses. Thus, a gold electrode surface was modified with amino-groups by formation a self-assembled monolayer of 4-ATP (a). Then, a homobifunctional crosslinker with a cleavable disulfide bond and a suitable spacer unit, DTSSP, was attached to the amino-modified surface (b). The target protein was immobilized by the formation of covalent amide bond between succinimide group of DTSSP and amino-group of lysine residues of IgG (c). A polymer matrix was formed by electrochemical polymerization of dopamine around the immobilized IgG (d). It was expected that the multiple non-covalent interactions (hydrogen bonding, van der Waals interactions, electrostatic and hydrophobic) between PDA and IgG molecule ensure the formation of complementary cavities in the growing polymer films. After subsequent removal of the protein by destruction of the DTSSP cleavable bond using 2-mercaptoethanol, and non-covalent bonds by the surfactant

Fig. 1 The strategy for preparation of the IgG-SIP thin films: (a) 4-ATP self-assembled monolayer creation Au electrode (b) attachment of DTSSP cleavable linker (c) IgG covalent immobilization (d) PDA electrodeposition (e) washing out the IgG molecules (f) rebinding of IgG



containing NaCl solution, the complementary binding sites of the target protein confined in the surface of the polymer film were created (e).

In order to choose the appropriate thickness of the electrodeposited PDA layer the length of immobilized structure—4-ATP/DTSSP/IgG—was theoretically estimated. The previously reported AFM and ellipsometry studies indicated a perpendicular orientation of 4-ATP molecules to the metal surface [25], suggesting thus that thickness of a 4-ATP monolayer would be close to the length of the 4-ATP molecule (0.7–0.8 nm). The DTSSP linker has a spacer arm length of 1.2 nm. IgG covalent attachment to a succinimidyl group of the DTSSP proceeds through lysine residues that are abundant in antibody, resulting in random immobilization with multiple orientations of IgG on the surface. Therefore, two limiting cases of antibody possible orientations were considered to estimate the size of the immobilized IgG by RasMol software: “end-on” (Fc fragment closer to the surface) or “head-on” (Fab fragment closer to the surface) orientations with the size approx. 18 nm and “side-on” orientation (Fc and one of the Fabs closer to the surface while another Fab is away from the surface) with size approx. 8.5 nm. Thus, the theoretically estimated height of the whole immobilized structure can vary from approx. 10.5 to 20 nm. The choice for the range of thicknesses of the electrodeposited PDA film needed to achieve surface imprinting of the target protein is determined, from one side, by the linker system length, and, from the other side, by the height of the whole immobilized structure. In this work the polymer films with thicknesses ranging from 4.4 to 22.1 nm (Fig. 1d) were applied in order to evaluate the different extent of polymer coverage on the IgG-modified surface.

IgG immobilization on the gold electrode surface. Cyclic voltammetry and electrochemical impedance spectroscopy studies

IgG immobilization on the QCM gold electrode was accomplished by a multistep procedure including electrode modification with 4-ATP self-assembled monolayer, DTSSP crosslinker attachment, and finally antibody covalent immobilization. CV and EIS techniques were employed to evaluate the changes of gold electrode electrochemical behavior after each modification step. It was already shown that CV and EIS techniques are effective methods for testing the blocking ability towards the electron transfer reactions across a surface modified electrode/electrolyte interface using the ferro/ferri cyanide redox couple as a probe molecule [26].

Figure 2 shows cyclic voltammograms of the Au electrode after the different modification stages. It can be seen that the bare Au electrode (Fig. 2a) shows a reversible peak for the redox couple indicating that the electron transfer reaction is under diffusion-controlled. Reversibility of the reaction at the Au/4-ATP is almost the same as that at the bare Au electrode, indicating that the 4-ATP monolayer exhibits rather poor

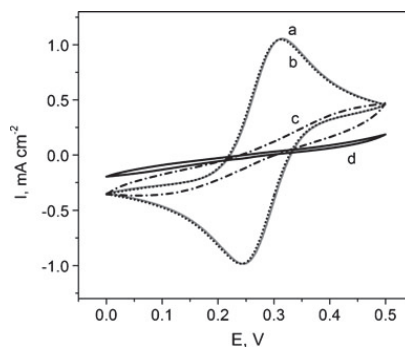


Fig. 2 Cyclic voltammograms of the bare Au (a), 4-ATP (b), 4-ATP/DTSSP (c), and 4-ATP/DTSSP/IgG (d) modified electrodes. The data were recorded in 1 M KCl containing 4 mM $\text{Fe}(\text{CN})_6^{3-}/\text{Fe}(\text{CN})_6^{4-}$ at scan rate of $50 \text{ mV} \cdot \text{s}^{-1}$

blocking ability. The poor barrier properties of a 4-ATP monolayer towards the redox reaction were reported earlier [26]. The CV and EIS studies of aromatic thiols SAMs on a gold surface performed by the authors demonstrated that the 4-ATP monolayer is formed with low surface coverage implying the existence of a large number of pinholes and defects within the monolayer. After subsequent attachment of the DTSSP linker to the 4-ATP modified electrode no well-defined current peaks were observed on the voltammogram indicating a significant barrier to a charge-transfer reaction involving the redox couple due to partial surface blocking and thicker layer formation. It is supposed that some DTSSP molecules were disrupted through S-S bond cleavage by contact with uncovered gold surface thus filling the defects of the 4-ATP monolayer and producing so called mixed monolayer, while the intact DTSSP molecules are attached directly to the amino-group of 4-ATP forming the outerlayer intended for IgG binding. When IgG was immobilized through covalent binding between the succinimidyl groups of DTSSP and the amino-groups of the protein, a denser insulating layer is formed on the electrode surface inhibiting more strongly the faradic process as indicates the featureless voltammogram (Fig. 2d).

The EIS spectra (Fig. S1 in the ESM) are in well agreement with the CV measurements, which further confirm the successful immobilization of the IgG via the DTSSP linker on the electrode surface. In spite of significant perturbation to electronic transport at the modified electrode surface, it is evidently not completely blocked, since an electronic current is still observed on the cyclic voltammogram (Fig. 2d). Thus, polymer matrix formation around the immobilized IgG by dopamine electropolymerization is expected to be feasible.

PDA films electrodeposition. Electrochemical QCM study

The PDA films on the 4-ATP/DTSSP/IgG-modified QCM electrodes were formed by electrochemical polymerization of

dopamine in order to provide a more accurate control of polymer film growth. The electrochemical QCM technique was used to simultaneously monitor voltamperometric and gravimetric responses during the polymer growth. Electrochemical QCM has proved to be a valuable in-situ tool to study electropolymerization processes, redox behaviour of electroactive polymers etc., which relates the mass changes during the electrochemical transformations at a QCM electrode to the observed changes in resonant frequency [27]. Considering the theoretical estimations for the range of a polymer bulk needed (Strategy for preparation of IgG-SIP thin films section), the PDA films with thicknesses of 4.4, 8.8, 13.3, 17.7 and 22.1 nm that correspond to the QCM frequency changes of 30, 60, 90, 120 and 150 Hz respectively, were electrodeposited on the 4-ATP/DTSSP/IgG modified QCM sensor electrode. Figure 3 shows a typical resonance frequency response of the QCM during PDA electrodeposition on its electrode. As it can be seen from Fig. 3a the PDA film grows non-linearly demonstrating a faster growth in the beginning of the process, following by its gradual slowing-down until the constant resonant frequency value is reached indicating the self-limiting polymerization. For comparison, the PDA film that is formed on a bare Au electrode, grows significantly faster as shown by Fig. 3b, due to lack of any layer hindering electron transfer at the electrode. In addition, it should be noted that due its insulating nature the PDA film electrochemical growth is self-limited achieving the maximum value of 22 nm in our experimental conditions. The SEM micrographs in Fig. S4 (see ESM) provide additional evidence for the PDA film deposition on the 4-ATP/DTSSP/IgG modified electrode, where this polymer with morphology of uniformly sized agglomerates of fine particles can be seen.

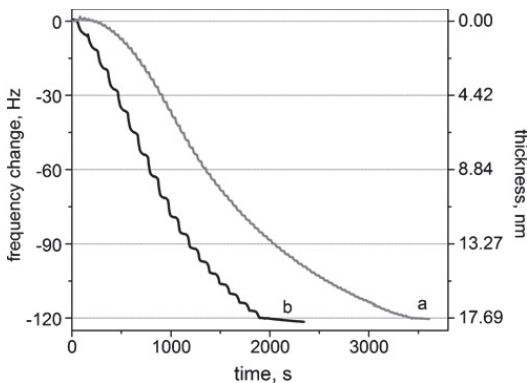


Fig. 3 The resonant frequency responses during dopamine electropolymerization on bare Au (b) and the Au/4-ATP/DTSSP/IgG modified (a) electrodes. The data were recorded with the QCM sensor upon potential cycling between -0.45 and $+0.55$ V at scan rate of $50 \text{ mV} \cdot \text{s}^{-1}$ in a PBS buffer solution containing 5 mM of dopamine

Evaluation of IgG-SIPs films rebinding capability

IgG rebinding capability of the IgG-SIPs prepared with the different PDA film thicknesses was studied by the QCM-FIA technique. To ascertain that the interaction between IgG and the IgG-SIP surface was specific, a control experiment was performed with the NIP modified electrode for each tested PDA film thickness. The sensor-to-sensor reproducibility reported as the relative standard deviation of the resonance frequency changes at saturation ($6.7 \mu\text{M}$ IgG) for the different sensors was 14.5% . Figure 4 shows typical frequency responses of the IgG-SIP and NIP modified QCM sensors with the thickness of PDA film of 8.8 nm upon consecutive injections of the solutions with increasing concentration of IgG in PBS buffer. A frequency drop associated with IgG binding is observed for the IgG-SIP modified QCM sensor already after the injection of $6.4 \cdot 10^{-5} \text{ mg} \cdot \text{mL}^{-1}$ IgG concentration, while the NIP modified sensor shows the non-significant frequency change. With the increasing concentration of IgG the frequency drop becomes more pronounced for both SIP and NIP films but at the same time the noticeably difference between the frequency responses of the IgG-SIP and NIP modified sensors is still observed. The higher rebinding capability of the IgG-SIP is more likely attributed to the presence of the imprint sites on the surface. However, there is also evidence of the significant non-specific adsorption appeared as the considerable frequency decrease recorded by the NIP modified QCM sensor.

Considering the experimental conditions of the QCM-FIA rebinding study, in particular, the low flow rate ($12 \mu\text{L} \cdot \text{min}^{-1}$) and the construction of the axial flow cell, where an injected solution flows about stagnation point, it can be assumed that the adsorption equilibrium is achieved after each successive injection of IgG. Therefore, the adsorption isotherm can be generated by plotting the appropriate accumulated frequency changes that are related to the amount of the bound protein on the Y axis, and the

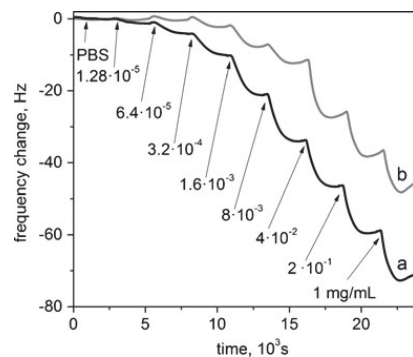


Fig. 4 The resonant frequency response of the IgG-SIP (a) and NIP (b) modified QCM Au electrode. The IgG-SIP and NIP are prepared with PDA film thickness of 8.8 nm . The data were upon successive injections of the different concentrations of IgG in 10 mM PBS buffer

IgG solution concentrations on the X axis (Fig. 5). Adsorption isotherms are useful in understanding the adsorption interaction mechanism of a template with a MIP surface.

A number of different models such as Langmuir [28], bi-Langmuir [29], Freundlich [30] and Freundlich-Langmuir (FL) [31] was used in order to obtain comparable and physically interpretable parameters, which describe the adsorption process. Since most of MIPs have heterogeneous binding sites, the models that account for heterogeneity (Freundlich and FL) should be considered primarily [32]. According to Shimidzu and co-workers [33] FL model (Eq. 2) is more universally applicable in characterizing MIPs

because it can provide heterogeneity information and is able to model adsorption behavior over the entire concentration range up to saturation:

$$B = \frac{B_{\max}(K_{FL}C)^m}{1 + (K_{FL}C)^m} \quad (2)$$

where C is the concentration of a protein in a solution, B and B_{\max} the fraction of bound protein and its saturation value, respectively, m is the heterogeneity index, which varies from 0 to 1 and with values <1 , the material is heterogeneous. K_{FL} is the association constant, which relates to the equilibrium

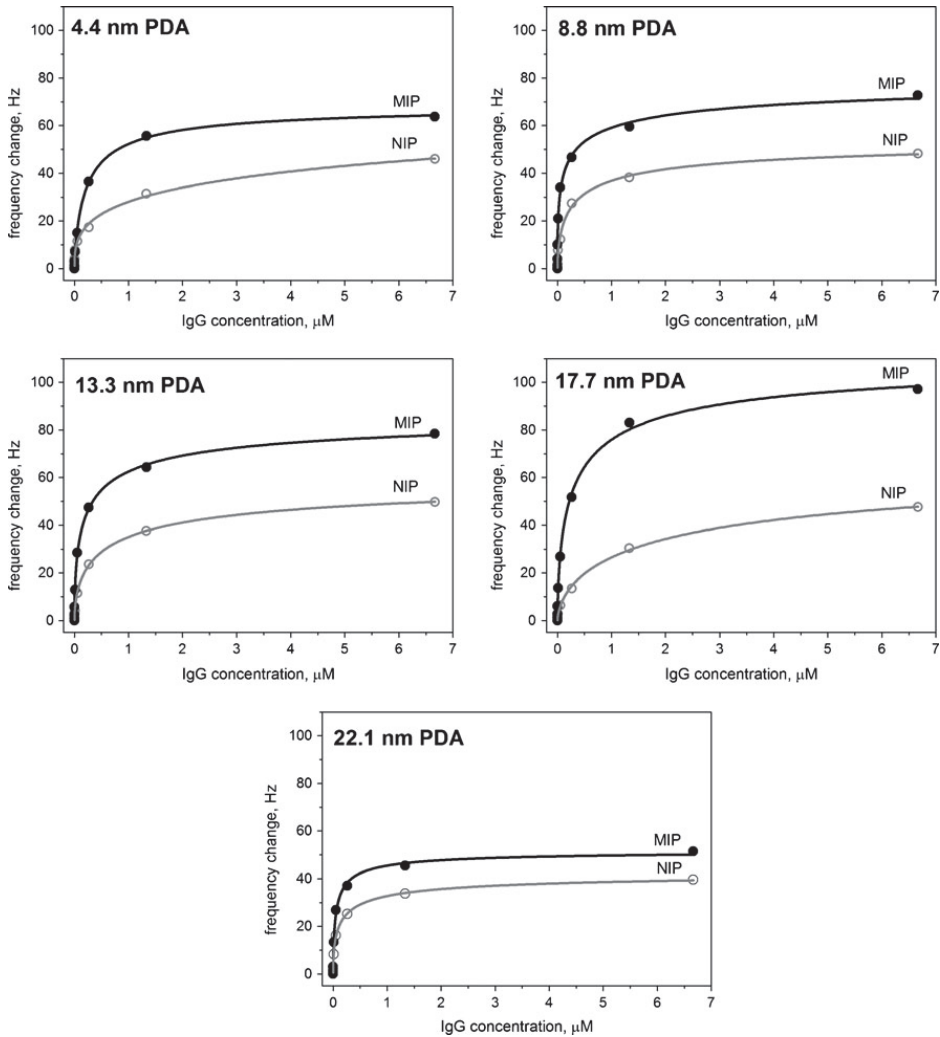


Fig. 5 The IgG adsorption isotherms for the IgG-SIP (*black circle*) and NIP (*hollow circle*) of the PDA various thicknesses. The curves represent fits of the data to Freundlich-Langmuir (FL) isotherm model

Table 1 The fitted binding parameters and corresponding correlation coefficients using the FL isotherm model

PDA thickness, nm	B_{\max} , Hz	m	K_{FL} , L μmol^{-1}	K_D , nmol L $^{-1}$	R^2	IF
IgG-SIP						
4.4	70.1 (2.0)	0.780 (0.049)	4.127 (0.488)	242 (28.6)	0.998	0.89
8.8	82.0 (3.9)	0.457 (0.032)	7.848 (2.239)	127 (36.3)	0.997	1.52
13.3	88.2 (1.8)	0.578 (0.020)	5.374 (0.546)	186 (18.9)	0.999	1.38
17.7	117.0 (4.0)	0.621 (0.035)	3.376 (0.531)	296 (46.6)	0.998	1.66
22.1	52.1 (1.9)	0.676 (0.064)	17.261 (3.277)	57.9 (11.0)	0.995	1.19
NIP						
4.4	78.1 (22.1)	0.459 (0.072)	0.262 (0.329)	3813 (4794)	0.990	–
8.8	53.8 (2.6)	0.621 (0.051)	3.813 (0.865)	262 (59.5)	0.996	–
13.3	64.0 (4.0)	0.566 (0.040)	1.413 (0.393)	708 (197)	0.998	–
17.7	70.3 (3.5)	0.583 (0.021)	0.394 (0.075)	2537 (481)	0.999	–
22.1	43.9 (1.1)	0.567 (0.024)	6.690 (0.843)	149 (18.9)	0.999	–

Values in parentheses are standard errors

dissociation constant (K_D) as $K_{FL}=1/K_D$. In this work K_D was used to assess the affinity of the prepared IgG-SIP film to the template protein. The experimental data of the adsorption isotherms were fitted to the FL model using a nonlinear regression and plotted in both normal and logarithmic forms (Figs. 5 and S5 in ESM for log plot). The fitted parameters are presented in the Table 1. The imprinting factor (IF) was calculated according to the following equation [34]:

$$IF = \frac{B_{\max}(MIP)}{B_{\max}(NIP)} \quad (3)$$

It can be seen from the graphical evaluation that for all tested IgG-SIPs and NIPs the FL model gives an excellent fit, which is confirmed by the high correlation coefficient R^2 values (0.990–0.999). The benefit of using the FL fitting model is also supported by the graphs presented in the log plot of the binding isotherms (Fig. S5 in ESM), which show both the linear regions at the low concentrations and the curvature at the high concentrations [33]. The values of m index in the range of 0.457 to 0.78 indicate that the adsorption sites along the IgG-SIPs and NIPs surface are energetically heterogeneous. Nevertheless, all the IgG-SIPs differing in PDA film thickness show somewhat higher binding capacity compared to the corresponding NIPs, that is most likely caused by the presence of the complementary cavities on the surface of the SIP films due to the imprinting phenomenon. Among the IgG-SIPs prepared with different PDA film thicknesses the most pronounced imprinting effect (IF 1.66) was observed for the IgG-SIP with PDA film of 17.7 nm thick. For this case the value of K_D , which is considered as a measure of IgG affinity toward the SIP, is found to be approximately one order of magnitude higher for the IgG-SIP than that for the corresponding NIP. Probably, at such PDA

film thickness the immobilized IgG molecules are appropriately confined in the polymer and high-affinity binding sites are formed at the polymer surface after the IgG removal procedure. However, binding isotherms observed for the IgG-SIP and NIP pair built-up of the thinnest PDA film (4.4 nm) are clearly inconsistent with the other ones showing the highest difference between the binding affinities of the SIP and NIP while the B_{\max} value of NIP exceeds B_{\max} of MIP giving the IF less than unity. This is perhaps due to the non-uniformity of the ultrathin polymer film that may contain significant number of the uncovered areas on the surface, enhancing thus the non-specific adsorption. On the other hand, the lower value of IF was obtained for the IgG-SIP with PDA film of 22 nm thick compared to the IgG-SIPs with other PDA film thicknesses (excl. 4.4 nm thick PDA). This may be explained by the decreasing of the number of the specific cavities on the surface of the polymer film supporting our hypothesis that the polymer film with thickness exceeding the height of the whole immobilized structure (approx. 18 nm) may entrap the template more rigorously.

A selectivity test for IgG-SIPs as well as IgA-SIP prepared by the described approach was carried out with respect to IgA and IgG. The preliminary study showed (Fig. S6 in the ESM) that the IgG-SIP binds ca. 2 times more IgG than IgA while the IgA-SIP binds ca. 1.5 times more IgA than IgG.

Conclusion

In summary, we have demonstrated a possibility of preparing the SIP thin films for IgG specific recognition based on a covalent immobilization of IgG through a cleavable cross-linker to a gold electrode of a QCM followed by controlled electropolymerization of the monomer to yield an ultrathin

polymeric matrix. The IgG rebinding study performed by the QCM-FIA revealed that the IgG-SIPs built-up of PDA film thickness starting from 8.8 nm and higher demonstrated an apparently enhanced affinity towards IgG when they are compared to the corresponding NIP films. The nanomolar range of K_D , estimated by fitting the adsorption isotherms to FL model, indicated strong polymer-template interaction that was expected to result from the multipoint attachment (multiple non-covalent bonds) of the protein to the polymer matrix. IgG-SIPs prepared with PDA thickness of 17.7 nm showed the most pronounced imprinting effect (IF 1.66) compared to other studied IgG-SIPs as well as the nanomolar range binding affinity (K_D 296 nM). It was concluded that at such PDA film thickness the immobilized IgG molecules were appropriately confined in the polymer and the more specific binding sites were formed at the polymer surface after the subsequent IgG removal procedure. Although further research is required in this field, we believe that the presented strategy offers a great promise for SIP-based biosensor development demonstrating a way for formation of SIP thin films directly on a sensor transducer surface, which in turn enables convenient real-time label-free detection of a target protein.

Acknowledgements This work has been supported by the Estonian Ministry of Education and Research (grant PUT150) and the Estonian Science Foundation (grant ETF8249).

References

- Ye L, Mosbach K (2008) Molecular imprinting: synthetic materials as substitutes for biological antibodies and receptors. *Chem Mater* 20(3):859–868. doi:10.1021/Cm703190w
- Tamayo FG, Turiel E, Martin-Esteban A (2007) Molecularly imprinted polymers for solid-phase extraction and solid-phase microextraction: recent developments and future trends. *J Chromatogr A* 1152(1–2):32–40. doi:10.1016/j.chroma.2006.08.095
- Pichon V, Haupt K (2006) Affinity separations on molecularly imprinted polymers with special emphasis on solid–phase extraction. *J Liq Chromatogr Relat Technol* 29(7–8):989–1023. doi:10.1080/10826070600574739
- Sellergren B, Allender CJ (2005) Molecularly imprinted polymers: a bridge to advanced drug delivery. *Adv Drug Deliv Rev* 57(12):1733–1741. doi:10.1016/j.addr.2005.07.010
- Wulff G (2002) Enzyme-like catalysis by molecularly imprinted polymers. *Chem Rev* 102(1):1–27. doi:10.1021/Cr980039a
- Shi H, Tsai WB, Garrison MD, Ferrari S, Ratner BD (1999) Template-imprinted nanostructured surfaces for protein recognition. *Nature* 398:593–597. doi:10.1038/19267
- Yilmaz E, Haupt K, Mosbach K (2000) The Use of immobilized templates—new approach in molecular imprinting. *Angew Chem Int Ed* 39:2115–2118
- Li Y, Yang HH, You QH, Zhuang ZX, Wang XR (2006) Protein recognition via surface molecularly imprinted polymer nanowires. *Anal Chem* 78:317–320
- Qin L, He X-W, Zhang W, Li W-Y, Zhang Y-K (2009) Surface-modified polystyrene beads as photografting imprinted polymer matrix for chromatographic separation of proteins. *J Chromatogr A* 1216:807–814. doi:10.1016/j.chroma.2008.12.007
- Titirici MM, Hall AJ, Sellergren B (2002) Hierarchically imprinted stationary phases: mesoporous polymer beads containing surface-confined binding sites for adenine. *Chem Mater* 14(1):21–23. doi:10.1021/Cm011207+
- Titirici MM, Sellergren B (2004) Peptide recognition via hierarchical imprinting. *Anal Bioanal Chem* 378:1913–1921. doi:10.1007/s00216-003-2445-5
- Nematollahzadeh A, Sun W, Aureliano CSA, Lutkemeyer D, Stute J, Abdekhodaie MJ, Shojaei A, Sellergren B (2011) High-capacity hierarchically imprinted polymer beads for protein recognition and capture. *Angew Chem Int Ed* 50(2):495–498. doi:10.1002/anie.201004774
- Lautner G, Kaev J, Reut J, Öpik A, Rappich J, Syritski V, Gyurcsányi RE (2011) Selective artificial receptors based on micropatterned surface-imprinted polymers for label-free detection of proteins by SPR imaging. *Adv Funct Mater* 21(3):591–597. doi:10.1002/adfm.201001753
- Menaker A, Syritski V, Reut J, Öpik A, Horváth V, Gyurcsányi RE (2009) Electrosynthesized surface-imprinted conducting polymer microrods for selective protein recognition. *Adv Mater* 21(22):2271–2275. doi:10.1002/adma.200803597
- Schirhagl R, Lieberzeit PA, Blaas D, Dickert FL (2010) Chemosensors for viruses based on artificial immunoglobulin copies. *Adv Mater* 22:2078–2081. doi:10.1002/adma.200903517
- Marx KA (2003) Quartz crystal microbalance: a useful tool for studying thin polymer films and complex biomolecular systems at the solution-surface interface. *Biomacromolecules* 4:1099–1120
- Arce L, Zougagh M, Arce C, Moreno A, Ríos A, Valcárcel M (2007) Self-assembled monolayer-based piezoelectric flow immunosensor for the determination of canine immunoglobulin. *Biosens Bioelectron* 22(12):3217–3223. doi:10.1016/j.bios.2007.02.014
- Zhang Q, Huang Y, Zhao R, Liu G, Chen Y (2008) Determining binding sites of drugs on human serum albumin using FIA-QCM. *Biosens Bioelectron* 24:48–54. doi:10.1016/j.bios.2008.03.009
- Syritski V, Reut J, Menaker A, Gyurcsányi RE, Öpik A (2008) Electrosynthesized molecularly imprinted polypyrrole films for enantioselective recognition of L-aspartic acid. *Electrochim Acta* 53(6):2729–2736. doi:10.1016/j.electacta.2007.10.032
- Malitesta C, Losito I, Zambonin PG (1999) Molecularly imprinted electrosynthesized polymers: new materials for biomimetic sensors. *Anal Chem* 71:1366–1370
- Liu K, Zeng J-X, Wei W-Z, Liu X-Y, Gao Y-P (2006) Application of a novel electrosynthesized polydopamine-imprinted film to the capacitive sensing of nicotine. *Anal Bioanal Chem* 385:724–729. doi:10.1007/s00216-006-0489-z
- Ouyang R, Lei J, Ju H (2008) Surface molecularly imprinted nanowire for protein specific recognition. *Chemical Communications*. 5761–5763. doi:10.1039/b810248a
- Zhou W-H, Tang S-F, Yao Q-H, Chen F-R, Yang H-H, Wang X-R (2010) A quartz crystal microbalance sensor based on mussel-inspired molecularly imprinted polymer. *Biosens Bioelectron* 26:585–589. doi:10.1016/j.bios.2010.07.024
- Orata D, Buttry DA (1987) Determination of ion populations and solvent content as functions of redox state and pH in polyaniline. *J Am Chem Soc* 109(12):3574–3581. doi:10.1021/ja00246a013
- Valério E, Abrantes LM, Viana AS (2008) 4-Aminothiophenol self-assembled monolayer for the development of a DNA biosensor aiming the detection of cylindrospermopsin producing cyanobacteria. *Electroanalysis* 20:2467–2474. doi:10.1002/elan.200804350
- Sabatani E, Cohen-Boulakia J, Bruening M, Rubinstein I (1993) Thioaromatic monolayers on gold: a new family of self-assembling monolayers. *Langmuir* 9:2974–2981
- Buttry DA, Ward MD (1992) Measurement of interfacial processes at electrode surfaces with the electrochemical quartz crystal microbalance. *Chem Rev* 92(6):1355–1379. doi:10.1021/cr00014a006

28. Langmuir I (1918) The adsorption of gases on plane surfaces of glass, mica and platinum. *J Am Chem Soc* 40(9):1361–1403. doi:[10.1021/ja02242a004](https://doi.org/10.1021/ja02242a004)
29. Shea KJ, Spivak DA, Sellergren B (1993) Polymer complements to nucleotide bases—selective binding of adenine-derivatives to imprinted polymers. *J Am Chem Soc* 115(8):3368–3369
30. Freundlich H (1906) Over the adsorption in solution. *Z Phys Chem* 57:385–471
31. Sips R (1948) On the structure of a catalyst surface. *J Chem Phys* 16(5):490–495
32. Umpleby RJ, Baxter SC, Chen YZ, Shah RN, Shimizu KD (2001) Characterization of molecularly imprinted polymers with the Langmuir-Freundlich isotherm. *Anal Chem* 73(19):4584–4591
33. Umpleby RJ, Baxter SC, Rampey AM, Rushton GT, Chen YZ, Shimizu KD (2004) Characterization of the heterogeneous binding site affinity distributions in molecularly imprinted polymers. *J Chromatogr B* 804(1):141–149. doi:[10.1016/j.jchromb.2004.01.064](https://doi.org/10.1016/j.jchromb.2004.01.064)
34. Muhammad T, Nur Z, Piletska EV, Yimit O, Piletsky SA (2012) Rational design of molecularly imprinted polymer: the choice of cross-linker. *Analyst* 137(11):2623–2628

PAPER III

Aleksei Tretjakov, Vitali Syritski, Jekaterina Reut, Roman Boroznjak, and Andres Öpik, Molecularly imprinted polymer film interfaced with Surface Acoustic Wave technology as a sensing platform for label-free protein detection, *Analytica Chimica Acta*, 902 (2016) 182-188.



Molecularly imprinted polymer film interfaced with Surface Acoustic Wave technology as a sensing platform for label-free protein detection



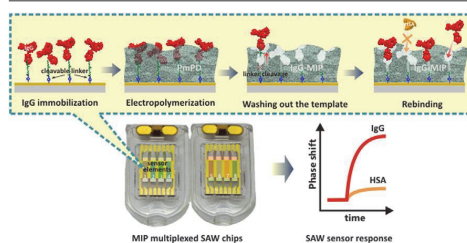
Aleksei Tretjakov, Vitali Syritski*, Jekaterina Reut, Roman Boroznjak, Andres Öpik

Department of Materials Science, Tallinn University of Technology, Ehitajate tee 5, 19086 Tallinn Estonia

HIGHLIGHTS

- A facile integration of protein-MIPs with SAW technology was firstly reported.
- IgG-MIP ultrathin films were interfaced with the multiplexed SAW chips by an electrosynthesis approach.
- The selectivity of IgG-MIP films toward IgG over IgA and HSA was demonstrated.

GRAPHICAL ABSTRACT



ARTICLE INFO

Article history:

Received 18 July 2015

Received in revised form 29 October 2015

Accepted 4 November 2015

Available online 17 November 2015

Keywords:

Molecularly imprinted polymer

Electrochemical polymerization

Immunoglobulin G

Surface acoustic wave

ABSTRACT

Molecularly imprinted polymer (MIP)-based synthetic receptors integrated with Surface Acoustic Wave (SAW) sensing platform were applied for the first time for label-free protein detection. The ultrathin polymeric films with surface imprints of immunoglobulin G (IgG-MIP) were fabricated onto the multiplexed SAW chips using an electrosynthesis approach. The films were characterized by analyzing the binding kinetics recorded by SAW system. It was revealed that the capability of IgG-MIP to specifically recognize the target protein was greatly influenced by the polymer film thickness that could be easily optimized by the amount of the electrical charge consumed during the electrodeposition. The thickness-optimized IgG-MIPs demonstrated imprinting factors towards IgG in the range of 2.8–4, while their recognition efficiencies were about 4 and 10 times lower toward the interfering proteins, IgA and HSA, respectively. Additionally, IgG-MIP preserved its capability to recognize selectively the template after up to four regeneration cycles. The presented approach of the facile integration of the protein-MIP sensing layer with SAW technology allowed observing the real-time binding events of the target protein at relevant sensitivity levels and can be potentially suitable for cost effective fabrication of a biosensor for analysis of biological samples in multiplexed manner.

© 2015 Elsevier B.V. All rights reserved.

1. Introduction

Today label-free detection of proteins has become of extensive demand in fundamental research as well as in clinical practice

providing an alternative to the widely used label-based detection methods that involves laborious, lengthy procedure and can influence the interfacial activity of the resulting protein–label complexes, and consequently the accuracy of measurement results [1]. Label-free detection can be implemented with the help of various transduction mechanisms, including, but not limited to, optical, electrochemical or piezoelectric, where the biochemical interaction between an analyte and a recognition element of the sensor

* Corresponding author.

E-mail address: vitali.syritski@ttu.ee (V. Syritski).

is recorded as a change in e.g., refractive index (SPR sensors), impedance (electrochemical sensors) or resonance frequency (QCM sensors), respectively.

Common recognition elements in biosensors are biomacromolecules such as antibodies, enzymes, or DNA, that can capture target analyte with very high affinity and specificity. However, due to the restricted operating conditions and high production cost of these biological receptors, the development of artificial systems with molecular recognition capability, so-called synthetic receptors, have gained a lot of interest as potential alternatives for biological recognition elements. Among a number of existing techniques for design of synthetic receptors, high expectations are set in the development of molecularly imprinted polymers (MIPs). The technique of molecular imprinting allows the formation of specific molecular recognition sites in highly reticulated polymeric network grown in the presence of analyte molecules, which are subsequently removed leaving behind the analyte specific cavities. MIPs have been shown to possess several advantages as an alternative recognition material for biosensor including low cost, the ease of preparation, storage stability, repeated operations without loss of activity, high mechanical strength, durability to heat and pressure, as well as applicability in harsh chemical media [2,3].

Although synthesis of MIP materials recognizing small molecular weight compounds has proven to be very successful, molecular imprinting of biomacromolecules, in particular proteins, obviously has encountered challenges due their inherent properties such as molecular size, complexity, conformational flexibility, and solubility [4]. Thus, the hindered mass transfer of a large biomolecule in highly reticulated polymeric networks prepared by conventional bulk imprinting leads to their entrapment during imprinting rather than to binding sites permitting free ligand exchange with the sample solution. A number of imprinting strategies were elaborated in order to address the issues associated with protein imprinting [4,5]. The surface imprinting approach leading to the formation of polymer with imprinted sites located at or close to the surface of MIPs, enabling easy access to the target macromolecules, was shown to be a promising way for protein-MIP preparation [6–8].

Many of the reported surface imprinting strategies take advantage of the facile integration of protein-MIP sensing layer with a transducer that is a key aspect in the design of a MIP-based sensor. Thus, the microcontact surface imprinting approach based on photopolymerization has been widely studied to prepare a surface imprinted polymer thin film directly on the surface for selective recognition of C-reactive protein [6], trypsin [9], bovine serum albumin [10]. In another surface imprinting approach, the sol-gel method was combined with a self-assembly technology to prepare a human serum albumin (HSA)-imprinted film on the surface of a QCM [11]. Electrosynthesis has been introduced recently as a convenient strategy for effectively interfacing protein-MIPs with transducers allowing rapid and controlled deposition of polymer films with tunable thickness [7,12–17]. It is worth to mention that in the most of the reported works using protein-MIPs for sensing applications QCM, SPR or electrochemical sensors are preferential choice. Meanwhile, Surface Acoustic Waves (SAW) may provide advances in fabrication of MIP-based sensors over these technologies. Generally, SAW devices share the similar principle of operation as QCMs, but utilize acoustic waves at surfaces rather than in the bulk of a piezoelectric material allowing to increase operating frequencies of SAW devices to the range of 100–500 MHz without compromising in their mechanical fragility. The Love Wave sensor, a special class of the shear-horizontal SAW having the acoustic energy propagation path strictly confined inside of the guiding layer coated onto the top of the sensor. This layer minimizes the energy dissipation losses into environmental media making thus the Love Wave sensors, besides their ex-

tremely high sensitivity towards surface effects, well suited for operation in liquids. Usually, owing to high operation frequencies SAW offers about an order of magnitude higher mass resolution than QCMs, while keeps sensor cost low and at the same time is fully compatible with large-scale fabrication and multiplexing technologies [18,19]. As compared to SPR, SAW technology is not limited to detect only mass loading onto the surface, but also useful to follow structural insights of sensing layers through use of dissipation factor of the acoustic wave propagating along the sensor surface.

Despite of the mentioned advantages, integration of SAW sensors with polymeric synthetic receptor materials has not yet been sufficiently displayed. While SAW gas sensors with a MIP-based recognition layer have been reported [20,21], there is no a report, however, on a sensor of similar type designed for protein selective recognition. To fill this void, here we have integrated the IgG-MIPs with SAW technology by facile electrochemical synthesis approach. The special attention was paid to the careful choice of optimal polymer thickness to prepare IgG-MIP with the improved recognition properties. The binding kinetics were analyzed to differentiate the equilibrium binding capacities and affinities of the targets to IgG-MIP and NIP surfaces. The regeneration, and thus reusability of the IgG-MIP-modified SAW chips after the repeated regeneration cycles was also examined.

2. Experimental

2.1. Chemicals and materials

IgG from human serum, IgA from human serum, HSA from human serum, 4-aminothiophenol (4-ATP), *m*-phenylenediamine (mPD), 2-mercaptoethanol, phosphate buffer saline (PBS) tablets, sodium chloride were obtained from Sigma-Aldrich. 3,3'-dithiobis[sulfosuccinimidylpropionate] (DTSSP) was purchased from ThermoFisher Scientific Inc. All chemicals were of analytical grade or higher and were used as received without any further purification. Ultrapure water (resistivity 18.2 M Ω cm, Millipore, USA) was used for preparation of all aqueous solutions. Phosphate buffered saline (PBS) solution (0.01 M, pH 7.4) was used to prepare synthesis and analyte solutions.

2.2. IgG-MIP film preparation

IgG-MIP films were fabricated directly on Love Wave-configured SAW chips (NanoTemper Technologies GmbH, München, Germany) according to the previously developed procedure (Fig. 1) [14]. The procedure was undergone some modifications with intention to improve analytical performance of the resulting films. In brief, the gold sensing surface of SAW chip consisting of four sensor elements was preliminary cleaned by a fresh base piranha solution (25% NH₄OH:30% H₂O₂:H₂O, 1:1:5 volume ratio) for 15 min, rinsed abundantly with ultrapure water, and treated in an UV/ozone cleaner followed by rinsing with ultrapure water and drying in a nitrogen stream. Then, IgG was immobilized on the cleaned surface through DTSSP cleavable crosslinker. For this purpose, the surface was functionalized with amino-groups by immersion in the ethanolic solution of 0.1 M 4-ATP for 1 h and then, DTSSP crosslinker was covalently attached by incubation in PBS buffer (pH 7.4) containing 10 mM of DTSSP for 30 min. After that, 0.1 mL of PBS containing 1 mg mL⁻¹ of IgG was dropped onto the modified sensing surface and allowed to react for 30 min, followed by additional rinsing with PBS buffer to remove the unbound IgG. The protein-modified SAW chip was placed into the 5-mL electrochemical cell designed to expose the modified sensing surface to the synthesis solution. The electrochemical cell accommodated

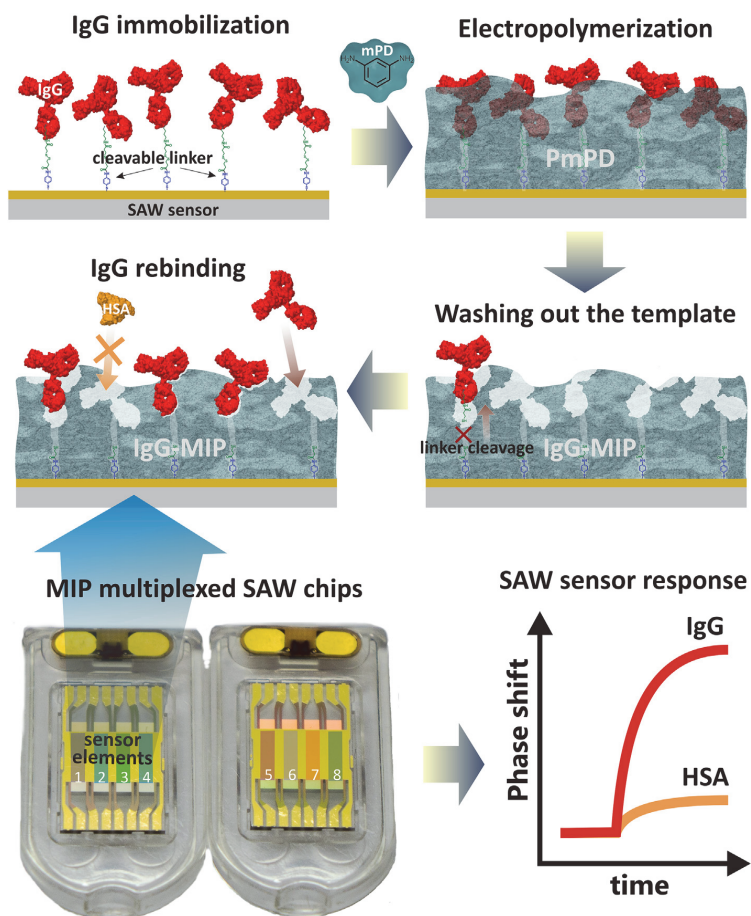


Fig. 1. Schematic representation of the synthesis concept for IgG-MIP sensing layer integration with SAW chip.

three electrodes, i.e. the sensing surface of SAW chip as a working electrode, a spiral shaped Pt wire as a counter electrode, and Ag/AgCl/KCl_{sat} as a reference electrode, all connected to an electrochemical workstation (Reference 600™, Gamry Instruments, Inc., USA). *m*-PD electropolymerization on the IgG-modified surface was carried out in PBS buffer solution containing 10 mM of *m*PD by imposing the constant potential of 0.9 V to the working electrode.

To yield the polymeric structures of defined thickness their growth were controlled by charge passed through the working electrode. Thicknesses were determined by a spectroscopic ellipsometer (SE 850 DUV, Sentech Instruments GmbH, Berlin, Germany). Ellipsometric parameters ψ and Δ were measured from three spots for each sample in ambient air confining the wavelength range between 380 and 850 nm at the angle of incidence of 70°. The spectra were fitted (SpectraRay 3 software) with the optical model containing a one-layer Cauchy layer on the top of the gold and the thicknesses were determined.

After the electrodeposition the PmPD film coated sensing surface was rinsed with ultrapure water and dried in a nitrogen stream. To remove the template protein, IgG, from the electrode-

posited PmPD film the modified sensing surface was immersed in aqueous solution of 0.1 M 2-mercaptoethanol, and heated in water bath up to 100 °C with stirring for 15 min. After that, the sensing surface was washed additionally in 3 M NaCl aqueous solution for 15 min and in DMSO for 30 min. The resulting IgG-MIP SAW chip was washed thoroughly with ultrapure water and subjected to the protein rebinding studies. To assess the IgG-MIPs in terms of their affinity to IgG molecule, control non-imprinted polymer (NIP) structures were also created using the very same conditions as for the IgG-MIP but excluding the linker cleavage stage by mercaptoethanol. In this case, the NIP films still contained the covalently bound target protein, but had no specific cavities on its surface.

2.3. IgG rebinding studies

Real-time rebinding of IgG on the prepared IgG-MIP-modified SAW chips was performed using a SAW biosensor system (SamX®, NanoTemper Technologies GmbH, München, Germany) capable to handle two SAW chips having four separate sensor elements each. The microfluidics of the system provided the option to deliver

analyte solutions to the modified sensor elements either individually or in serial fashion.

The sensor elements were preconditioned at constant flow (25 $\mu\text{L min}^{-1}$) of the degassed PBS buffer solution (pH = 7.4) until a constant baseline was reached. Subsequently, various concentrations (from 0.4 nM to 53 nM) of analytes prepared from the same buffer were injected into the flow stream via an autosampler using a 430 μL injection loop and allowed to interact with the IgG-MIP or IgG-NIP modified SAW chip.

The SAW sensor system capable of both phase and amplitude signal measurement, reflecting changes in mass and in viscoelastic properties of a material at the sensor surface, respectively. In this work, phase-shift response was analyzed to evaluate rebinding properties of IgG-MIPs. Data analysis was performed using Origin 9.1 (Northampton, MA). Raw data were exported, cut and analyzed by individual fits using two kinetic models for sorption from liquid solution represented by the first- and second-order equations as described in the Results and Discussion section. Affinity constants and K_D values were determined from plot of the equilibrium signal (Q_{eq}) versus analyte concentration using Langmuir–Freundlich equation for the data fitting. Regeneration of the film-modified chips was done by their immersion in 3 M NaCl aqueous solution for 2 h with stirring and heating up to 100 $^{\circ}\text{C}$.

3. Results and discussion

3.1. IgG-MIP fabrication

In contrast to the previously reported synthesis strategy [14], some modifications were introduced here in order to improve the selectivity of the resulting IgG-MIPs. mPD was used as a functional monomer for polymer matrix formation instead of dopamine. Electropolymerization of mPD proceeds faster than that of dopamine therefore the surface-immobilized IgG is less exposed to the synthesis solution as well as to the applied potential that significantly reduces the possibility of conformational changes of IgG. In addition, the computational modeling using molecular docking and quantum chemical approach revealed that mPD as a functional monomer minimally affected the conformation of IgG and was able to create molecular memory via multiple hydrogen bonds, van der Waal's and lipophilic interactions between the polymer matrix and IgG [22]. Moreover, taking into account the types of possible interactions between PmPD and IgG, the template washing out procedure was also modified by including the treatment with 3 M NaCl solution and DMSO in addition to the cleavage of DTSSP linker with mercaptoethanol.

The electrosynthesis approach to the preparation of MIP films allowed a fine control of the polymer thickness by monitoring the electrical charge passed during the synthesis. For the surface imprinting strategy used in this study the deposition of a polymer film with an appropriate thickness is one of the most important task in order to produce protein-MIP film with specific binding sites located on the surface [23,24]. The influence of the electrodeposited polymer thickness on the specific recognition properties of IgG-MIP has been already demonstrated in the previous study [14]. Thereby, in this study to avoid irreversible entrapment of the template the special attention was paid to the careful choice of optimal polymer thickness through control of the charge passed during the in-situ electrodeposition and subsequent correlation of the data with the *ex-situ* ellipsometry measurements (Fig. 2). As it can be seen, the deposited polymer thickness varied nearly linearly ($R^2 = 0.996$) across the applied electric charge range making thus its prediction between ca. 3 nm and 30 nm quite certain. Since the height of IgG with the immobilizing linker system above the surface may spread from ca. 10.5 till 20 nm [14] PmPD films with the thicknesses in the range of 5.7 nm and 28.4 nm were synthesized

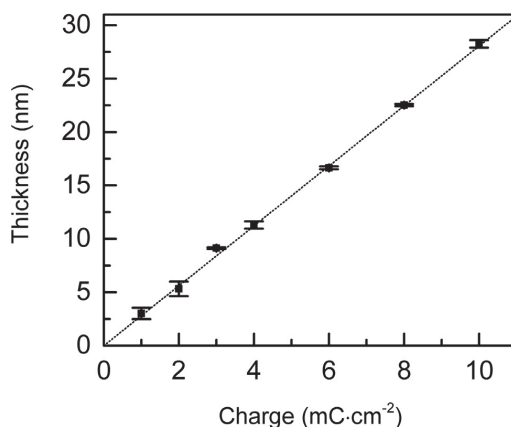


Fig. 2. The calibration graph representing the dependence of the polymeric film thickness, as measured by the spectroscopic ellipsometry, on the amount of the charge consumed during the electropolymerization of *m*-PD on IgG-modified gold electrode.

on the IgG-modified SAW chips by applying the respective charge between 2 and 10 mC cm^{-2} . The influence of the polymer film thickness on IgG-MIP capability to specifically recognize the target protein was evaluated in the course of IgG rebinding study as discussed below.

3.2. IgG rebinding study

The fabricated IgG-MIPs were characterized in term of their affinity to IgG by monitoring the binding kinetics with SAW system. Typical sensorgrams of IgG rebinding at the different concentrations to the surface of SAW chip modified with 11 nm thick IgG-MIP and NIP are presented in Fig. 3a. The association phase of the sensorgrams was analyzed in order to determine the equilibrium signal for the IgG to IgG-MIP and NIP surfaces by fitting the response to the pseudo-first order and pseudo second order kinetic Eqs. (1) and (2), respectively:

$$Q = Q_{eq}[1 - e^{-k_1 t}] \quad (1)$$

$$Q = [Q_{eq}^2 k_2 t] / [1 + Q_{eq} k_2 t] \quad (2)$$

where Q is the phase-shift response upon IgG rebinding at time t , Q_{eq} is its value at equilibrium, k_1 is a pseudo-first order rate constant, k_2 is a pseudo-second order rate constant. The first and second order rate models have been widely used to describe adsorption data obtained under non-equilibrium conditions [25]. According to the first order kinetics model, the adsorbate binds only to a single active site on the adsorbent surface and the interactions of adsorbate and adsorbent are of physical nature; the rate of occupation of adsorption sites is proportional to the number of unoccupied sites [26,27]. The pseudo-second order model recognizes that the rate-limiting step is chemisorption involving sharing or exchange of electrons between adsorbent and adsorbate and the rate of occupation of adsorption sites is proportional to the square of the number of unoccupied sites [27,28]. Both models have been applied to describe the adsorption kinetics on the MIP surfaces [29–31].

The kinetics parameters obtained by fitting the sensorgrams in Fig. 3a to the Eqs. (1) and (2) are listed in Table 1. As it can be seen both models provided excellent fit to the experimental data with the correlation coefficients (R^2) in the range of

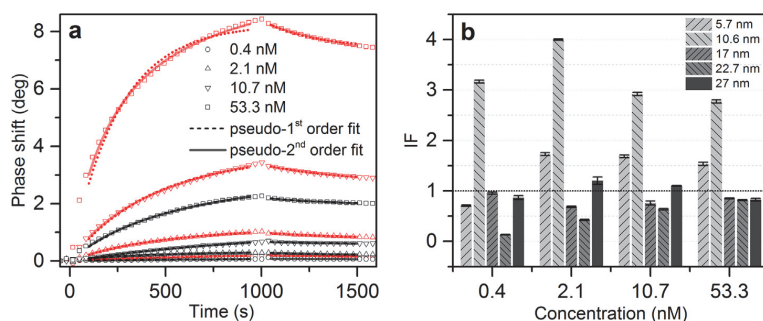


Fig. 3. (a) Typical phase-shift responses of the IgG-MIP (red) and NIP (black) modified SAW chips (PmPD film thickness of 11 nm) upon consecutive injections of IgG in PBS buffer. The dotted and solid lines represent the fits to the Eq. (1) and Eq. (2), respectively; (b) The calculated IF values for IgG-MIPs prepared with PmPD films of different thicknesses as a function of the IgG concentration. (For interpretation of the references to color in this figure legend, the reader is referred to the web version of this article.)

Table 1

The kinetics parameters obtained by fitting the sensorgrams in Fig. 3a to the pseudo-first order and pseudo-second order kinetic models.

C (nM)	Q_{eq} (MIP) (deg)	k^a	R^2	Q_{eq} (NIP) (deg)	k^a	R^2
Pseudo-first order model						
0.4	0.24	1.51E-03	0.994	0.08	1.83E-03	0.965
2.1	1.13	2.15E-03	0.998	0.30	3.01E-03	0.994
10.7	3.65	2.37E-03	0.994	1.06	9.90E-04	0.999
53.3	8.25	3.98E-03	0.978	2.58	2.09E-03	0.997
Pseudo-second order model						
0.4	0.38	2.72E-03	0.995	0.12	1.15E-02	0.965
2.1	1.64	1.00E-03	0.999	0.41	6.18E-03	0.995
10.7	5.17	3.66E-04	0.999	1.77	3.43E-04	0.999
53.3	10.43	3.90E-04	0.997	3.76	4.21E-04	0.999

^a Pseudo-first order rate constant (s^{-1}) or pseudo-second order rate constant ($deg^{-1} s^{-1}$).

0.965–0.999, although, at the higher analyte concentrations, somewhat higher values were obtained for the second order adsorption model. The latter might be explained by the fact that Q_{eq} in the pseudo-second order model can be determined independently of the kinetic mechanism of the adsorption process [32] and is less prone to the random experimental errors as compared to the first order rate equation [27]. Thus, Q_{eq} values determined by the pseudo-second rate model were used further to assess the degree of recognition capability of MIP towards the target molecule calculating imprinting factor (IF). Actually, IF shows a binding ratio between MIP and NIP:

$$IF = Q_{eq}(MIP)/Q_{eq}(NIP) \quad (3)$$

where Q_{eq} (MIP) and Q_{eq} (NIP) are phase-shift responses at equilibrium for MIP and NIP, respectively. As a measure of the presence of selective cavities, IF was taken into account to optimize the thickness of the PmPD film in IgG-MIP. SAW chips modified with IgG-MIP and NIP of different thicknesses in the range of ca 6 and 27 nm were subjected to interact with various IgG concentrations between 0.4 and 53.3 nM. Fig. 3b clearly indicates that for all IgG concentrations studied the highest IF values in the range of 2.8–4.0 were obtained for the IgG-MIP with PmPD film of 11 nm. This polymer thickness corresponds to the half of the height of immobilized IgG that was estimated to be around 20 nm assuming the IgG “end-on” orientation (through the Fc region). Obviously, at such polymer film thickness the immobilized IgG molecules might be appropriately confined in the polymer leading to the increasing number of high-affinity binding sites at the polymer surface after the IgG removal procedure. Thus, the thickness-optimized IgG-MIP films were employed for subsequent analysis of equilibrium parameters, regeneration and selectivity studies.

Adsorption isotherms are of particular interest as they represent the dependence of the equilibrium concentration of a bound analyte on the concentration of a free analyte in a solution and can provide useful information on the binding properties of the material by fitting the isotherm to specific binding models. The isotherm of IgG rebinding to IgG-MIP was constructed using the values of Q_{eq} determined from analysis of the experimental kinetic data fitting them to Eq. (2) (Fig. 4). Considering the binding site heterogeneity was frequently encountered in noncovalent MIPs [33] the analyte rebinding was modeled by the Langmuir–Freundlich (LF) isotherm (Eq. (4)).

$$Q = Q_{max}C^m / (K_D + C^m) \quad (4)$$

Here C is the concentration of an analyte in a solution, Q and Q_{max} the phase-shift responses upon IgG rebinding at concentration C and its saturation value, respectively, m is the heterogeneity index, which varies from 0 to 1 and with values < 1 , the material is heterogeneous, K_D – equilibrium dissociation constant. According to Fig. 4 LF model gives an excellent fit ($R^2 = 0.999$) for both IgG-MIP and NIP films tested in this study. The calculated m value of IgG-MIP indicates the somewhat heterogeneity of the binding sites in comparison to NIP, whose heterogeneity index equals to 1 corresponding to a homogeneous material. This can be well explained through assumption that NIP films might possess the exclusively nonspecific binding sites of equal adsorption energy, while the imprinting process introduced the binding sites with varying degrees of affinity resulting in the heterogeneity of the polymer surface. Furthermore, the obtained value of the signal at saturated binding to IgG-MIP was about 3 times higher than that to corresponding NIP (15.0 vs 5.3 deg) while the only modest difference in the dissociation constants (K_D) between two polymers was observed. One possible explanation for the observed phenomenon could be that despite of the total number of binding sites was increased in MIP relative to the NIP, the fraction of the higher-affinity binding sites was still low to contribute significantly to the overall affinity of IgG-MIP. Similarly, Shimizu and co-workers reported on the inconsistency between the difference in binding capacities and binding affinities of MIP and corresponding NIP [34].

3.3. Regeneration of IgG-MIPs

In order to verify the stability and reusability of the fabricated IgG-MIPs, the films with the optimal thickness after first IgG rebinding were subjected to the regeneration procedure. Since the nature of the interactions between the imprinted material and the target protein was insufficiently known, the regeneration

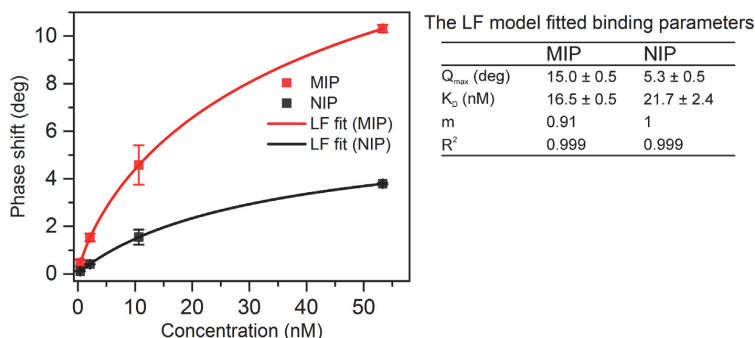


Fig. 4. The binding isotherms obtained using Q_{eq} determined from fitting of the kinetic data to Eq. (2). The solid lines represent fits of the data to Langmuir–Freundlich (LF) isotherm model. The table summarizes the fitted binding parameters.

experiments disrupting hydrogen, ionic and electrostatic bonds were performed. It was found that solutions of 1 M NaOH and 10 mM HCl affected significantly on reproducibility of further binding events making difference between MIP and NIP films barely noticed (results are not shown), while MIPs retained their affinity towards the target after the treatment in 3 M NaCl solution (100 °C) suggesting that electrostatic interactions might play a role in the given MIP-protein system. Therefore, the treatment in the hot 3 M NaCl solution was chosen as a method for regeneration of the fabricated IgG-MIPs. The changes in Q_{max} of the polymers for IgG after the subsequent rebinding-regeneration cycles are depicted in Fig. 5. As it can be seen, although both MIP and NIP polymers showed irreversible adsorption of the target, their rebinding capacities were about to stabilize after the 3rd regeneration cycle while still demonstrating MIP preferential affinity and relevant sensitivity levels towards the target. The noticed decrease in the adsorption capacity may indicate that the regeneration method left behind to some extent the target entrapped in the polymeric matrix altering thus the following rebinding. Still, the phenomenon cannot be explained purely by the target entrapment since the nonspecific adsorption, displayed by NIP film response, was suppressed significantly after the very 1st regeneration cycle. Thus, the films might also undergo morphological changes upon contact with the high temperature and ionic strength solutions resulting

in loss of a fraction of the polymeric material from the sensing surface.

3.4. Selectivity study

Selectivity of IgG imprinted films towards the template was studied by injecting $8 \mu\text{g mL}^{-1}$ solutions of other serum proteins: HSA and IgA that may cause serious interference when analyzing real samples. Selectivity factor S , which is the ratio of IF of an interfering substance to that toward the template molecule, was used to assess cross-reactivity of IgG-MIP:

$$S = IF_{(interf)} / IF_{(IgG)} \quad (5)$$

where $IF_{(IgG)}$ is the imprinting factor of IgG-MIP for IgG and $IF_{(interf)}$ is the imprinting factor of IgG-MIP for interfering protein, IgA or HSA. $IF_{(interf)}$ values for IgA and HSA were calculated according to Eq. (3), where the values of Q_{eq} upon HSA and IgA adsorption onto IgG-MIP and NIP were determined from the kinetics data using the similar analysis procedure as described for IgG rebinding study (Section 3.2). As it can be seen in Fig. 6, IgG-MIP demonstrated the preferential binding to the original template molecule (IgG) over the IgA and HSA with the S values of 0.3 and 0.09, respectively. The data suggests that the both interfering proteins have lower binding affinity to IgG-MIP than IgG, even though the molecular size and shape of IgG and IgA are similar. Thus, IgG-MIP can recognize the

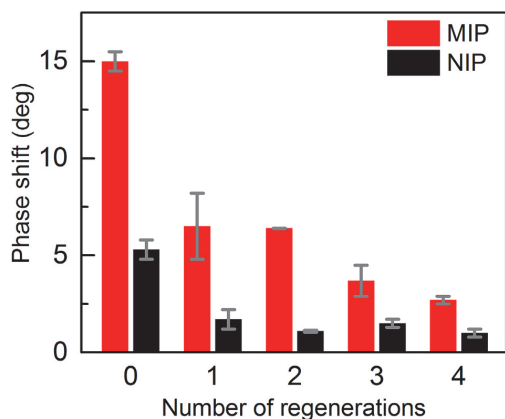


Fig. 5. SAW sensor response at saturated binding (Q_{max}) for IgG-MIP and NIP after various number of regeneration cycles. The initial responses of freshly fabricated sensors are presented at 0 value of regeneration cycle.

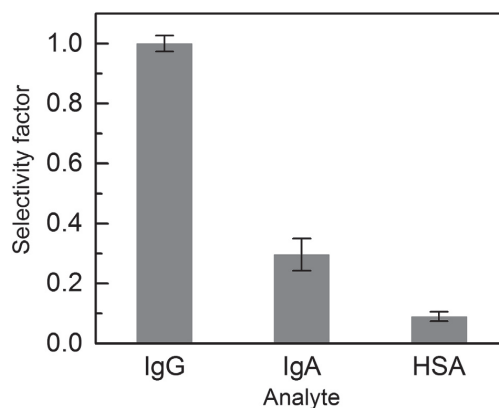


Fig. 6. Selectivity factors (S) of IgG-MIP for the template (IgG) and non-template (IgA, HSA) proteins.

target protein confirming the presence of IgG imprints in the polymer matrix that are able to discriminate on the basis of molecular shape and size as well as functional groups arrangement.

4. Conclusions

In this study, the protein imprinted polymers, IgG-MIPs, were used for the first time as sensing layers of SAW sensor platform. The thin films of IgG-MIP were successfully interfaced with SAW chips using the electrosynthesis approach. The binding kinetic analysis with the pseudo second-order rate model allowed the determination of equilibrium binding response and thus, the calculation and comparison of the imprinting factors for the IgG-MIP of different polymer thicknesses. It was found that IgG-MIP films with the thickness of 11 nm had higher specific recognition ability towards IgG as compared to the other studied IgG-MIP counterparts. The thickness optimized MIPs demonstrated imprinting factors in the range of 2.8–4.

The analysis of the isotherm data by fitting them to Langmuir-Freundlich adsorption model suggested a certain degree of heterogeneity of the binding sites in IgG-MIP films. Although, the binding capacity of IgG-MIP was about 3 times higher than that of NIP, their dissociation constants were somewhat comparable. This is more likely attributed to the disproportionately low contribution of the high affinity binding sites to the increased binding capacity of IgG-MIP. The prepared IgG-MIPs demonstrated good selectivity towards IgG over the interfering proteins such as IgA and HSA as well preserved their capability to recognize selectively the template after up to four regeneration cycles in hot 3 M NaCl solution.

The realized concept for facile integration of protein-MIPs with SAW technology allowed observing the real-time binding events of the target protein at relevant sensitivity levels and can be potentially suitable for cost effective fabrication of a biosensor for analysis of biological samples in multiplexed manner.

Acknowledgments

This work was supported by the Estonian Ministry of Education and Research (grant PUT150). The authors thank Dr. J. Rappich for the opportunity to perform the ellipsometry measurements at Helmholtz-Zentrum Berlin für Materialien und Energie GmbH.

References

- [1] S. Ray, G. Mehta, S. Srivastava, Label-free detection techniques for protein microarrays: prospects, merits and challenges, *Proteomics* 10 (2010) 731–748.
- [2] S. Li, Y. Ge, S.A. Piletsky, J. Lunec, *Molecularly Imprinted Sensors: Overview and Applications*, Elsevier, 2012, p. 388.
- [3] L. Ye, K. Haupt, Molecularly imprinted polymers as antibody and receptor mimics for assays, sensors and drug discovery, *Anal. Bioanal. Chem.* 378 (2004) 1887–1897.
- [4] N.W. Turner, C.W. Jeans, K.R. Brain, C.J. Allender, V. Hlady, D.W. Britt, From 3D to 2D: A review of the molecular imprinting of proteins, *Biotechnol. Prog.* 22 (2006) 1474–1489.
- [5] H. Nishino, C.S. Huang, K.J. Shea, Selective protein capture by epitope imprinting, *Angew. Chem. Int. Ed.* 45 (2006) 2392–2396.
- [6] P.C. Chou, J. Rick, T.C. Chou, C-reactive protein thin-film molecularly imprinted polymers formed using a micro-contact approach, *Anal. Chim. Acta* 542 (2005) 20–25.
- [7] G. Lautner, J. Kaev, J. Reut, A. Öpik, J. Rappich, V. Syritski, R.E. Gyurcsanyi, Selective Artificial receptors based on micropatterned surface-imprinted polymers for label-free detection of proteins by SPR imaging, *Adv. Funct. Mater.* 21 (2011) 591–597.
- [8] A. Menaker, V. Syritski, J. Reut, A. Öpik, V. Horvath, R.E. Gyurcsanyi, Electrosynthesized surface-imprinted conducting polymer microrods for selective protein recognition, *Adv. Mater.* 21 (2009) 2271–2275.
- [9] O. Hayden, C. Haderspock, S. Krassnig, X.H. Chen, F.L. Dickert, Surface imprinting strategies for the detection of trypsin, *Analyst* 131 (2006) 1044–1050.
- [10] D.R. Kryscio, N.A. Peppas, Surface imprinted thin polymer film systems with selective recognition for bovine serum albumin, *Anal. Chim. Acta* 718 (2012) 109–115.
- [11] Z.H. Zhang, Y.M. Long, L.H. Nie, S.Z. Yao, Molecularly imprinted thin film self-assembled on piezoelectric quartz crystal surface by the sol-gel process for protein recognition, *Biosens. Bioelectron.* 21 (2006) 1244–1251.
- [12] J. Rick, T.C. Chou, Using protein templates to direct the formation of thin-film polymer surfaces, *Biosens. Bioelectron.* 22 (2006) 544–549.
- [13] P.S. Sharma, A. Pietrzyk-Le, F. D'Souza, W. Kutner, Electrochemically synthesized polymers in molecular imprinting for chemical sensing, *Anal. Bioanal. Chem.* 402 (2012) 3177–3204.
- [14] A.S. Tretjakov, V. Syritski, J. Reut, O. Volobujeva, A. Öpik, Surface molecularly imprinted polydopamine films for recognition of immunoglobulin G, *Mikrochim. Acta* 180 (2013) 1433–1442.
- [15] J. Bognar, J. Szucs, Z. Dorko, V. Horvath, R.E. Gyurcsanyi, Nanosphere lithography as a versatile method to generate surface-imprinted polymer films for selective protein recognition, *Adv. Funct. Mater.* 23 (2013) 4703–4709.
- [16] D. Cai, L. Ren, H.Z. Zhao, C.J. Xu, L. Zhang, Y. Yu, H.Z. Wang, Y.C. Lan, M.F. Roberts, J.H. Chung, M.J. Naughton, Z.F. Ren, T.C. Chiles, A molecular-imprint nanosensor for ultrasensitive detection of proteins, *Nat. Nanotechnol.* 5 (2010) 597–601.
- [17] D. Dechtrirat, N. Gajovic-Eichelmann, F.F. Bier, F.W. Scheller, Hybrid material for protein sensing based on electrosynthesized MIP on a mannose terminated self-assembled monolayer, *Adv. Funct. Mater.* 24 (2014) 2233–2239.
- [18] T.M.A. Gronewold, Surface acoustic wave sensors in the bioanalytical field: recent trends and challenges, *Anal. Chim. Acta* 603 (2007) 119–128.
- [19] K. Länge, B.E. Rapp, M. Rapp, Surface acoustic wave biosensors: a review, *Anal. Bioanal. Chem.* 391 (2008) 1509–1519.
- [20] V.V. Losev, A.V. Medved, A.V. Roshchin, R.G. Kryshal, B.I. Zapadinski, I.D. Epinat'ev, I.V. Kumpanenko, An acoustic study of the selective absorption of vapors by microporous polymer films, *Russ. J. Phys. Chem. B* 3 (2009) 990–1003.
- [21] W. Wen, S.T. He, S.Z. Li, M.H. Liu, P. Yong, Enhanced sensitivity of SAW gas sensor coated molecularly imprinted polymer incorporating high frequency stability oscillator, *Sens. Actuators B Chem.* 125 (2007) 422–427.
- [22] R. Boroznjak, A. Tretjakov, V. Syritski, J. Reut, A. Öpik, Unpublished results, (2015).
- [23] M. Bosserdt, J. Erdossy, G. Lautner, J. Witt, K. Kohler, N. Gajovic-Eichelmann, A. Yarman, G. Wittstock, F.W. Scheller, R.E. Gyurcsanyi, Microelectrospotting as a new method for electrosynthesis of surface-imprinted polymer microarrays for protein recognition, *Biosens. Bioelectron.* 73 (2015) 123–129.
- [24] K.J. Jetzschmann, G. Jagerszki, D. Dechtrirat, A. Yarman, N. Gajovic-Eichelmann, H.D. Gilsing, B. Schulz, R.E. Gyurcsanyi, F.W. Scheller, Vectorially Imprinted Hybrid Nanofilm for Acetylcholinesterase Recognition, *Adv. Funct. Mater.* 25 (2015) 5178–5183.
- [25] Y. Liu, L. Shen, From Langmuir kinetics to first- and second-order rate equations for adsorption, *Langmuir ACS J. Surf. Coll.* 24 (2008) 11625–11630.
- [26] S. Lagergren, Zur theorie der sogenannten adsorption gelöster stoffe, *Kungliga Svenska Vetenskapsakademiens Handlingar* 24 (1898) 1–39.
- [27] W. Plazinski, W. Rudzinski, A. Plazinska, Theoretical models of sorption kinetics including a surface reaction mechanism: a review, *Adv. Colloid Interfac.* 152 (2009) 2–13.
- [28] Y.S. Ho, Review of second-order models for adsorption systems, *J. Hazard Mater.* 136 (2006) 681–689.
- [29] C.Y. Chen, C.H. Wang, A.H. Chen, Recognition of molecularly imprinted polymers for a quaternary alkaloid of berberine, *Talanta* 84 (2011) 1038–1046.
- [30] K. da Mata, M.Z. Corazza, F.M. de Oliveira, A.L. de Toffoli, C.R.T. Tarley, A.B. Moreira, Synthesis and characterization of cross-linked molecularly imprinted polyacrylamide for the extraction/preconcentration of glyphosate and aminomethylphosphonic acid from water samples, *React. Funct. Polym.* 83 (2014) 76–83.
- [31] Q.P. You, Y.P. Zhang, Q.W. Zhang, J.F. Guo, W.H. Huang, S.Y. Shi, X.Q. Chen, High-capacity thermo-responsive magnetic molecularly imprinted polymers for selective extraction of curcuminoids, *J. Chromatogr. A* 1354 (2014) 1–8.
- [32] W. Rudzinski, W. Plazinski, On the applicability of the pseudo-second order equation to represent the kinetics of adsorption at solid/solution interfaces: a theoretical analysis based on the statistical rate theory, *Adsorption* 15 (2009) 181–192.
- [33] R.J. Umpleby 2nd, S.C. Baxter, Y. Chen, R.N. Shah, K.D. Shimizu, Characterization of molecularly imprinted polymers with the Langmuir–Freundlich isotherm, *Anal. Chem.* 73 (2001) 4584–4591.
- [34] A.M. Rampey, R.J. Umpleby, G.T. Rushton, J.C. Iseman, R.N. Shah, K.D. Shimizu, Characterization of the imprint effect and the influence of imprinting conditions on affinity, capacity, and heterogeneity in molecularly imprinted polymers using the Freundlich isotherm-affinity distribution analysis, *Anal. Chem.* 76 (2004) 1123–1133.

APPENDIX B

CURRICULUM VITAE

1. Personal data

Name Aleksei Tretjakov
Date and place of birth 28.05.1988, Tallinn
E-mail address aleksei.tretjakov@gmail.com

2. Education

Educational institution	Graduation year	Education (field of study/degree)
Tallinn 48th Secondary School	2007	Secondary education
Tallinn University of Technology	2010	Chemical and Environmental Technology / BSc
Tallinn University of Technology	2012	Materials and Processes of Sustainable Energetics / MSc

3. Language competence/skills

Language	Level
Russian	Native
Estonian	Fluent
English	Average

4. Special courses

Period	Educational or other organisation
2012-2014	Graduate school "Functional materials and technologies FMTDK", Tallinn University of Technology, Estonia

5. Professional employment

Period	Organisation	Position
2009-2012	Tallinn University of Technology, Department of Materials Science	Scientific projects participant
2012-2014	Tallinn University of Technology, Department of Materials Science	Engineer

6. Research activity, including honours and thesis supervised **Projects**

01.01.2006 - 31.12.2011	Electrically Conductive Polymers for Functional Materials and Electron Devices. Investigation of the physical and chemical properties and possibilities for practical applications	SF0142714s06
01.11.2008 - 31.12.2010	Synthetic receptors based on molecularly imprinted conducting polymers	B612
01.01.2010 - 31.12.2012	Surface-Imprinted Electrosynthesized Conducting Polymers for Biorecognition	ETF8249
01.01.2012 - 31.12.2014	The New Technology for Wastewater Treatment by Photoelectrolytic Oxidation Combined with Molecularly Imprinted Polymers as Analytical Sensors	AR12046
01.01.2013 - 31.12.2016	Investigation and development of new generation biosensing selective recognition elements based on Molecularly Imprinted Polymers	PUT150

Honours

Award for the best publication in the field of natural and exact sciences in 2015 at Tallinn University of Technology: Akinrinade George Ayankojo, **Aleksei Tretjakov**, Jekaterina Reut, Roman Boroznjak, Andres Öpik, Jörg Rappich, Andreas Furchner, Karsten Hinrichs, and Vitali Syritski, Molecularly Imprinted Polymer Integrated with a Surface Acoustic Wave Technique for Detection of Sulfamethizole, *Analytical Chemistry*, 88(2) (2016) 1476–1484.

Theses supervised

Akinrinade George Ayankojo, Preparation of Antibiotic-imprinted Polymer Films by Electrochemical Approach: Towards the Development of a Label-free Chemical Sensor, MSc thesis, *Faculty of Chemical and Materials Technology: Department of Materials Science: Chair of Physical Chemistry* (2014), Supervisor: Vitali Sõritski, Co-supervisors: **Aleksei Tretjakov**, Jekaterina Reut.

ELULOOKIRJELDUS

1. Isikuandmed

Ees- ja perekonnanimi Aleksi Tretjakov
Sünniaeg ja -koht 28.05.1988, Tallinn
Kodakondsus Eesti
E-posti aadress aleksei.tretjakov@gmail.com

2. Hariduskäik

Õppeasutus (nimetus lõpetamise ajal)	Lõpetamise aeg	Haridus (eriala/kraad)
Tallinna 48. keskkool	2007	Keskharidus
Tallinna Tehnikaülikool	2010	Keemia- ja keskkonnakaitsetehnoloogia / bakalaureusekraad
Tallinna Tehnikaülikool	2012	Materjalid ja protsessid jäätkeusuutlikus energeetikas / magistrikraad

3. Keelteoskus

Keel	Tase
Vene	Emakeel
Eesti	Kõrgtase
Inglise	Kesktase

4. Täiendusõpe

Õppimise aeg	Täiendusõppe korraldaja nimetus
2012-2014	TÜ ja TTÜ doktorikool "Funktsionaalsed materjalid ja tehnoloogiad" (FMTDK), Eesti

5. Teenistuskäik

Töötamise aeg	Tööandja nimetus	Ametikoht
2009-2012	Tallinna Tehnikaülikool, materjaliteaduse instituut	Teadusprojektide täitja
2012-2014	Tallinna Tehnikaülikool, materjaliteaduse instituut	Insener

6. Teadustegevus, sh tunnustused ja juhendatud lõputööd

Projektid

01.01.2006 31.12.2011	Elektrit juhtivate polümeermaterjalide omaduste uurimine ja modifitseerimine kasutamiseks funktsionaalsete materjalidena ning elektronseadiste komponentidena	SF0142714s06
01.11.2008 31.12.2010	Süntetilised retseptorid molekulaarselt jäljendatud elektrit juhtivatest polümeeridest	B612
01.01.2010 31.12.2012	Biotundlikud süsteemid pindmiste mälupesadega molekulaarselt jäljendatud elektrit juhtivatest polümeeridest	ETF8249
01.01.2012 31.12.2014	Uus tehnoloogia keskkonnaohtlike mikrosaasteainete lagundamiseks vesifaasis: molekulaarselt jäljendatud polümeeridest analüütiliste sensoritega varustatud fotokatalüütiline puhastusseade	AR12046
01.01.2013 31.12.2016	Uue põlvkonna biotundlike süsteemide uurimine ja väljatöötamine molekulaarselt jäljendatud polümeeride baasil	PUT150

Tunnustused

TTÜ 2015. aasta parim teadusartikkel loodus-, täppis- ja terviseteaduste valdkonnas: Akinrinade George Ayankojo, **Aleksei Tretjakov**, Jekaterina Reut, Roman Boroznjak, Andres Öpik, Jörg Rappich, Andreas Furchner, Karsten Hinrichs, and Vitali Syritski, Molecularly Imprinted Polymer Integrated with a Surface Acoustic Wave Technique for Detection of Sulfamethizole, *Analytical Chemistry*, 88(2) (2016) 1476–1484.

Juhendatud lõputööd

Ayankojo, Akinrinade George, Preparation of Antibiotic-imprinted Polymer Films by Electrochemical Approach: Towards the Development of a Label-free Chemical Sensor, magistr töö, *Tallinna Tehnikaülikool, keemia ja materjalitehnoloogia teaduskond, materjaliteaduse instituut, füüsikalise keemia õppetool* (2014), juhendaja: Vitali Sõritski; kaasjuhendajad: **Aleksei Tretjakov**, Jekaterina Reut.

**DISSERTATIONS DEFENDED AT
TALLINN UNIVERSITY OF TECHNOLOGY ON
NATURAL AND EXACT SCIENCES**

1. **Olav Kongas**. Nonlinear Dynamics in Modeling Cardiac Arrhythmias. 1998.
2. **Kalju Vanatalu**. Optimization of Processes of Microbial Biosynthesis of Isotopically Labeled Biomolecules and Their Complexes. 1999.
3. **Ahto Buldas**. An Algebraic Approach to the Structure of Graphs. 1999.
4. **Monika Drews**. A Metabolic Study of Insect Cells in Batch and Continuous Culture: Application of Chemostat and Turbidostat to the Production of Recombinant Proteins. 1999.
5. **Eola Valdre**. Endothelial-Specific Regulation of Vessel Formation: Role of Receptor Tyrosine Kinases. 2000.
6. **Kalju Lott**. Doping and Defect Thermodynamic Equilibrium in ZnS. 2000.
7. **Reet Koljak**. Novel Fatty Acid Dioxygenases from the Corals *Plexaura homomalla* and *Gersemia fruticosa*. 2001.
8. **Anne Paju**. Asymmetric oxidation of Prochiral and Racemic Ketones by Using Sharpless Catalyst. 2001.
9. **Marko Vendelin**. Cardiac Mechanoenergetics *in silico*. 2001.
10. **Pearu Peterson**. Multi-Soliton Interactions and the Inverse Problem of Wave Crest. 2001.
11. **Anne Menert**. Microcalorimetry of Anaerobic Digestion. 2001.
12. **Toomas Tiivel**. The Role of the Mitochondrial Outer Membrane in *in vivo* Regulation of Respiration in Normal Heart and Skeletal Muscle Cell. 2002.
13. **Olle Hints**. Ordovician Scolecodonts of Estonia and Neighbouring Areas: Taxonomy, Distribution, Palaeoecology, and Application. 2002.
14. **Jaak Nõlvak**. Chitinozoan Biostratigraphy in the Ordovician of Baltoscandia. 2002.
15. **Liivi Kluge**. On Algebraic Structure of Pre-Operad. 2002.
16. **Jaanus Lass**. Biosignal Interpretation: Study of Cardiac Arrhythmias and Electromagnetic Field Effects on Human Nervous System. 2002.
17. **Janek Peterson**. Synthesis, Structural Characterization and Modification of PAMAM Dendrimers. 2002.
18. **Merike Vaher**. Room Temperature Ionic Liquids as Background Electrolyte Additives in Capillary Electrophoresis. 2002.
19. **Valdek Mikli**. Electron Microscopy and Image Analysis Study of Powdered Hardmetal Materials and Optoelectronic Thin Films. 2003.
20. **Mart Viljus**. The Microstructure and Properties of Fine-Grained Cermets. 2003.
21. **Signe Kask**. Identification and Characterization of Dairy-Related *Lactobacillus*. 2003.
22. **Tiiu-Mai Laht**. Influence of Microstructure of the Curd on Enzymatic and Microbiological Processes in Swiss-Type Cheese. 2003.
23. **Anne Kuusksalu**. 2–5A Synthetase in the Marine Sponge *Geodia cydonium*. 2003.
24. **Sergei Bereznev**. Solar Cells Based on Polycrystalline Copper-Indium Chalcogenides and Conductive Polymers. 2003.
25. **Kadri Kriis**. Asymmetric Synthesis of C₂-Symmetric Bimorpholines and Their Application as Chiral Ligands in the Transfer Hydrogenation of Aromatic Ketones. 2004.

26. **Jekaterina Reut.** Polypyrrole Coatings on Conducting and Insulating Substrates. 2004.
27. **Sven Nõmm.** Realization and Identification of Discrete-Time Nonlinear Systems. 2004.
28. **Olga Kijatkina.** Deposition of Copper Indium Disulphide Films by Chemical Spray Pyrolysis. 2004.
29. **Gert Tamberg.** On Sampling Operators Defined by Rogosinski, Hann and Blackman Windows. 2004.
30. **Monika Übner.** Interaction of Humic Substances with Metal Cations. 2004.
31. **Kaarel Adamberg.** Growth Characteristics of Non-Starter Lactic Acid Bacteria from Cheese. 2004.
32. **Imre Vallikivi.** Lipase-Catalysed Reactions of Prostaglandins. 2004.
33. **Merike Peld.** Substituted Apatites as Sorbents for Heavy Metals. 2005.
34. **Vitali Syritski.** Study of Synthesis and Redox Switching of Polypyrrole and Poly(3,4-ethylenedioxythiophene) by Using *in-situ* Techniques. 2004.
35. **Lee Põllumaa.** Evaluation of Ecotoxicological Effects Related to Oil Shale Industry. 2004.
36. **Riina Aav.** Synthesis of 9,11-Secosterols Intermediates. 2005.
37. **Andres Braunbrück.** Wave Interaction in Weakly Inhomogeneous Materials. 2005.
38. **Robert Kitt.** Generalised Scale-Invariance in Financial Time Series. 2005.
39. **Juss Pavelson.** Mesoscale Physical Processes and the Related Impact on the Summer Nutrient Fields and Phytoplankton Blooms in the Western Gulf of Finland. 2005.
40. **Olari Ilison.** Solitons and Solitary Waves in Media with Higher Order Dispersive and Nonlinear Effects. 2005.
41. **Maksim Säkki.** Intermittency and Long-Range Structurization of Heart Rate. 2005.
42. **Enli Kiipli.** Modelling Seawater Chemistry of the East Baltic Basin in the Late Ordovician–Early Silurian. 2005.
43. **Igor Golovtsov.** Modification of Conductive Properties and Processability of Polyparaphenylene, Polypyrrole and polyaniline. 2005.
44. **Katrin Laos.** Interaction Between Furcellaran and the Globular Proteins (Bovine Serum Albumin β -Lactoglobulin). 2005.
45. **Arvo Mere.** Structural and Electrical Properties of Spray Deposited Copper Indium Disulphide Films for Solar Cells. 2006.
46. **Sille Ehala.** Development and Application of Various On- and Off-Line Analytical Methods for the Analysis of Bioactive Compounds. 2006.
47. **Maria Kulp.** Capillary Electrophoretic Monitoring of Biochemical Reaction Kinetics. 2006.
48. **Anu Aaspõllu.** Proteinases from *Vipera lebetina* Snake Venom Affecting Hemostasis. 2006.
49. **Lyudmila Chekulayeva.** Photosensitized Inactivation of Tumor Cells by Porphyrins and Chlorins. 2006.
50. **Merle Uudsemaa.** Quantum-Chemical Modeling of Solvated First Row Transition Metal Ions. 2006.
51. **Tagli Pitsi.** Nutrition Situation of Pre-School Children in Estonia from 1995 to 2004. 2006.

52. **Angela Ivask.** Luminescent Recombinant Sensor Bacteria for the Analysis of Bioavailable Heavy Metals. 2006.
53. **Tiina Lõugas.** Study on Physico-Chemical Properties and Some Bioactive Compounds of Sea Buckthorn (*Hippophae rhamnoides* L.). 2006.
54. **Kaja Kasemets.** Effect of Changing Environmental Conditions on the Fermentative Growth of *Saccharomyces cerevisiae* S288C: Auxo-accelerostat Study. 2006.
55. **Ildar Nisamedtinov.** Application of ¹³C and Fluorescence Labeling in Metabolic Studies of *Saccharomyces* spp. 2006.
56. **Alar Leibak.** On Additive Generalisation of Voronoï's Theory of Perfect Forms over Algebraic Number Fields. 2006.
57. **Andri Jagomägi.** Photoluminescence of Chalcopyrite Tellurides. 2006.
58. **Tõnu Martma.** Application of Carbon Isotopes to the Study of the Ordovician and Silurian of the Baltic. 2006.
59. **Marit Kauk.** Chemical Composition of CuInSe₂ Monograin Powders for Solar Cell Application. 2006.
60. **Julia Kois.** Electrochemical Deposition of CuInSe₂ Thin Films for Photovoltaic Applications. 2006.
61. **Ilona Oja Açıık.** Sol-Gel Deposition of Titanium Dioxide Films. 2007.
62. **Tiia Anmann.** Integrated and Organized Cellular Bioenergetic Systems in Heart and Brain. 2007.
63. **Katrin Trummal.** Purification, Characterization and Specificity Studies of Metalloproteinases from *Vipera lebetina* Snake Venom. 2007.
64. **Gennadi Lessin.** Biochemical Definition of Coastal Zone Using Numerical Modeling and Measurement Data. 2007.
65. **Enno Pais.** Inverse problems to determine non-homogeneous degenerate memory kernels in heat flow. 2007.
66. **Maria Borissova.** Capillary Electrophoresis on Alkylimidazolium Salts. 2007.
67. **Karin Valmsen.** Prostaglandin Synthesis in the Coral *Plexaura homomalla*: Control of Prostaglandin Stereochemistry at Carbon 15 by Cyclooxygenases. 2007.
68. **Kristjan Piirimäe.** Long-Term Changes of Nutrient Fluxes in the Drainage Basin of the Gulf of Finland – Application of the PolFlow Model. 2007.
69. **Tatjana Dedova.** Chemical Spray Pyrolysis Deposition of Zinc Sulfide Thin Films and Zinc Oxide Nanostructured Layers. 2007.
70. **Katrin Tomson.** Production of Labelled Recombinant Proteins in Fed-Batch Systems in *Escherichia coli*. 2007.
71. **Cecilia Sarmiento.** Suppressors of RNA Silencing in Plants. 2008.
72. **Vilja Mardla.** Inhibition of Platelet Aggregation with Combination of Antiplatelet Agents. 2008.
73. **Maie Bachmann.** Effect of Modulated Microwave Radiation on Human Resting Electroencephalographic Signal. 2008.
74. **Dan Hüvonen.** Terahertz Spectroscopy of Low-Dimensional Spin Systems. 2008.
75. **Ly Villo.** Stereoselective Chemoenzymatic Synthesis of Deoxy Sugar Esters Involving *Candida antarctica* Lipase B. 2008.
76. **Johan Anton.** Technology of Integrated Photoelasticity for Residual Stress Measurement in Glass Articles of Axisymmetric Shape. 2008.
77. **Olga Volobujeva.** SEM Study of Selenization of Different Thin Metallic Films. 2008.

78. **Artur Jõgi**. Synthesis of 4'-Substituted 2,3'-dideoxynucleoside Analogues. 2008.
79. **Mario Kadastik**. Doubly Charged Higgs Boson Decays and Implications on Neutrino Physics. 2008.
80. **Fernando Pérez-Caballero**. Carbon Aerogels from 5-Methylresorcinol-Formaldehyde Gels. 2008.
81. **Sirje Vaask**. The Comparability, Reproducibility and Validity of Estonian Food Consumption Surveys. 2008.
82. **Anna Menaker**. Electrosynthesized Conducting Polymers, Polypyrrole and Poly(3,4-ethylenedioxythiophene), for Molecular Imprinting. 2009.
83. **Lauri Ilison**. Solitons and Solitary Waves in Hierarchical Korteweg-de Vries Type Systems. 2009.
84. **Kaia Ernits**. Study of In₂S₃ and ZnS Thin Films Deposited by Ultrasonic Spray Pyrolysis and Chemical Deposition. 2009.
85. **Veljo Sinivee**. Portable Spectrometer for Ionizing Radiation "Gammamapper". 2009.
86. **Jüri Virkepu**. On Lagrange Formalism for Lie Theory and Operadic Harmonic Oscillator in Low Dimensions. 2009.
87. **Marko Piirsoo**. Deciphering Molecular Basis of Schwann Cell Development. 2009.
88. **Kati Helmja**. Determination of Phenolic Compounds and Their Antioxidative Capability in Plant Extracts. 2010.
89. **Merike Sõmera**. Sobemoviruses: Genomic Organization, Potential for Recombination and Necessity of P1 in Systemic Infection. 2010.
90. **Kristjan Laes**. Preparation and Impedance Spectroscopy of Hybrid Structures Based on CuIn₃Se₅ Photoabsorber. 2010.
91. **Kristin Lippur**. Asymmetric Synthesis of 2,2'-Bimorpholine and its 5,5'-Substituted Derivatives. 2010.
92. **Merike Luman**. Dialysis Dose and Nutrition Assessment by an Optical Method. 2010.
93. **Mihhail Berezovski**. Numerical Simulation of Wave Propagation in Heterogeneous and Microstructured Materials. 2010.
94. **Tamara Aid-Pavlidis**. Structure and Regulation of BDNF Gene. 2010.
95. **Olga Bragina**. The Role of Sonic Hedgehog Pathway in Neuro- and Tumorigenesis. 2010.
96. **Merle Randrüüt**. Wave Propagation in Microstructured Solids: Solitary and Periodic Waves. 2010.
97. **Marju Laars**. Asymmetric Organocatalytic Michael and Aldol Reactions Mediated by Cyclic Amines. 2010.
98. **Maarja Grossberg**. Optical Properties of Multinary Semiconductor Compounds for Photovoltaic Applications. 2010.
99. **Alla Maloverjan**. Vertebrate Homologues of Drosophila Fused Kinase and Their Role in Sonic Hedgehog Signalling Pathway. 2010.
100. **Priit Pruunsild**. Neuronal Activity-Dependent Transcription Factors and Regulation of Human *BDNF* Gene. 2010.
101. **Tatjana Knjazeva**. New Approaches in Capillary Electrophoresis for Separation and Study of Proteins. 2011.
102. **Atanas Katerski**. Chemical Composition of Sprayed Copper Indium Disulfide Films for Nanostructured Solar Cells. 2011.

103. **Kristi Timmo.** Formation of Properties of CuInSe_2 and $\text{Cu}_2\text{ZnSn}(\text{S},\text{Se})_4$ Monograin Powders Synthesized in Molten KI. 2011.
104. **Kert Tamm.** Wave Propagation and Interaction in Mindlin-Type Microstructured Solids: Numerical Simulation. 2011.
105. **Adrian Popp.** Ordovician Proetid Trilobites in Baltoscandia and Germany. 2011.
106. **Ove Pärn.** Sea Ice Deformation Events in the Gulf of Finland and This Impact on Shipping. 2011.
107. **Germo Väli.** Numerical Experiments on Matter Transport in the Baltic Sea. 2011.
108. **Andrus Seiman.** Point-of-Care Analyser Based on Capillary Electrophoresis. 2011.
109. **Olga Katargina.** Tick-Borne Pathogens Circulating in Estonia (Tick-Borne Encephalitis Virus, *Anaplasma phagocytophilum*, *Babesia* Species): Their Prevalence and Genetic Characterization. 2011.
110. **Ingrid Sumeri.** The Study of Probiotic Bacteria in Human Gastrointestinal Tract Simulator. 2011.
111. **Kairit Zovo.** Functional Characterization of Cellular Copper Proteome. 2011.
112. **Natalja Makarytsheva.** Analysis of Organic Species in Sediments and Soil by High Performance Separation Methods. 2011.
113. **Monika Mortimer.** Evaluation of the Biological Effects of Engineered Nanoparticles on Unicellular Pro- and Eukaryotic Organisms. 2011.
114. **Kersti Tepp.** Molecular System Bioenergetics of Cardiac Cells: Quantitative Analysis of Structure-Function Relationship. 2011.
115. **Anna-Liisa Peikolainen.** Organic Aerogels Based on 5-Methylresorcinol. 2011.
116. **Leeli Amon.** Palaeoecological Reconstruction of Late-Glacial Vegetation Dynamics in Eastern Baltic Area: A View Based on Plant Macrofossil Analysis. 2011.
117. **Tanel Peets.** Dispersion Analysis of Wave Motion in Microstructured Solids. 2011.
118. **Liina Kaupmees.** Selenization of Molybdenum as Contact Material in Solar Cells. 2011.
119. **Allan Olsper.** Properties of VPg and Coat Protein of Sobemoviruses. 2011.
120. **Kadri Koppel.** Food Category Appraisal Using Sensory Methods. 2011.
121. **Jelena Gorbatšova.** Development of Methods for CE Analysis of Plant Phenolics and Vitamins. 2011.
122. **Karin Viipsi.** Impact of EDTA and Humic Substances on the Removal of Cd and Zn from Aqueous Solutions by Apatite. 2012.
123. **David Schryer.** Metabolic Flux Analysis of Compartmentalized Systems Using Dynamic Isotopologue Modeling. 2012.
124. **Ardo Illaste.** Analysis of Molecular Movements in Cardiac Myocytes. 2012.
125. **Indrek Reile.** 3-Alkylcyclopentane-1,2-Diones in Asymmetric Oxidation and Alkylation Reactions. 2012.
126. **Tatjana Tamberg.** Some Classes of Finite 2-Groups and Their Endomorphism Semigroups. 2012.
127. **Taavi Liblik.** Variability of Thermohaline Structure in the Gulf of Finland in Summer. 2012.
128. **Priidik Lagemaa.** Operational Forecasting in Estonian Marine Waters. 2012.

129. **Andrei Errapart.** Photoelastic Tomography in Linear and Non-linear Approximation. 2012.
130. **Külliki Krabbi.** Biochemical Diagnosis of Classical Galactosemia and Mucopolysaccharidoses in Estonia. 2012.
131. **Kristel Kaseleht.** Identification of Aroma Compounds in Food using SPME-GC/MS and GC-Olfactometry. 2012.
132. **Kristel Kodar.** Immunoglobulin G Glycosylation Profiling in Patients with Gastric Cancer. 2012.
133. **Kai Rosin.** Solar Radiation and Wind as Agents of the Formation of the Radiation Regime in Water Bodies. 2012.
134. **Ann Tiiman.** Interactions of Alzheimer's Amyloid-Beta Peptides with Zn(II) and Cu(II) Ions. 2012.
135. **Olga Gavrilova.** Application and Elaboration of Accounting Approaches for Sustainable Development. 2012.
136. **Olesja Bondarenko.** Development of Bacterial Biosensors and Human Stem Cell-Based *In Vitro* Assays for the Toxicological Profiling of Synthetic Nanoparticles. 2012.
137. **Katri Muska.** Study of Composition and Thermal Treatments of Quaternary Compounds for Monograin Layer Solar Cells. 2012.
138. **Ranno Nahku.** Validation of Critical Factors for the Quantitative Characterization of Bacterial Physiology in Accelerostat Cultures. 2012.
139. **Petri-Jaan Lahtvee.** Quantitative Omics-level Analysis of Growth Rate Dependent Energy Metabolism in *Lactococcus lactis*. 2012.
140. **Kerti Orumets.** Molecular Mechanisms Controlling Intracellular Glutathione Levels in Baker's Yeast *Saccharomyces cerevisiae* and its Random Mutagenized Glutathione Over-Accumulating Isolate. 2012.
141. **Loreida Timberg.** Spice-Cured Sprats Ripening, Sensory Parameters Development, and Quality Indicators. 2012.
142. **Anna Mihhalevski.** Rye Sourdough Fermentation and Bread Stability. 2012.
143. **Liisa Arike.** Quantitative Proteomics of *Escherichia coli*: From Relative to Absolute Scale. 2012.
144. **Kairi Otto.** Deposition of In₂S₃ Thin Films by Chemical Spray Pyrolysis. 2012.
145. **Mari Sepp.** Functions of the Basic Helix-Loop-Helix Transcription Factor TCF4 in Health and Disease. 2012.
146. **Anna Suhhova.** Detection of the Effect of Weak Stressors on Human Resting Electroencephalographic Signal. 2012.
147. **Aram Kazarjan.** Development and Production of Extruded Food and Feed Products Containing Probiotic Microorganisms. 2012.
148. **Rivo Uiboupin.** Application of Remote Sensing Methods for the Investigation of Spatio-Temporal Variability of Sea Surface Temperature and Chlorophyll Fields in the Gulf of Finland. 2013.
149. **Tiina Kriščiunaite.** A Study of Milk Coagulability. 2013.
150. **Tuuli Levandi.** Comparative Study of Cereal Varieties by Analytical Separation Methods and Chemometrics. 2013.
151. **Natalja Kabanova.** Development of a Microcalorimetric Method for the Study of Fermentation Processes. 2013.
152. **Himani Khanduri.** Magnetic Properties of Functional Oxides. 2013.
153. **Julia Smirnova.** Investigation of Properties and Reaction Mechanisms of Redox-Active Proteins by ESI MS. 2013.

154. **Mervi Sepp**. Estimation of Diffusion Restrictions in Cardiomyocytes Using Kinetic Measurements. 2013.
155. **Kersti Jääger**. Differentiation and Heterogeneity of Mesenchymal Stem Cells. 2013.
156. **Victor Alari**. Multi-Scale Wind Wave Modeling in the Baltic Sea. 2013.
157. **Taavi Päll**. Studies of CD44 Hyaluronan Binding Domain as Novel Angiogenesis Inhibitor. 2013.
158. **Allan Niidu**. Synthesis of Cyclopentane and Tetrahydrofuran Derivatives. 2013.
159. **Julia Geller**. Detection and Genetic Characterization of *Borrelia* Species Circulating in Tick Population in Estonia. 2013.
160. **Irina Stulova**. The Effects of Milk Composition and Treatment on the Growth of Lactic Acid Bacteria. 2013.
161. **Jana Holmar**. Optical Method for Uric Acid Removal Assessment During Dialysis. 2013.
162. **Kerti Ausmees**. Synthesis of Heterobicyclo[3.2.0]heptane Derivatives via Multicomponent Cascade Reaction. 2013.
163. **Minna Varikmaa**. Structural and Functional Studies of Mitochondrial Respiration Regulation in Muscle Cells. 2013.
164. **Indrek Koppel**. Transcriptional Mechanisms of BDNF Gene Regulation. 2014.
165. **Kristjan Pilt**. Optical Pulse Wave Signal Analysis for Determination of Early Arterial Ageing in Diabetic Patients. 2014.
166. **Andres Anier**. Estimation of the Complexity of the Electroencephalogram for Brain Monitoring in Intensive Care. 2014.
167. **Toivo Kallaste**. Pyroclastic Sanidine in the Lower Palaeozoic Bentonites – A Tool for Regional Geological Correlations. 2014.
168. **Erki Kärber**. Properties of ZnO-nanorod/In₂S₃/CuInS₂ Solar Cell and the Constituent Layers Deposited by Chemical Spray Method. 2014.
169. **Julia Lehner**. Formation of Cu₂ZnSnS₄ and Cu₂ZnSnSe₄ by Chalcogenisation of Electrochemically Deposited Precursor Layers. 2014.
170. **Peep Pitk**. Protein- and Lipid-rich Solid Slaughterhouse Waste Anaerobic Co-digestion: Resource Analysis and Process Optimization. 2014.
171. **Kaspar Valgepea**. Absolute Quantitative Multi-omics Characterization of Specific Growth Rate-dependent Metabolism of *Escherichia coli*. 2014.
172. **Artur Noole**. Asymmetric Organocatalytic Synthesis of 3,3'-Disubstituted Oxindoles. 2014.
173. **Robert Tsanev**. Identification and Structure-Functional Characterisation of the Gene Transcriptional Repressor Domain of Human Gli Proteins. 2014.
174. **Dmitri Kartofelev**. Nonlinear Sound Generation Mechanisms in Musical Acoustic. 2014.
175. **Sigrid Hade**. GIS Applications in the Studies of the Palaeozoic Graptolite Argillite and Landscape Change. 2014.
176. **Agne Velthut-Meikas**. Ovarian Follicle as the Environment of Oocyte Maturation: The Role of Granulosa Cells and Follicular Fluid at Pre-Ovulatory Development. 2014.
177. **Kristel Hälvin**. Determination of B-group Vitamins in Food Using an LC-MS Stable Isotope Dilution Assay. 2014.
178. **Mailis Päri**. Characterization of the Oligoadenylate Synthetase Subgroup from Phylum Porifera. 2014.

179. **Jekaterina Kazantseva**. Alternative Splicing of *TAF4*: A Dynamic Switch between Distinct Cell Functions. 2014.
180. **Jaanus Suurväli**. Regulator of G Protein Signalling 16 (RGS16): Functions in Immunity and Genomic Location in an Ancient MHC-Related Evolutionarily Conserved Synteny Group. 2014.
181. **Ene Viiard**. Diversity and Stability of Lactic Acid Bacteria During Rye Sourdough Propagation. 2014.
182. **Kristella Hansen**. Prostaglandin Synthesis in Marine Arthropods and Red Algae. 2014.
183. **Helike Lõhelaid**. Allene Oxide Synthase-lipoxygenase Pathway in Coral Stress Response. 2015.
184. **Normunds Stivriņš**. Postglacial Environmental Conditions, Vegetation Succession and Human Impact in Latvia. 2015.
185. **Mary-Liis Kütt**. Identification and Characterization of Bioactive Peptides with Antimicrobial and Immunoregulating Properties Derived from Bovine Colostrum and Milk. 2015.
186. **Kazbulat Šogenov**. Petrophysical Models of the CO₂ Plume at Prospective Storage Sites in the Baltic Basin. 2015.
187. **Taavi Raadik**. Application of Modulation Spectroscopy Methods in Photovoltaic Materials Research. 2015.
188. **Reio Põder**. Study of Oxygen Vacancy Dynamics in Sc-doped Ceria with NMR Techniques. 2015.
189. **Sven Siir**. Internal Geochemical Stratification of Bentonites (Altered Volcanic Ash Beds) and its Interpretation. 2015.
190. **Kaur Jaanson**. Novel Transgenic Models Based on Bacterial Artificial Chromosomes for Studying BDNF Gene Regulation. 2015.
191. **Niina Karro**. Analysis of ADP Compartmentation in Cardiomyocytes and Its Role in Protection Against Mitochondrial Permeability Transition Pore Opening. 2015.
192. **Piret Laht**. B-plexins Regulate the Maturation of Neurons Through Microtubule Dynamics. 2015.
193. **Sergei Žari**. Organocatalytic Asymmetric Addition to Unsaturated 1,4-Dicarbonyl Compounds. 2015.
194. **Natalja Buhhalko**. Processes Influencing the Spatio-temporal Dynamics of Nutrients and Phytoplankton in Summer in the Gulf of Finland, Baltic Sea. 2015.
195. **Natalia Maticiuc**. Mechanism of Changes in the Properties of Chemically Deposited CdS Thin Films Induced by Thermal Annealing. 2015.
196. **Mario Öeren**. Computational Study of Cyclohexylhemicucurbiturils. 2015.
197. **Mari Kalda**. Mechanoenergetics of a Single Cardiomyocyte. 2015.
198. **Ieva Grudzinska**. Diatom Stratigraphy and Relative Sea Level Changes of the Eastern Baltic Sea over the Holocene. 2015.
199. **Anna Kazantseva**. Alternative Splicing in Health and Disease. 2015.
200. **Jana Kazarjan**. Investigation of Endogenous Antioxidants and Their Synthetic Analogues by Capillary Electrophoresis. 2016.
201. **Maria Safonova**. SnS Thin Films Deposition by Chemical Solution Method and Characterization. 2016.
202. **Jekaterina Mazina**. Detection of Psycho- and Bioactive Drugs in Different Sample Matrices by Fluorescence Spectroscopy and Capillary Electrophoresis. 2016.